

UNIVERSITY OF TURKISH AERODYNAMIC ASSOCIATION
AERONAUTICS AND ASTRONAUTICS

**THERMAL CHARACTERISTICS OF PHASE CHANGE MATERIAL USED
AS THERMAL STORAGE SYSTEM BY USING SOLAR ENERGY**

MASTER THESIS

AMEER HASSAN AL-MAMOORI

ID: 1406080005

Institute of Science and Technology

Mechanical and Aeronautical Engineering Department

Master Thesis Program

April, 2017

**UNIVERSITY OF TURKISH AERODYNAMIC ASSOCIATION
AERONAUTICS AND ASTRONAUTICS**

**THERMAL CHARACTERISTICS OF PHASE CHANGE MATERIAL USED
AS THERMAL STORAGE SYSTEM BY USING SOLAR ENERGY**

MASTER THESIS

AMEER HASSAN AL-MAMOORI

ID: 1406080005

Re. NO:10145961

**IN PARTIAL FULFILLMENT OF THE REQUIREMENT FOR THE
DEGREE OF MASTER OF SCIENCE IN MECHANICAL AND
AERONAUTICAL ENGINEERING**

Supervisor: Assist. Prof. Dr. Munir ElFarra

CO. Supervisor: Dr. Kadhim Fadhil Nasir

بِسْمِ اللَّهِ الرَّحْمَنِ الرَّحِيمِ

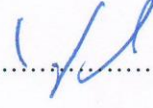
((قَالَ سِبْحَانُكَ لَا أَعْلَمُ لَنَا إِلَّا مَا عَلَّمْتَنَا

إِنَّكَ أَنْتَ الْعَلِيمُ الْحَكِيمُ))

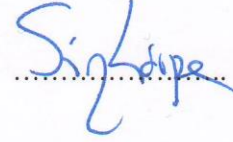
(البقرة ٢٢٢)

Türk Hava Kurumu Üniversitesi Fen Bilimleri Enstitüsü'nün 1406080005 numaralı Yüksek Lisans öğrencisi "Ameer AL-Mamoori" ilgili yönetmeliklerin belirlediği gerekli tüm şartları yerine getirdikten sonra hazırladığı " Thermal characteristics of phase change material used as thermal storage system by using solar energy " başlıklı tezini, aşağıda imzaları bulunan jüri önünde başarı ile sunmuştur.

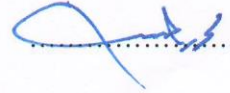
Tez Danışmanı : Yrd. Doç. Dr. Munir Elferra
Ankara Yıldırım Beyazıt Üniversitesi



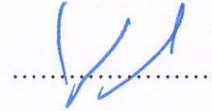
Jüri Üyeleri : Yrd. Doç. Dr. Durmuş Sinan Körpe
Türk Hava Kurumu Üniversitesi



: Yrd. Doç. Dr. Mohamed S. Elmnefi
Türk Hava Kurumu Üniversitesi



: Yrd. Doç. Dr. Munir Elferra
Ankara Yıldırım Beyazıt Üniversitesi



Tez Savunma Tarihi: 21.04.2017

STATEMENT OF NON-PLAGIARISM PAGE

I hereby declare that all information in this document has been obtained and presented in accordance with academic rules and ethical conduct. I also declare that, as required by these rules and conduct, I have fully cited and referenced all material and results that are not original to this work.

Ameer AL-Mamoori

21.04.2017

Acknowledgements

I would like to express my sincere gratitude to Dr. Asst .Pro . Miner Ali, my director, for her direction supervision, and sharing of expertise which guided me through my research period. I am also very grateful to my second supervisor D. Kadhim Al - Dulaimimy for their valuable suggestions I would also like to thank Dean Technical Institute Musayyib D. Asst. Jabber Abbas Japer . His supports and thoughtful advices to my research work

I am sincerely and heartily acknowledge my colleagues, advice relating to my research that they gave me. In the same way, I appreciate all the help and support from my friends me throughout my study.

Finally, I would like to express my deepest gratitude to all my family members: my father and mother my brother and sister, who constantly provided their emotional support to me during my research years. Batool Ngaem, my wife, deserves special thanks for her caring of our family during these years. Your encouragement and support without regrets get me through those difficult times. Nobody knows how much I owe them.

And last but not least, a heartfelt thanks to all my flat mates for the great time spent together. It has been a wonderful experience!

April 2017

Ameer AL-Mamoori

Contents

Aknowledgements	iii
Contents	iv
List of tables	vi
List of figures.....	vii
Abstract.....	x
Özet.....	xi
List of Symbols.....	xii
Chapter one.....	1
Introduction	1
1.1 Background	1
1.2 Thermal Energy Storage.....	1
1.3 Classification of Phase Transition To Pcm	2
1.3.1 Sensible Heat Storage	3
1.3.2 Latent Heat of Solid – Liquid Phase Change.....	3
1.4 Desired Characteristics In a Pcm.....	4
1.4.1 Thermal Properties.....	4
1.4.2 Thermodynamic Properties.....	4
1.5 Phase Changing Materials (Pcm).	4
1.6 Objectives	4
Chapter Two	5
Literature Review	5
2.1 Introduction	5
2.2 Thermal Energy Storage (Tes) With Phase Change Material (Pcm)	5
2.3 Summary of Previous Researches	14
Chapter Three	15
Experimental Work	15
3.2 Experimental Setup	15
3.2.1 Solar Water Collector	17
3.2.2 Shell And Tube Heat Exchanger	17
3.2.3 Water Pump	18
3.2.4 Connecting Pipes	18
3.2.5 Insulations	19
3.2.6 Valves	19
3.2.7 Storage Container	19
3.3 Phase Change Material	19
3.4 Measurements And Instrumentation	20
3.4.1 Temperature Measurements Thermocouples.....	21
3.4.2 Water Flow Meter.....	21
3.4.3 Solar Radiation Measurements	22
3.4.4 Wind Speed Measurements	22
3.5 Thermal Performance Analysis	22

3.5.1 The Steps Adopted Before Each Experimental Test Are	23
Chapter Four	25
Results and Discussion	25
4.1 Introduction	25
4.2 Collector Performance.....	25
4.3 Pcm1 on Summer Season	28
4.4 Pcm1 on Winter Season.	38
4.5 Pcm2 on Summer Season	48
4.6 Pcm2 Winter Season	58
4.7 Summary	69
Chapter Five.....	70
Conclusion and Recommendations	70
5.1 Conclusion.....	70
5.2 Recommendations	71
References.....	72

List of Tables

Table 3.1 Thermo physical properties of paraffin PCM2 [28,29, 30, 31,32, 33].....	20
Table 3.2 Thermo physical properties of paraffin PCM1 [28,29, 30, 31,32, 33].....	20
Table 3.3 Data of Experimenter Test	24

List of figures

Figure 1.1 various types of thermal of solar energy[5].....	2
Figure 1.2 Heat storage as latent heat for the case of solid-liquid phase change.....	3
Figure 2.1 Schematic of PCM storage tank unit and storage cell, [15].	7
Figure 2.2 Solar water heater, Sharma and Chen, [17].	8
Figure 2.3 Experimental setup (a) Photographic view (b) Schematic of LTES system, [20].	9
Figure 2.4 High temperature pilot plant, [21]	10
Figure 2.5 Experimental test rig for testing the phase change behavior of PCM, [23].	11
Figure 2.6 (a) Section view of the heat exchanger and (b) real photo of heat exchanger, [25].	12
Figure 2.7 The experimental setup of utilization of paraffin and beeswax as heat energy storage on infant incubator, [27].	14
3.1 Experimental Rig	15
Figure 3.2. A schematic diagram of the comprehensive experimental system.	16
3.3 Water Pump.....	18
3.4 storage container	19
Figure 3.5 Paraffin Black Iraqi and Paraffin white German	20
Figure 3.6 Temperature measurements thermocouples type (K).	21
Figure 3.7 Water Flow meter	22
Figure 4.1 Solar radiation for flow rate of 200 and 500 lph.	26
Figure 4.2 Collector thermal efficiency for flow rate of 200 and 500 lph.	26
Figure 4.3 Operation curve of Solar Collector for flow rate of 200 lph.	27
Figure 4.4 Operation curve of Solar Collector for flow rate of 500 lph	27
Figure 4.5 PCM1 temperatures for flow rate of 200 lph on 5th Aug 2016.	28
Figure 4.6 PCM1 temperatures for flow rate of 300 lph on 7th Aug 2016.	29
Figure 4.7 PCM1 temperatures for flow rate of 500 lph on 11 Aug 2016.	30
Figure 4.8 PCM1 temperatures (T3, T4, T5) for flow rate of 200 lph on 5th Aug. 2016.	31
Figure 4.9 PCM1 temperatures (T6, T7, T8) for flow rate of 200 lph on 5th Aug. 2016.	31
Figure 4.10 PCM1 middle temperatures (T4) on 5th ,7th ,11th Aug 2016.	32
Figure 4.11 PCM1 middle temperatures (T7) on 5th ,7th ,11th Aug 2016.	33
Figure 4.12 Inlet water temperature (Tin) for PCM1 on 5th ,7th ,11th Aug 2016. ..	34
Figure 4.13 Ambient temperature (Tamb) for PCM1 on 5th ,7th ,11th Aug 2016. .	34
Figure 4.14 Heat gained for PCM1 on 5th ,7th ,11th Aug 2016.	35
Figure 4.15 Water temperature difference of inner tube for PCM1 on 5th ,7th ,11th Aug 2016.	36
Figure 4.16 : Raising of temperature for middle sensor (T4) for PCM1 on 5th ,7th ,11th Aug 2016.	37

Figure 4.17: Raising percentage of temperature for middle sensor (T4) for PCM1 on 5 th , 7 th , 11 th 5 th Aug 2016.	38
Figure 4.18 PCM1 temperatures for flow rate of 200 lph on 26 th and 27 th Jan 2017.	39
Figure 4.19 PCM1 temperatures for flow rate of 300 lph on 28 th , 29 th Jan 2017.	39
Figure 4.20 PCM1 temperatures for flow rate of 500 lph on 30 th and 31 th Jan 2017.	40
Figure 4.21 PCM1 temperatures (T3, T4, T5) for flow rate of 200 lph on 26 th and 27 th Jan 2017.	41
Figure 4.22 PCM1 temperatures (T6, T7, T8) for flow rate of 200 lph on 26 th and 27 th Jan 2017.	41
Figure 4.23 PCM1 middle temperatures (T4) of 200 lph on 26 th , 27 th , 28 th , 29 th , 30 th and 31 th Jan 2017.	42
Figure 4.24 PCM1 middle temperatures (T7) of 200 lph on 26 th , 27 th , 28 th , 29 th , 30 th and 31 th Jan 2017.	43
Figure 4.25 Inlet water temperature (T _{in}) for PCM1 on 26 th , 27 th , 28 th , 29 th , 30 th and 31 th Jan 2017.	44
Figure 4.26 Ambient temperature (T _{amb}) for PCM1 on 26 th , 27 th , 28 th , 29 th , 30 th and 31 th Jan 2017.	44
Figure 4.27 Ambient temperature (T _{amb}) for PCM1 on 26 th , 27 th , 28 th , 29 th , 30 th and 31 th Jan 2017.	45
Figure 4.28 Heat gained for PCM1 on 26 th , 27 th , 28 th , 29 th , 30 th and 31 th Jan 2017.	46
Figure 4.29 Water temperature difference of inner tube for PCM1 on 26 th , 27 th , 28 th , 29 th , 30 th and 31 th Jan 2017.	46
Figure 4.30 Raising of temperature for middle sensor (T4) for PCM1 on 26 th , 27 th , 28 th , 29 th , 30 th and 31 th Jan 2017.	47
Figure 4.31 Raising percent of temperature for middle sensor (T4) for PCM1 on 26 th , 27 th , 28 th , 29 th , 30 th and 31 th Jan 2017.	48
Figure 4.32 PCM2 temperatures for flow rate of 200 lph on 16 th Aug 2016.	49
Figure 4.33 PCM2 temperatures for flow rate of 300 lph on 15 th Aug 2016.	49
Figure 4.34 PCM2 temperatures for flow rate of 500 lph on 14 th Aug 2016.	50
Figure 4.35 PCM2 temperatures (T3, T4, T5) for flow rate of 200 lph on 16 th Aug - 2016.	51
Figure 4.36 PCM2 temperatures (T6, T7, T8) for flow rate of 200 lph 16 th Aug 2016.	51
Figure 4.37 PCM2 middle temperatures (T4) of 200 lph on 16 th Aug-2016.	52
Figure 4.38 PCM2 middle temperatures (T7) of 200 lph on 16 th Aug-2016.	53
Figure 4.39 Inlet water temperature (T _{in}) for PCM2 on 14 th , 15 th , 16 th Aug -2016.	54
Figure 4.40 Ambient temperature (T _{amb}) for PCM2 on 14 th , 15 th , 16 th Aug 2016.	54
Figure 4.41 Heat gained for PCM2 on 14 th , 15 th , 16 th Aug 2016.	55
Figure 4.42 Inlet water temperature difference of inner tube for PCM2 on 14 th , 15 th , 16 th Aug 2016.	56
Figure 4.43: Raising of temperature for middle sensor (T4) for PCM1 on 14 th , 15 th , 16 th Aug 2016.	57
Figure 4.44 Raising percentage of temperature for middle sensor (T4) for PCM2 on 14 th , 15 th , 16 th Aug 2016.	58
Figure 4.45 PCM2 temperatures for flow rate of 200 lph on 19 th , 20 th Dec 2016.	59
Figure 4.46 PCM2 temperatures for flow rate of 300 lph on 21 th , 22 th Dec 2016.	59
Figure 4.47 PCM2 temperatures for flow rate of 500 lph on 27 th , 28 th Dec 2016.	60

Figure 4.48 PCM2 temperatures (T3, T4, T5) for flow rate of 200 lph on 19 th and 20 th Dec 2016	61
Figure 4.49: PCM2 temperatures (T6, T7, T8) for flow rate of 200 lph 19 th and 20 th Dec 2016	61
Figure 4.50: PCM2 middle temperatures (T4) of 200 lph on 19 th , 20 th , 21 th , 22 th , 27 th and 28 th Dec 2016.	62
Figure 4.51 Inlet water temperature (T _{in}) for PCM2 on 19 th , 20 th , 21 th , 22 th , 27 th and 28 th Dec 2016.....	63
Figure 4.52 Ambient temperature (T _{amb}) for PCM2 on 19 th , 20 th , 21 th , 22 th , 27 th and 28 th Dec 2016.....	63
Figure 4.53 Ambient temperature (T _{amb}) for PCM2 on 19 th , 20 th , 21 th , 22 th , 27 th and 28 th Dec 2016.....	64
4.54 Heat gained for PCM2 on 19 th , 20 th , 21 th , 22 th , 27 th and 28 th Dec 2016.....	65
Figure 4.55 Inlet water temperature difference of inner tube for PCM2 on 19 th , 20 th , 21 th , 22 th , 27 th and 28 th Dec 2016.....	65
Figure 4.56: Raising of temperature for middle sensor (T4) for PCM2 on 19 th , 20 th Dec 2016.....	66
Figure 4.57 Raising percentage of temperature for middle sensor (T4) for PCM2 on 19 th , 20 th Dec 2016	67
Figure 4.58 Latent Heat of PCM2.....	68
Figure 4.59 Compares on between the present work and (Yongcai Li) work [39]....	69

Abstract

Thermal characteristics of phase change material used as thermal storage system by using solar energy

Ameer AL-Mamoori

Master. Department of Aeronautics and Mechanical Engineering

Supervisor: Assist. Prof. Dr. Munir Elfarra

April, 2017, 92 Pages

Abstract

In this study, the melting processes of PCM in a circular shell and rectangular tube heat exchanger by using solar thermal energy have been studied experimentally to evaluate thermal storage performance of PCM. All experimental were conducted outdoor at AL- Musayyib city-Babylon-Iraq. In this study two different types of Paraffin are tested; PCM1 (which is produced in Iraq) and PCM2 which is produced in Germany. The main experimental procedure in the present work is included using the solar collector type of evacuated tube for melting PCM in shell regime. Different volume flow rates of the water flow within the inner tube of the heat exchanger namely (200, 300, and 500 lph) were used for each season from August 2016 to January 2017. The experimental results indicated that inlet temperature of the inner tube and ambient temperature has significant effects on the melting point compared with the volume flow rates. Studying PCM temperature distribution, it is exposed that a melting temperatures of the PCM in summer season needed time of (3-4) hours only, while it needed more time; about (14-16) hours in winter season. Increasing the ambient temperature and the solar radiation reduces the melting time for both PCM types. Increasing water temperature difference of inner tube increased the heat gained for PCM. The present experimental results compared with the available previous studied and give a good agreement.

Key words: solar radiation, thermal, storage energy, paraffin, PCM, shell and tube, heat exchanger

Özet

güneş enerjisi kullanılarak termal depolama sistemi olarak kullanılan faz değişim malzemesinin termal karakteristikle

Yüksek Lisans Tezi, Makine Mühendisliği Anabilim Dalı

Tez Danışmanı: Yrd. Doç. Dr. Munir El-Farra

2017, 92 sayfa

Özet

Bu araştırmada, güneş ısı enerjisi kullanılarak dairesel kabuk ve üçgen tüp şeklindeki ısı eşanjöründe PCM erime süreçleri; PCM'nin ısı depolama performansını değerlendirmek için sayısal olarak ve deneysel olarak araştırılmıştır. Tüm deneyler dış mekanda Irak'ın Babil şehrinde AL-Musayyib'de yapılmıştır. (Irak'ta üretilen) PCM1 ve Almanya'da üretilen olmak üzere bu çalışmada farklı türlerde iki parafin test edilmiştir. Şu anki çalışmada ana deney işlemi, kabuk rejiminde PCM eritimi için boşaltılmış tüpteki güneş kolektörü kullanılarak yapılır. 2016 Ağustos ayından 2015 Ocak ayına kadar her sezon için ısı eşanjörü içerisindeki iç tüpteki suyun farklı hacimli akış oranları şu şekilde (200, 300 ve 500 lph) kullanılmıştır. Deney sonuçları iç tüp ve ortam sıcaklığı giriş sıcaklığının hacim akış oranlarına göre erime noktasında önemli etkileri olduğunu göstermiştir. PCM sıcaklık dağılımı incelendiğinde PCM 'nin yaz mevsiminde erime sıcaklıkları için gerekli zamanın sadece (3-4) ay, kış sezonunda ise yaz sezonuna göre daha fazla zaman gerektiği bunun da yaklaşık (14-16) saat olduğunu göstermiştir. Ortam sıcaklığı ve güneş radyasyonu artımı her iki PCM türlerini erime süresini azaltmaktadır. İç tüpün sıcaklık derecesi farklılığının atması PCM için elde edilen ısıyı artırmıştır. Bu araştırmanın deney ve sayısal sonuçları ve PCM ile ilgili önceki elde edilen araştırma sonuçları karşılaştırılmış.

Anahtar kelimeler: Güneş radyasyonu, ısı, depolanmış enerji, parafin, PCM, kabuk ve tüp, ısı eşanjörü

List of symbols

Symbol	Definition	Units
C_p	Specific heat	J/kg.k
C_{ps}	Average specific heat	J/kg.k
C_{pL}	Average specific heat	
d	Diameter of the tube	m
V_o	Volume flow rate in inner tube	lpm
Q_o	Volume flow rate in annular region	lpm
F	Collector efficiency factor	
g	Acceleration due to gravity	m/s^2
h	Heat transfer coefficient	$W/m^2.k$
I	Incident solar radiation	W/m^2
I_{tur}	Turbulence intensity	
k	Thermal conductivity, turbulent kinematic energy per unit mass	$W/m.k, m^2/s^2$
LCT	Local time	hr
L_t	Tube length	m
l	Length	m
m	Constant	Kg
\dot{m}	Mass flow rate	Kg
\dot{m}_c	Mass flow rate of cold fluid in (inner tube)	Kg/s
C_μ	Turbulence model constant	
P	Pressure	$N/m^2(Pa)$
Q	Heat transfer rate	W
Q_o	Total quantity of heat stored in PCM	kJ
Q_u	Useful energy gained from collector	J

q_L	Heat loss	J
r	Radius	m
S	Absorbed solar radiation	W/m^2
T	Temperature	$^{\circ}C$
T_i	Inlet fluid	$^{\circ}C$
T_o	Out fluid	$^{\circ}C$
T_f	Final temperature	$^{\circ}C$
T_m	Melting temperature	$^{\circ}C$
T_1	Initial temperature	$^{\circ}C$
T_{1-8}	Thermocouples type (K)	$^{\circ}C$
t	Time	s
Δh_m	Fusion heat per unit mass	(J/kg)
h	Convection coefficient	$W\ m^{-2}\ K^{-1}$
V	Velocity	m/s
W	Weight	kg

Greek symbols

α	Solar altitude, Thermal diffusivity	degree, m^2/s
β	Tilt angle	degree
η_{th}	Efficiency of collector	%
ϕ	Coefficient for the TFM without surface coefficient for heat flux	
μ	Dynamic viscosity	Kg/m.s
ν	Kinematic viscosity	m^2/s
ρ	Density	kg/m^3
θ	,Incident angle	degree
ΔT	Temperature difference	$^{\circ}C$

Subscripts

a	Air, ambient, aperture
exp	Experimental
h	Hot in annular region,
i	Inlet, inner, inside, tensor symbol
max	Maximum
min	Minimum
th	Theoretical

Abbreviations

ASHRAE	American Society of Heating, Refrigeration and Air Conditioning Engineers
DSM	Demand Side Management
HTF	Heat transfer fluid
SHPH	Solar heat pump heating system
VTSC	Vacuum tubes solar collector
RANS	Reynolds-Averaged Navier-Stokes
TES	Thermal energy storage
PCM	Phase Change Material
SHS	Sensible heat storage
LHTES	Latent heat thermal energy storage than sensible energy storage

Chapter one

Introduction

1.1 Background

Regrettably the global traditional fuels in reserves are running out while the world energy consumption is mounting very rapid. Whole scientists agreed that Renewable energies are one of the better solutions for energy ready in many parts of the world. Renewable energy sources such as wind energy, solar energy and tidal energy are described by their intermittent nature, as they not obtainable all the time. This sporadic problem can be disbanded by energy storage. Energy storage component improves the energy efficiency of systems by decreasing the mismatch between demand and supply. For this purpose, phase-change materials are particularly attractive since they supply a high energy at constant temperature and storage density that corresponds to the phase transference temperature of the material.

1.2 Thermal energy storage

Thermal energy storage (TES) is recognized as the temporary holding of thermal energy in the form of cold or hot substances for later utilization [1]. Energy request change on seasonal, weekly and daily, bases. These request can be matched with the help systems that a labor synergistically, and the agree with the storage of energy by heating ,cooling ,melting, vaporizing or solidifying a material and the thermal energy be obtainable when the process is reversed. A considerable technology in systems included renewable energies as well as other energy resources as it can make their process more efficient, particularly by bridging the interval between intervals when energy is harvested and intervals when it is necessary. That is beneficial for balancing between the equipping and request of energy. Thermal Energy Storage is foundation to overcome the mismatches between the equipping and consumption of energy or primary energy source divergence. Such as patrol variations of solar energy. Phase Change Material (PCM) used for Latent Heat Storage has received senior attention attributed to its isothermal nature and density high storage and of heat storage and release. There are many type of PCM. This

makes them catchy in applications such as; heat utilization, and water heating, waste and space air conditioning, and cooling and thermal oversight applications [2]. The main types of are sensible and latent. Sensible systems store energy by variable the temperature of the storage medium, [3, 4].

1.3 Classification of Phase Transition to PCM

The physical states involved in the phase transition to PCM can be classified in four categories regarding:

1. Solid-liquid
2. Solid-gas
3. Liquid-gas
4. Solid- Solid

The transitions in close gas phase are not workable because of the large volumes or high pressures required to store the materials, while solid-solid PCMs have typically a very slow phase change and lower heat of transition. Hence solid-liquid PCMs are the most appropriate technology for storing thermal energy in buildings. Solid-liquid phase change materials as shown Fig.1.1.

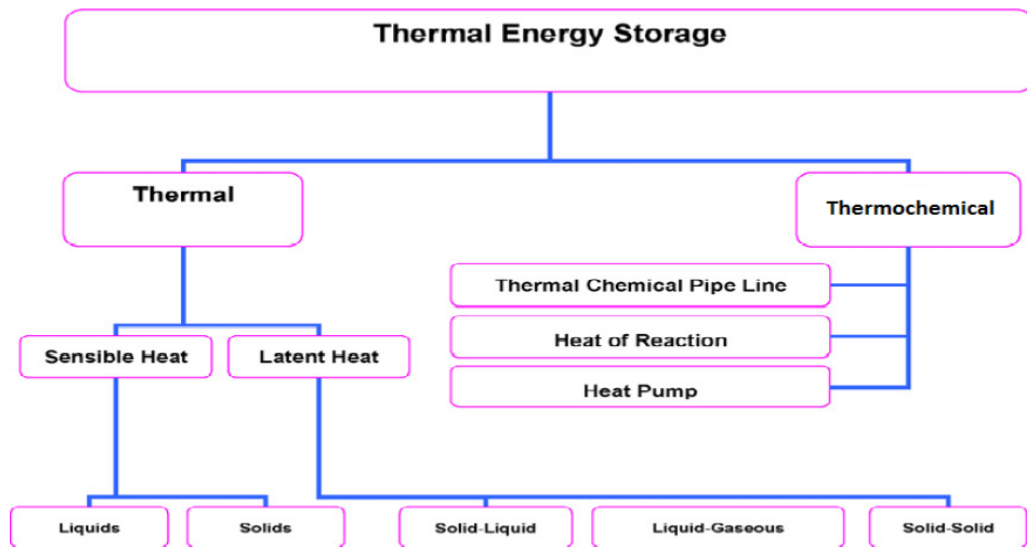


Figure 1.1 various types of thermal of solar energy[5].

1.3.1 Sensible heat storage

In sensible heat storage (SHS), thermal energy is stored by hike the temperature of a material, practically a solid or liquid. The system uses the heat amplitude and the alteration in temperature of the material during the operation of charging and discharging. The amount of heat stored depends on the specific heat of the medium, the temperature alteration and the amount of storage material. Fig.1.2 shows, heat convey to the storage medium leads to a temperature boost of the storage medium. A sensor can disclose this temperature boost and the heat stored is thus called sensible heat.

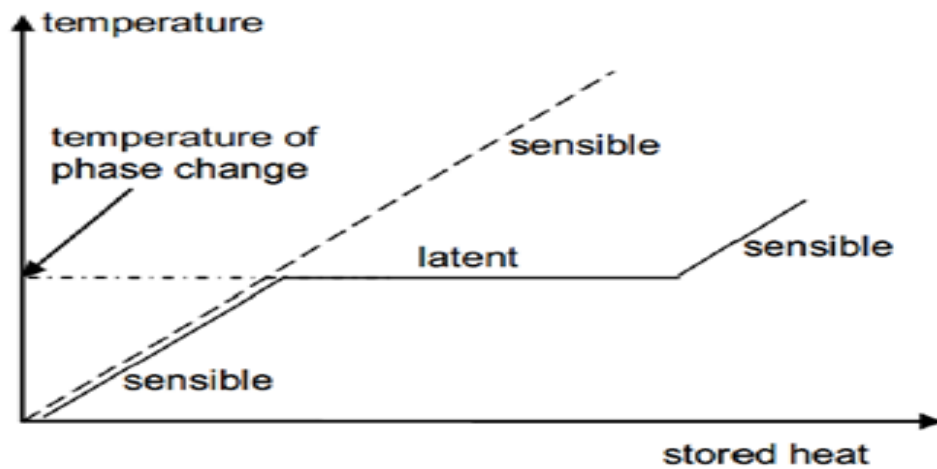


Figure 1.2 Heat storage as latent heat for the case of solid-liquid phase change.

1.3.2 Latent heat of solid – liquid phase change.

There are diverse choices of energy storage with solid – liquid phase alteration with featured advantages and disadvantages. As compared to sensible heat storage, the phase change by melting and solidification can store large amounts of heat or cold, if a suitable material is selected. Melting is feature by a small volume alteration, commonly less than 10%. If a container can fit the phase with the larger volume, commonly the liquid, the pressure is not changed significantly and consequently melting and solidification of the storage material proceed at a stationary temperature. Upon melting, while heat is convey to the storage material, the material still keeps its temperature stationary at the melting temperature, also called phase change temperature [6]. (Fig. 1.2).

1.4 Desired characteristics in a PCM

1.4.1 Thermal properties

- Suitable phase change temperature (the value depends on the application).
- Large latent heat of fusion, to achieve high storage density.
- High thermal conductivity, to be able to absorb and release the heat in a short time.
- Reproducible phase change, also called cycling stability, to store the heat as many times as necessary.

1.4.2 Thermodynamic properties

1. Melting temperature in the desired operating temperature range.
2. High latent heat of fusion per unit volume.
3. High specific heat, high density and high thermal conductivity.
4. Small volume changes on phase transformation and small vapor pressure at operation temperatures to reduce the containment problem.
5. Congruent melting [7,8].

1.5 Phase changing materials (PCM).

Phase change materials (PCM) are thermal store materials, and are used to control the temperature fluctuations in various applications, such as buildings. The privacy it has is the ability to store latent heat by changing their physical condition. During the past 20 years, it has been marketed several forms of the largest phase material encapsulated for solar applications negative and positive change, including the achievement of immediate gains. However, most of the encapsulated products business area is insufficient to provide heat to the building after it melted PCM of solar collectors directly. [9,10].

1.6 Objectives

This work is to evaluate the thermal characteristics of Phase change materials used for providing thermal energy experimentally under outdoor test for Iraq climate conditions.

Chapter Two

Literature Review

2.1 Introduction

Socaciu, L.G., (2012) [11]. Systems of thermal energy storage (TES) supply varied alternatives for efficient energy conservation and use. Phase change material (PCM) for TES is material providing thermal arranging at specific phase change temperatures by emitting and absorbing the medium heat. Generally the TES and specifically PCM, have been a major subject in research for the last 30 years. During the heating process, PCM absorb energy and phase change happen and release energy to the ambience in the phase change range during process of reverse cooling. With a certain temperature, latent thermal energy of PCM change its state. PCM for TES is generally liquid-solid phase change material, thus they need encapsulation. TES systems that using PCM as a storage medium, offering advantages such as small unit size, high TES capacity and isothermal behavior during discharging and charging when compared to the sensible TES.

Al-Abidi, *et al.*, (2012) [12]. TES is very important to enucleate the contradiction between energy demand and energy supply and to upgrade the energy efficiency of solar energy system. High storage capacity per unit mass/volume at approximately constant temperatures led to more benefit from Latent heat thermal energy storage than sensible energy storage. It is expected that the design of LHTES will reduce the volume and the cost of networks and air conditioning systems,

2.2 Thermal Energy Storage (TES) with Phase Change Material (PCM)

Peng, *et al.*, (2004), [13]. was investigated low melt temperature paraffin as a phase change material (PCM) and describing of a group of thermal energy storage (TES) composites that combine TES and structural functionality was done. A thermoplastic SEBS/paraffin and three different epoxy systems system with different glass transition temperatures were studied. Epoxy matrices was used to encapsulate Paraffin particles. The thermal conductivity, particle size distribution, thermal diffusivity, contact resistance, and latent heat of the composites were measured. It was noted that the thermal conductivity of the composites was increased when the phase change material was a liquid, partly because of best wetting of the epoxy by

the liquid paraffin and because volume expansion of the paraffin liquid in the composite. The interaction between components of paraffin/epoxy, provide appropriate thermal and mechanical performance. The thermoplastic SEBS/paraffin system display excellent mechanical performance and thermal.

Kenisarin and Mahkamov, (2007), [14]. were focused on various PCMs thermal properties and its assessment on heat storage design configurations facilities and methods of heat transfer enhancement that were used as a part of solar active and passive space heating systems, solar cooking and greenhouses. The analysis of data published in the open previous literature leaded to the following conclusions. Differential thermal analysis and differential scanning calorimetric methods were the main methods used in studying the thermal properties of PCM and considerably differ from strict thermo-physical methods.

Qi, *et al.*, (2008), [15]. Were studied seasonal latent heat thermal storage (SLHTS -SHPH) with a solar heat pump heating system as shown in Fig.2.1. A mathematical model was build up for the system and simulation to the operating performances of the system were done. The simulation showed that the solar energy can be seasonally stored and can be used in the winter. It showed that the temperature of the PCM in a storage tank could be maintained near its melting point and was lowest than that of water in a central solar heating system. Hence, the SHPH-SLHTS system, energy losses from the storage tank to ambient reduced and the efficiency of solar collectors was increased. The storage volume of a SHPH-SLHTS system was smallest than central solar heating system with seasonal storage using water.

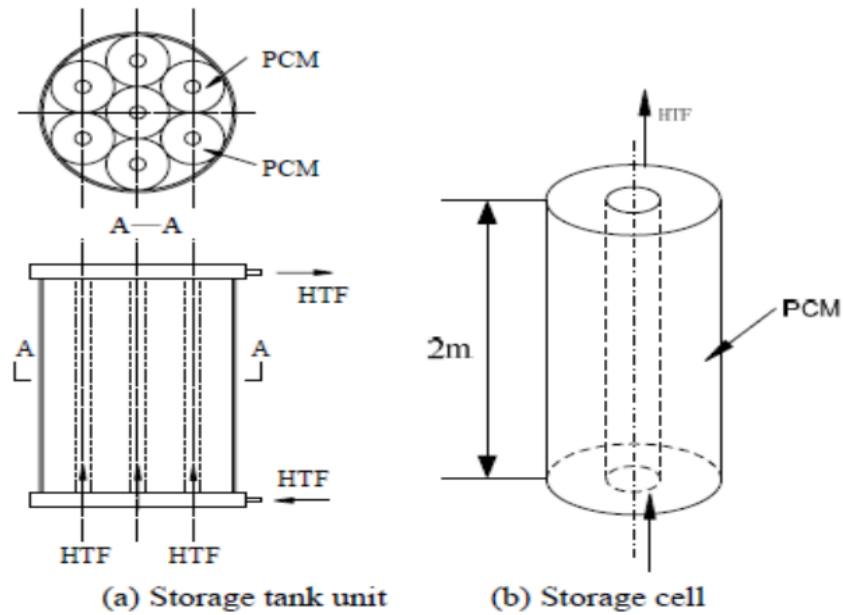


Figure 2.1 Schematic of PCM storage tank unit and storage cell, [15].

Qureshi, et al., (2008), [16]. presented ideas for two sides of Demand Side Management (DSM) methods were performed for residential loads. Electrical utilities was used to modify network loading and also to conserve energy during shortages. Application of price was examined, based on demand side management in built environment using PCM like Paraffin RT20. Two advantages were delivered from price based DSM:

- Reduced cost of electricity consumption for consumer,
- Shifting price responsive peak load during period of high electricity claim for the distribution network.

The PCM provided energy efficiency gains and thus saving energy cost.

Sharma and Chen, (2009),[17]. Summarized the investigation of the solar water heating system incorporating with Phase Change Materials as shown in Fig. 2.2. Suitable PCM became specified easily and provided malty designs for solar water heating systems.

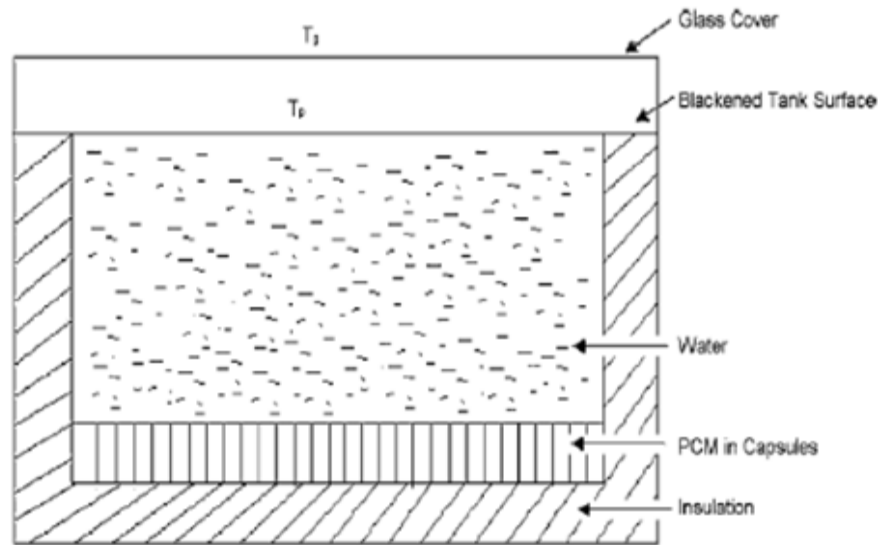


Figure 2.2 Solar water heater, Sharma and Chen, [17].

Bhatt, et al., (2010),[18].Reviewed more than sixty phase changing materials including inorganic, organic, eutectic and ionic liquids with considering to the capacity of their thermal energy storage. This review was based on properties like heat of fusion, melting temperature, density and thermal conductivity. After a studied of their properties, prepared a list of nine favorable phase changing materials, suitable for thermal energy storage.

Quanying, et al.,(2010),[19].Studied the thermal properties and prepared experimentally the shape-stabilized PCMs. Mixtures of liquid paraffin and n-Octadecane or 46#, 48# paraffin, and n-mixtures of n-Heptad cane and 48#paraffin were used in the experiments. Phase change temperatures that used in this experiment are between 20°C and 30 °C, and its latent heat are high. The proportions of 50, 60%, 70%, 80% and 90% with paraffin mixtures mixed polyethylene of high-density. Prepared shape-stabilized PCM was the ideal thermal storage material for wall using. The phase change latent heat proportion directly with the paraffin mixture mass content. The appropriate percentage for mass content of paraffin mixtures was seventy percent in the shape-stabilized PCM.

Zhang, et al., (2011), [20]. Investigated experimentally a shell and tube LTES system built for hot water supply and room heating as shown in Fig. 2.3. Composite of paraffin/EG and only paraffin were used as the heat storage material. The EG/paraffin composite PCM improved the heat storage/retrieval rates of the LTES system. The LTES system with paraffin/EG composite reduced the heat storage duration and the retrieval duration in amount 44% and 69% respectively as it compared with the system using pure paraffin. The LTES system filled with paraffin/EG composite increased the outlet water temperature more than that with paraffin and maintained at a higher level for a longer term. EG with 7% mass fraction of Paraffin/EG composite PCM was enhanced paraffin heat transfer.

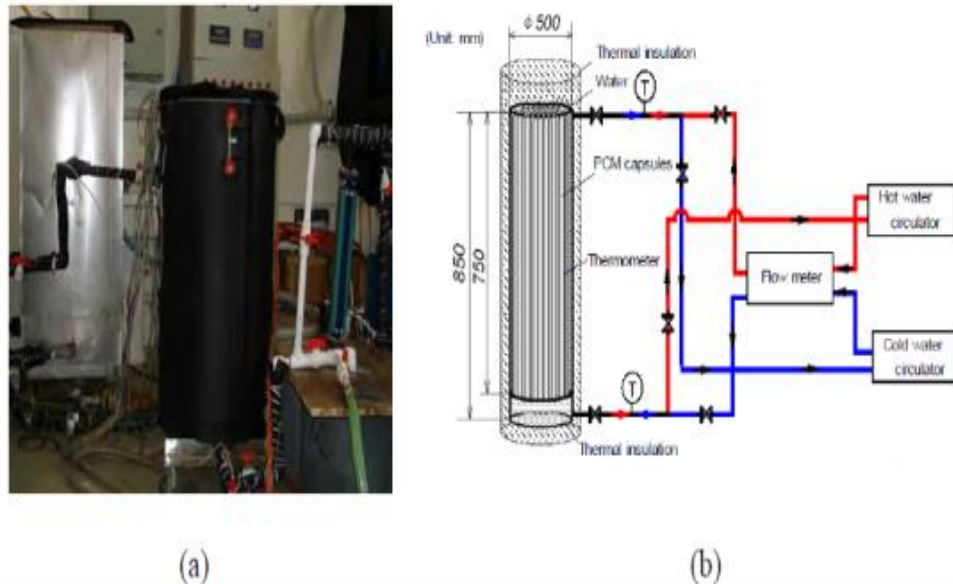


Figure 2.3 Experimental setup (a) Photographic view (b) Schematic of LTES system, [20].

Oró, et al., (2012), [21]. Was used pilot plant as was shown in Fig. 2.4 to implement and tested a thermal energy storage (TES) system through using different phase change materials (PCM) that was used for solar cooling and refrigeration applications. Pilot plant consist from cooling system, heating system, and different storage tanks. Synthetic thermal oil (working at range of temperature from 100 °C to 400 °C) was used as heat transfer fluid in the pilot plant. Two types of PCM were

selected, d-mannitol has 167 °C phase change temperature and hydroquinone which has 172.2 °C melting temperature. Experiments for solar cooling applications were done with different heat transfer fluid (HTF) temperatures and mass flow rates. Calculation to the effective heat transfer coefficient between the HTF and storage material was done. The effective heat transfer coefficient was 0.86 and 0.88 for hydroquinone and d-mannitol PCM respectively. During the charging and the discharging process with the same boundary conditions, the enhancement in energy stored was 30% and 20% for d-mannitol and hydroquinone, in spite of 10 and 16% latent heat enhancement respectively.

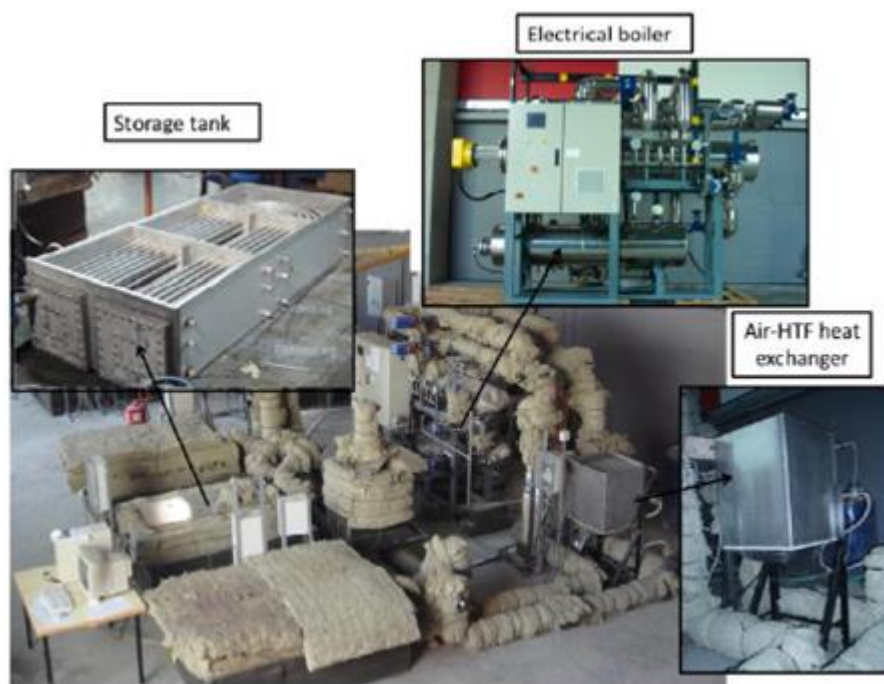


Figure 2.4 High temperature pilot plant, [21]

Warzoha, et al., (2012),[22]. Investigated experimentally the effect of infiltration method on paraffin PCM saturation rate within graphite foams. The foam was infiltrated by two methods: a vacuum infiltration technique and a simple submersion technique. Paraffin when infiltrated graphite foams, became effective for energy storage, but the foam was not easy saturated with paraffin. The influence of the infiltration method on the rate of paraffin saturation, yielding better results with the vacuum system.

Harikrishnan and Kalaiselvam, (2013),[23]. Presented nan fluid preparation, which consisted of TiO₂ nanoparticles as solid embedded into liquid of melting plasmatic acid. Then investigated the heat transfer and thermal characteristics of nano based PCM during release processes and energy storage. Sol-gel method was used to synthesized size of the TiO₂ nanoparticles and measured was done by using transmission electron microscope. Experimental test rig was used for analyzing the characteristics of melting and solidification of composite PCM during cooling and heating processes as was shown in Fig.2.5. Measurements were done by using differential scanning calorimetric to obtain the phase change temperature and latent heat of Nano fluid for melting and solidification process. The heat-transfer characteristics of plasmatic acid had enhanced when dispersed in it the nanoparticles, which led to accelerate the energy storage and with faster release rates as compared to pure plasmatic acid.

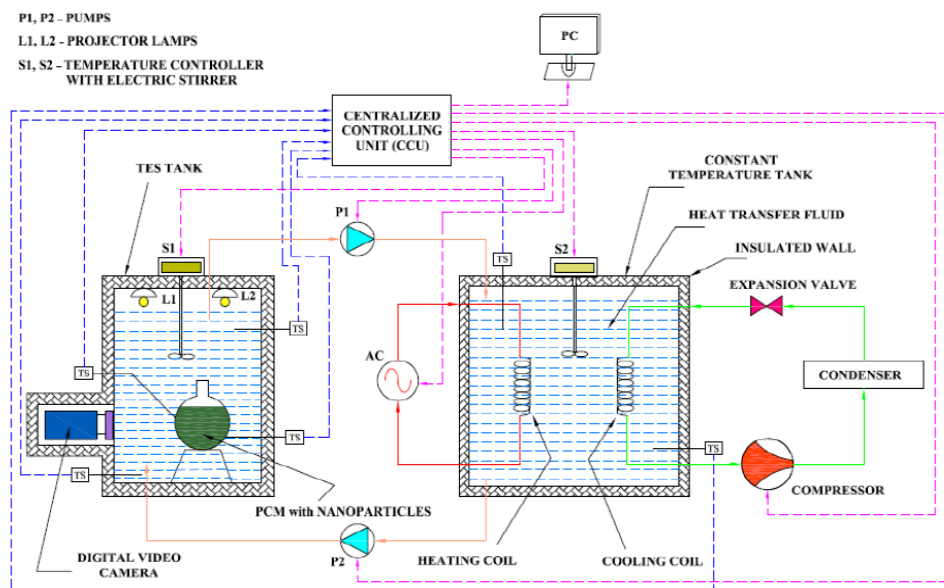
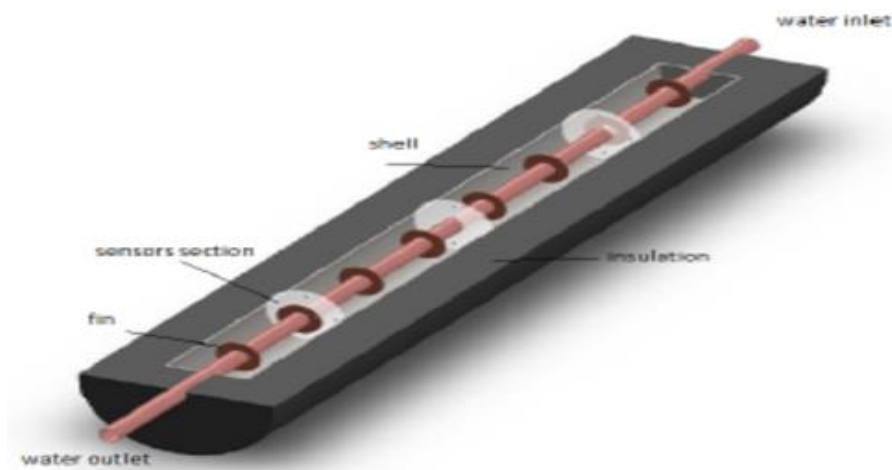


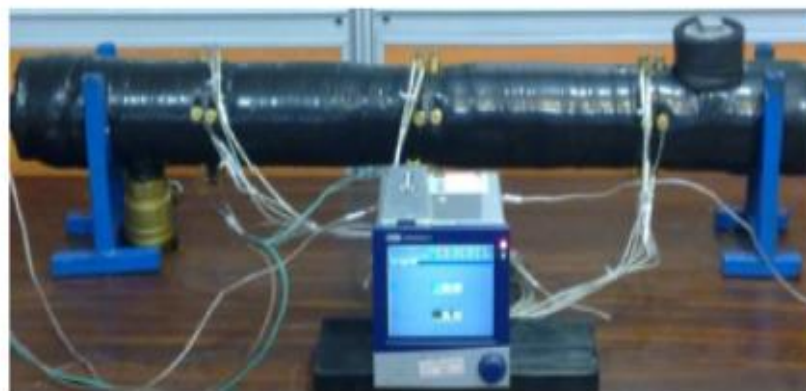
Figure 2.5 Experimental test rig for testing the phase change behavior of PCM, [23].

Chen, et al., (2014), [24]. reviewed the kinds of metal foam that were used in PCM and the effective thermal conductivity and convection heat transfer of the composite PCMs. Also reviewed the research methods that were used in the investigation of convective, conductive, and phase change heat transfer process in composite PCM.

Hosseini, et al., (2015), [25]. Investigated numerically and experimentally the effect of Stefan number and fins' height on effectiveness of shell and tube heat exchanger where PCM inside it as shown in Fig. 2.6. Solidification and melting time, mass fraction of liquid, melting and solidification front and different directions temperature distribution (longitudinal, radial and angular) are the criteria for heat exchangers' comparison. Melting and solidification fronts were studied for different sections of fin section, the shell, and mid-section, for different height fin during the processes of charging and discharging. These two parameters (Melting and solidification fronts) played important roles in the performance of heat exchanger. Increasing Stefan number and/ or fins' height led to reduces in the melting time. The solidification time effected than melting with higher fins.



(a)



(b)

Figure 2.6 (a) Section view of the heat exchanger and (b) real photo of heat exchanger, [25].

Kumar and Shukla, (2015), [26]. Have been studied the literatures of thermal energy storage unit with PCM and had chosen the best suitable PCM and material for the test bench design for the thermal energy storage unit. Multi types of storage unit were described but the assertion was given to thermal energy storage unit. Storage system of latent heat thermal energy, stores heat 5 to 14 times more than storage material of sensible heat thermal energy. The latent heat thermal energy storage was more economical and store much energy to supply continuously to the solar cavity receiver system of helical coil. For air conditioning purposes, materials that has melting temperature below 15°C was selected, while materials that had melting temperature above 90°C were used for absorption refrigeration system. All other materials that melt between 15°C and 90°C can be applied in heat load leveling applications and for solar heating. Efficient thermal energy storage unit was coupled with the selection of PCM and its compatibility with the containment where PCM encapsulated.

Sinaringati, *et al.*, (2016), [27]. Investigated experimentally the utilization of the paraffin and beeswax materials as a heat energy sources for infant incubator as and made comparison between them shown in Fig.2.7. The results showed that the phase change material can keep heat energy in the infant incubator room at temperature above 32°C for more than 8 hours. The beeswax performed better heat energy storage than paraffin and best performance when used beeswax as the PCM for infant incubator or any other practical application.

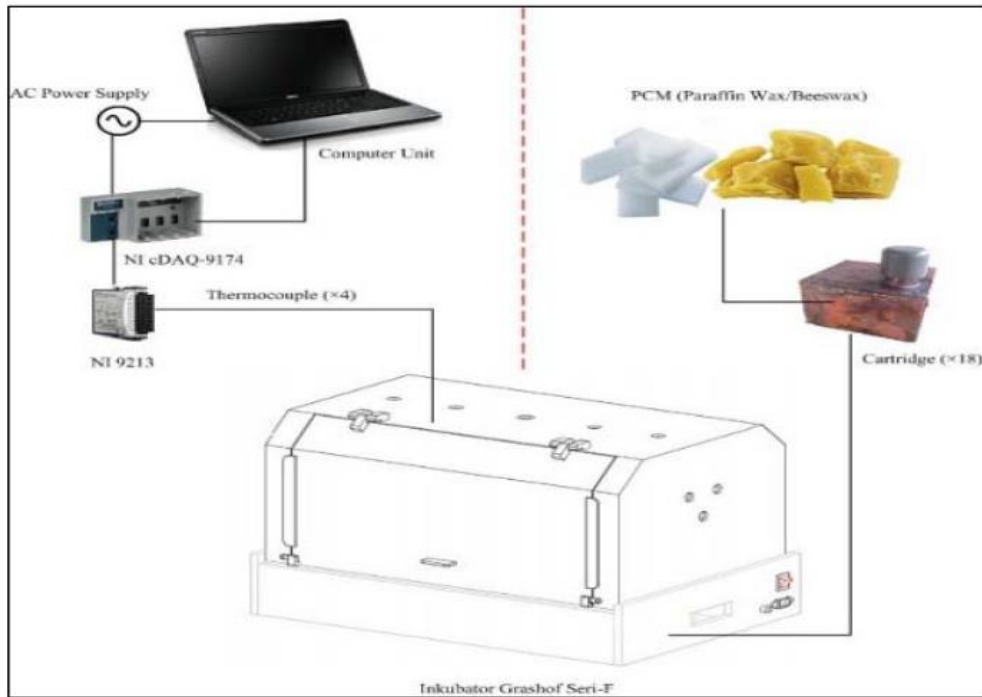


Figure 2.7 The experimental setup of utilization of paraffin and beeswax as heat energy storage on infant incubator, [27].

2.3 Summary of Previous Researches

This survey is showed the previous studies on thermal energy storage that used for the application of PCM and air conditioning systems in different parts of the air distribution network, air conditioning networks, microencapsulated slurries, chilled water network, heat rejection of the absorption cooling and thermal power. Recently, researchers are focused on study the heat transfer enhancement of the TES with PCM due to the PCM has low thermal conductivity, which led to a long period of charging and discharging process.

Chapter Three

Experimental work

An experimental study was carried out for investigation the effect of using solar energy on the thermal characteristics of two types of phase change materials (PCM) with variable climatic conditions, which include solar radiation wind speed and ambient temperature. Outdoor tests were carried out at Musayyib, Babylon-Iraq climatic conditions from August 2016 to Jun 2017 at the roof of a building elevation 7m from the ground floor at (Lat. 32.5 ° North and Long. 44.2 ° East) with tilt angle of 32.5°.

3.1 Experimental Setup

The Experimental rig includes vacuum tubes solar collector (VTSC) using with shell and tube heat exchanger is designed and fabricated in order to study the effect of different ambient conditions and collector water flow conditions on the thermal performance of PCM. The experimental rig shown in 3.1. A schematic diagram of the comprehensive experimental system in Fig 3.2. The location of the different temperatures measured ($T_1=T_{in}$, $T_2 =T_{out}$, $T_3... T_8$) are shown in the schematic of Figure 3.2.



3.1 Experimental Rig

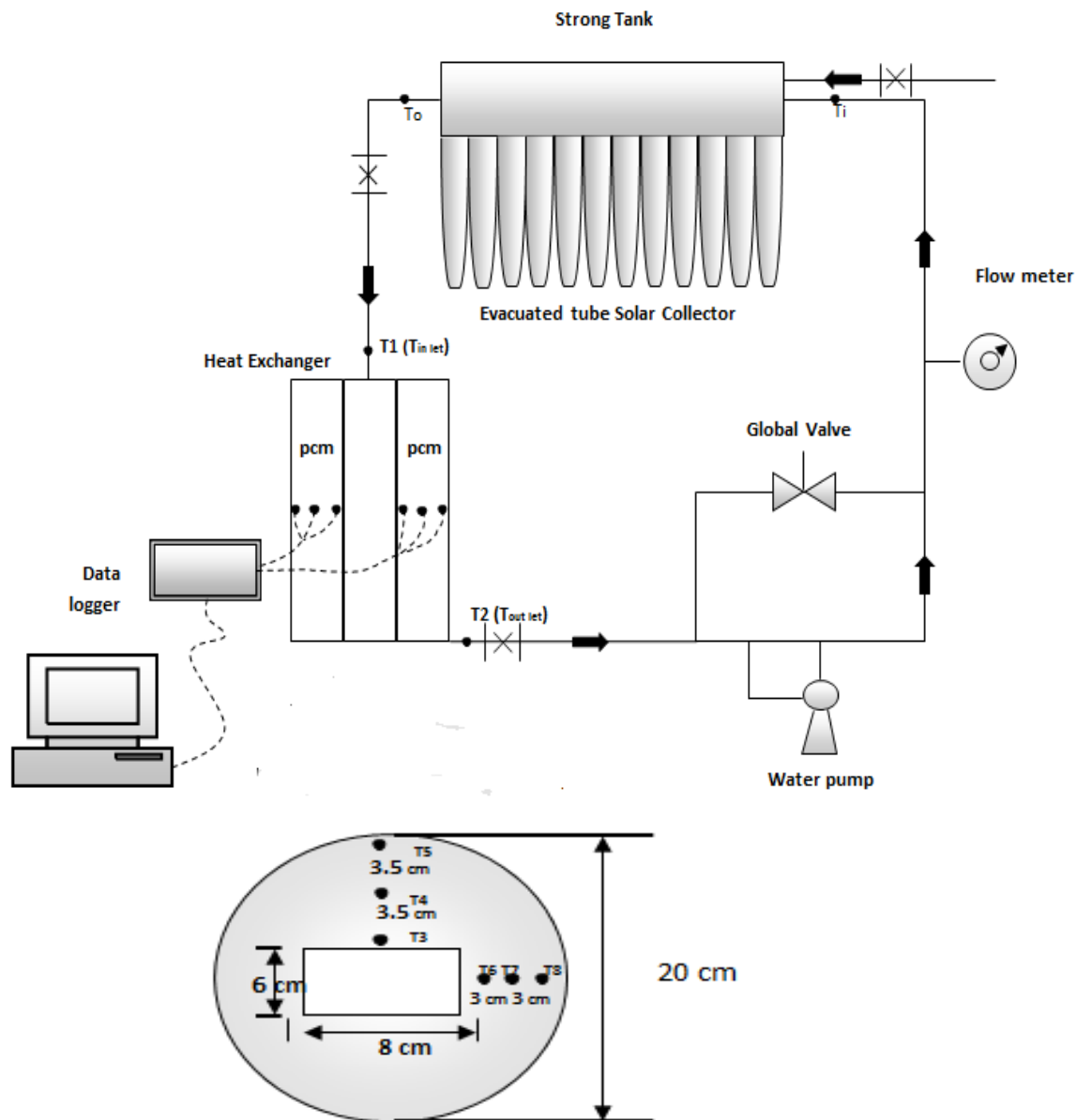


Figure 3.2. A schematic diagram of the comprehensive experimental system.

The experimental rig consists of the following items:

3.1.1 Solar Water collector

This collector is evacuated tube type consists of storage tank of 80 liter capacity and 12 evacuated tube as shown in the Fig.3.3.



Figure 3.3 Solar Water collector.

3.1.2 Shell and tube heat exchanger

Shell and tube heat exchanger was used in this work consists of rectangular tube with dimensions of (8cm x 6cm) had external longitudinal fins to improve heat transfer through the PCM, inside which the hot water that discharged from the solar collector is flow and the shell regime had a cylindrical shape with 60 cm long and 20 cm diameter which filled with PCM as shown in the Fig. 3.4.

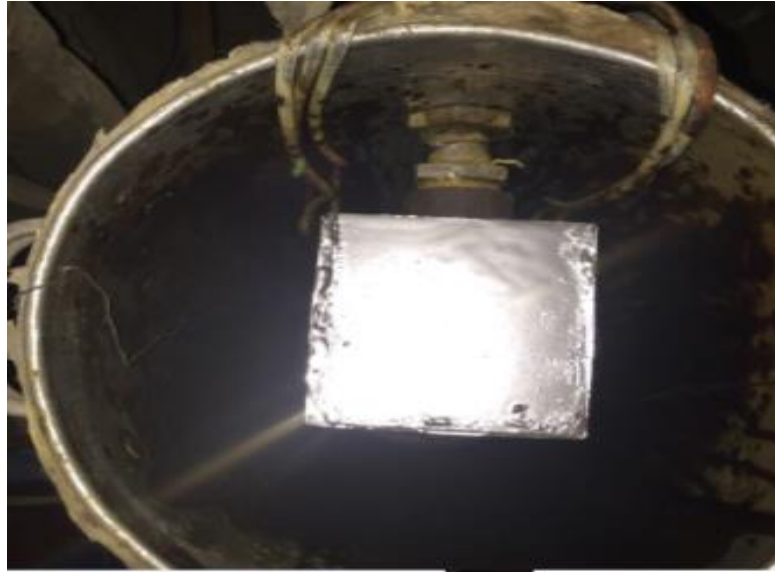


Figure 3.4 Heat Exchanger.

3.1.3 Water Pump

The water pumps used are electric AC water pumps to circulate water, which manufactured in china Pump Industrial Company. LTD. As shown in Fig 3.5. It has specifications of (0.37kW) power, (30m) maximum head, and(30lph)maximum discharge.



3.3 Water Pump.

3.1.4 Connecting pipes

Plastic pipes of (1/2 inch) are used to connect the parts of the setup system.

3.1.5 Insulations

Glass wool has a thickness of 15 mm had been used to insulate all system pipes and heat exchanger.

3.1.6 Valves

Global valves used for controlling the amount of water flow and Senior safety valves system used for preventing exposed to high-pressure upon the arrival of water at high temperatures.

3.1.7 Storage container

A container made of aluminum length 600 mm width 200mm, thickness of 1.5 mm where put inside the heat exchanger and the solid paraffin and bottom of the container, and there is a tube after Process Melt.as shown Fig 3.6 .



3.4 storage container

3.2 Phase Change Material

There are two types of PCM that are used in this work, the first type is black Iraqi origin Paraffin with amount of 12 kg and it is called PCM1. The physical properties of PCM1 are listed in Table 3.1. The other type is white German Origin Paraffin with amount of 12 kg and it is called PCM2. The physical properties of PCM2 are listed in Table 3.2. The shapes of PCM1 and PCM2 are shown as shown in the Fig. 3.7.

Table 3.1 Thermo physical properties of paraffin PCM2 [28, 29, 30, 31, 32, 33].

C ₂₂ H ₄₆ weight PCM2	12kg
Density	Solid/Liquid 912 ^S , 769 ^L kg/m ³
Melting Temperature	40.2 ± 0.5
Heat Capacities Solid/Liquid	2.4/2.0 kJ/kg·K ± 3 %
Thermal Conductivities	Solid/Liquid 0.21 /0.224 W/m·K
Heat of fusion	189 kJ/kg
Specific heat	2.1 kJ/kg .k
Viscosity	3.701Pa.s

Table 3.2 Thermo physical properties of paraffin PCM1 [28,29, 30, 31,32, 33].

C ₂₁ H ₄₄ Black PCM1	12kg
Density	Solid/Liquid 912 ^S , 769 ^L kg/m ³
Melting Temperature	44.0 ± 0.5
Heat Capacities Solid/Liquid	2.4/2.0 kJ/kg·K ± 3 %
Thermal Conductivities	Solid/Liquid 0.21 /0.224 W/m·K
Heat of fusion	189 kJ/kg
Specific heat	kJ/kg .k 2.1
Viscosity	3.588Pa.s



Figure 3.5 Paraffin Black Iraqi and Paraffin white German

3.3 Measurements and Instrumentation

The measurement devices that used in the this work are arrangement as following:

3.3.1 Temperature measurements thermocouples

Twelve standard thermocouples type (K) with 0.4 mm diameter and 1 m long are used in this work. These thermocouples are connected to Digital data logger type of 12 channels temperature recorder with SD card data logger model BTM-4208SD manufactured by Lutron company of Taiwan for reading and recording the values of temperature with an accuracy of ($\pm 4\%$). The temperature measurements range of (-50 to 999.9 °C) and resolution of 0.1 °C. A thermocouple is shown in Fig.3.8.

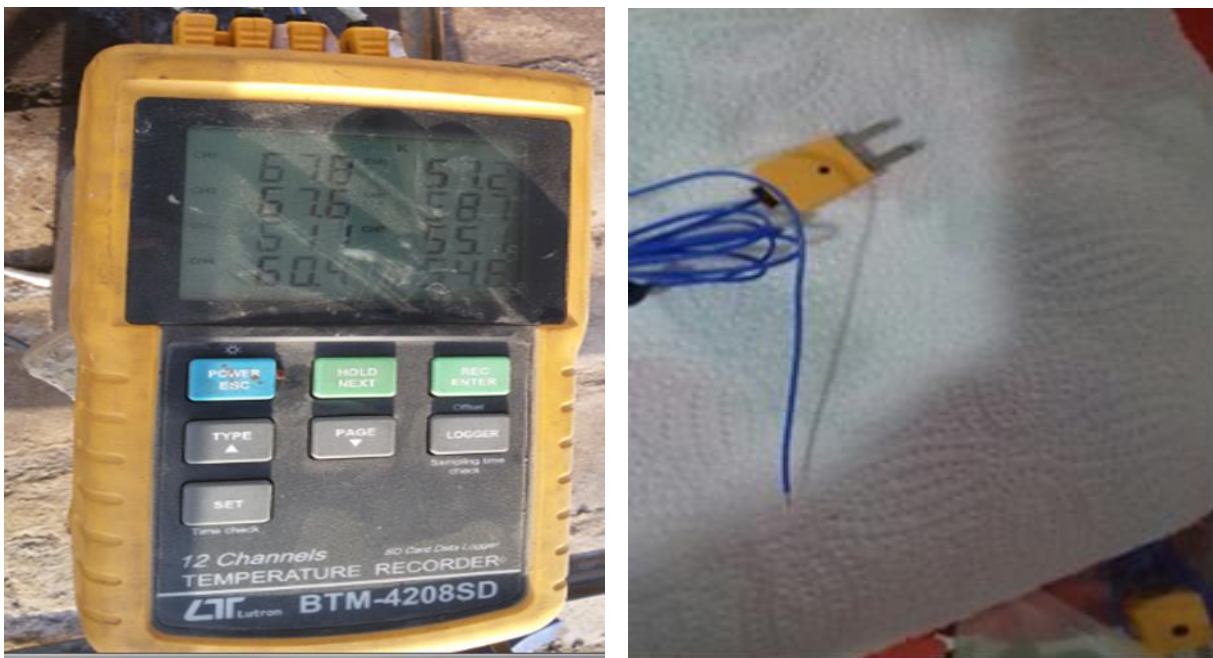


Figure 3.6 Temperature measurements thermocouples type (K).

3.3.2 Water Flow meter

Flow Meters is a device for measuring and controlling the quantity of water drainage outside of the pump to the centrifugal pumps of Solar collector heater tank discharge Flow Meters rate measurement of 100- 1500 L / h Water volumetric flow rate is measured using Nuritech flow meter instruments model (Z-3002) with an accuracy of ($\pm 4\%$) as shown in Fig.3.9.



Figure 3.7 Water Flow meter

3.3.3 Solar radiation measurements

Solar intensity was measured with a Kipp and Zonen class one Pyrometer model CMP22 which has a measuring range of up to 4000 W/m² (error < 5 W/m²). It was installed on the collector at tilt angle of 32.5 ° with the horizontal.

3.3.4 Wind speed measurements

The wind speed was measured using a Lutron multifunctional anemometer device model (ABH-4225) made in Taiwan, with an accuracy of (±3%). The measurement range of the anemometer is (0.4-30) m/s and resolution of 0.1 m/s .

3.4 Thermal Performance analysis

The value of instantaneous thermal efficiency η_{th} for the water solar collector has been calculated from the energy balance of the receiver which shown in the figure (3). The useful energy as heat gain (Q_u) transported to the receiver defined as [34].

$$Q_u = mc_p(T_o - T_i) \text{-----(1)}$$

Where: T_i and T_o represent the inlet fluid and exit fluid temperatures, respectively.

The instantaneous thermal efficiency of the water solar collector defined as the ratio of heat gain (Q_u) supplied to as, and the solar radiation (I) which is incident on the area of aperture [35,36].

$$\eta_{th} = \frac{mc_p(T_o - T_i)}{I A_a} \text{-----(2)}$$

Thermal energy is stored in the sensible heat storage (SHS), by increasing the temperature of the solids or liquids. SHS system employs the change in the temperature and the heat capacity of the material during of the charging and the discharging processes. The quantity of the heat storage depending on the medium specific heat, the quantity of storage material and the temperature change, sensible heat storage system of a PCM medium is specified[36]. as:

$$Q_s = mc_p(T_{in} - T_{out}) \text{-----(3)}$$

In the latent heat storage system the charging and the discharging phenomenon occur as soon as the storage material experiences phase change from solid to liquid, liquid to gaseous or solid to solid. The storage capacity for latent heat storage system with a PCM medium is specified as :

$$Q_u = mc_{ps}(T_m - T_1) + m \cdot \Delta hm + mc_{pL}(T_f - T_m) \text{-----(4)}$$

Where T_m is melting temperature ($^{\circ}\text{C}$), C_{ps} is the average specific heat between T_1 and T_m (kJ/kg K), Δhm is fusion heat per unit mass (J/kg) and C_{pL} is the average specific heat between T_m and T_f (J/kg K), T_1 is the initial temperature and T_f is the final temperature[37].

In the present analysis, it considers the transport and thermal properties of the water to be dependent on the temperature as:

$$\text{Density: } \rho = 0.00001 * T^3 - 0.0056 * T^2 + 0.0037 * T + 1000.3 \text{-----(5)}$$

$$\text{Specific heat: } C_p = -0.0000001 * T^3 + 0.00003 * T^2 - 0.0017 * T + 4.2084 \text{-----(6)}$$

$$\text{Thermal conductivity: } k = 0.00000002 * T^3 - 0.00001 * T^2 + 0.0023 * T + 0.5568 \text{-----(7)}$$

$$\text{Viscosity: } \mu = -0.000002 * T^3 + 0.0005 * T^2 - 0.0428 * T + 1.6944 \text{-----(8)}$$

3.4.1 The steps adopted before each experimental test are

1. Lift the cover of system which protects it from rain and dust.
2. Clean the glass cover of ETSC with cleaner fluid.

3. Connect all thermocouples to data loggers, then adjusted date and time recorder of data loggers. Data from all thermocouples were recorded every 30 minutes then checked.
4. Connect all pressure transducers to digital data loggers then checked.
5. Fill the storage tank with source water through the intake valve.
6. Close the intake valve after the water exit from ventilation pipe
7. Check all parts of the system to ensure there is no water leakage.
8. Ensure that all valves are open in the circulation path.
9. minute by LOGBOX data logger.
10. Adjust the global valve until the specified flow rate is reached.
11. Make sure to put paraffin material inside the container.

The experimental tests were carried out for melting PCM, experimental data was collected the summer and winter as shown in table 4.1.2016 with each test starting at 8:00 am and terminated at 17:00 pm. Eight different water circulating flow rates were employed through the system for experimental range. The experimental tests were implemented for different weather conditions which included partly cloudy, dusty sky, and clear sky.

Table 3.3 Data of Experiment Test

Material	Water flow rate lph	Date
PCM1 Simmer	200	5 AUG 2016
	300	7 AUG 2016
	500	11 AUG 2016
PCM1 Winter	200	26 and 27 Jan 2017
	300	28 and 29 Jan 2017
	500	30 and 31 Jan 2017
PCM2 Simmer	200	14 AUG 2016
	300	15 AUG 2016
	500	16 AUG 2016
PCM2 Winter	200	19 and 20 DEC 2016
	300	21 and 22 DEC 2016
	500	27 and 28 DEC 2016

Chapter Four

Results and Discussion

4.1 Introduction

In this section the results of the pilot study and discussion are presented. Particular focus will be on the main topic of the thesis.

4.2 Collector performance

Fig.4.1 displays the solar radiation power per square meter that falls on the present solar collector for selected clear days on August 2016. It is clear that the solar radiation increases from low values at morning to maximum values on noon then decreases to low values on afternoon. The comparison of the solar radiation measured data for two clear days shows the same behavior due to no cloud and dust in the sky. Fig. 4.2 illustrates the day hourly variation of the solar collector thermal efficiency on August 2016 for two tests days. It indicates that the thermal efficiency increases till 12:30 pm after that it is decreased. The operation curve for the tests on two clear days are shown in Figures 4.3 and 4.4. The thermal efficiency of the ETSC system is found by computing the instantaneous thermal efficiency for high values of incident solar radiation, water temperature in the collector and ambient temperatures. This wanted experimentally measured of the incident solar radiation onto ETSC under quasi-steady state conditions. That's occurs over the period from 11:00 am to 14:00 pm. The relationship between the thermal efficiency and $(T_i - T_a)/I$. The coefficients are obtained from the plots in Figures 4.3 and 4.4 is found as:

For 9 Aug. 2016

$$\eta_{th} = 0.3432 - 15.716 \left(\frac{T_i - T_a}{I} \right) \text{-----(5.1)}$$

For 11 Aug. 2016

$$\eta_{th} = 0.3309 - 4.8801 \left(\frac{T_i - T_a}{I} \right) \text{-----(5.2)}$$

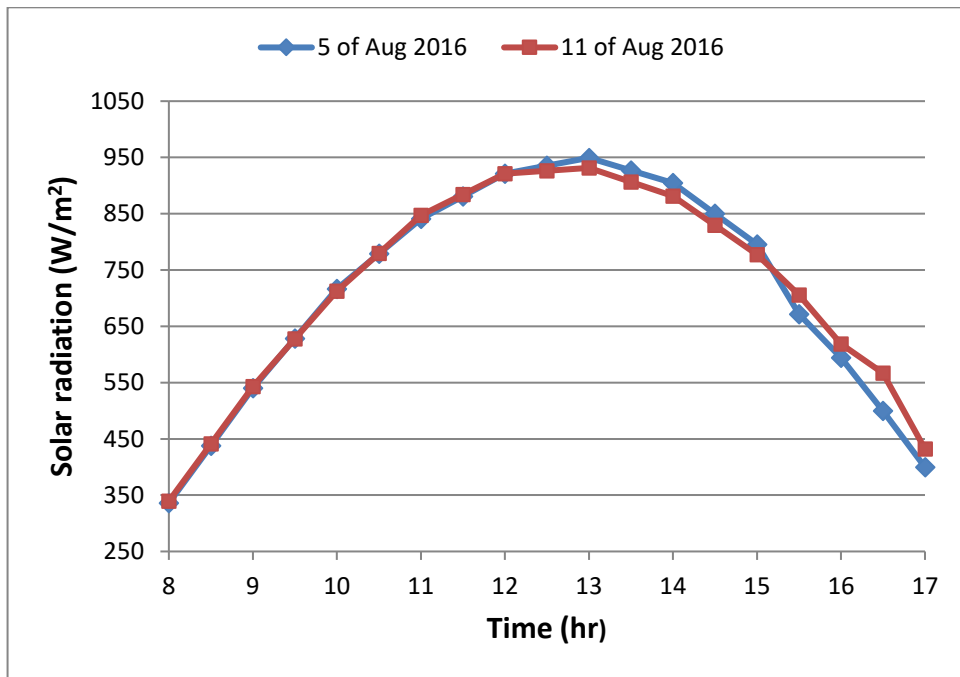


Figure 4.1 Solar radiation for flow rate of 200 and 500 lph.

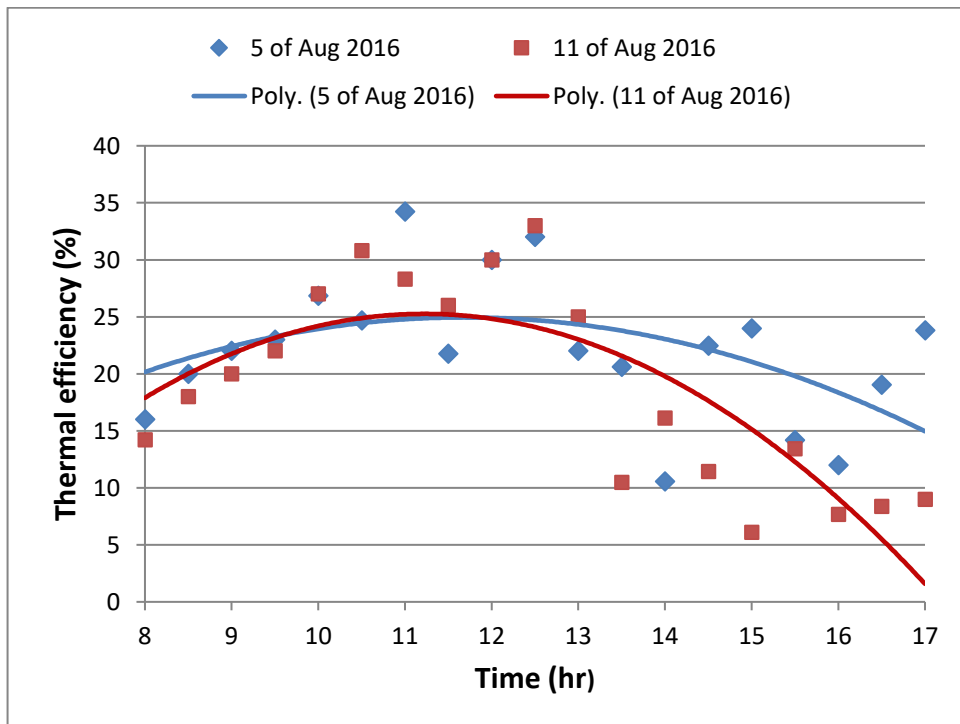


Figure 4.2 Collector thermal efficiency for flow rate of 200 and 500 lph.

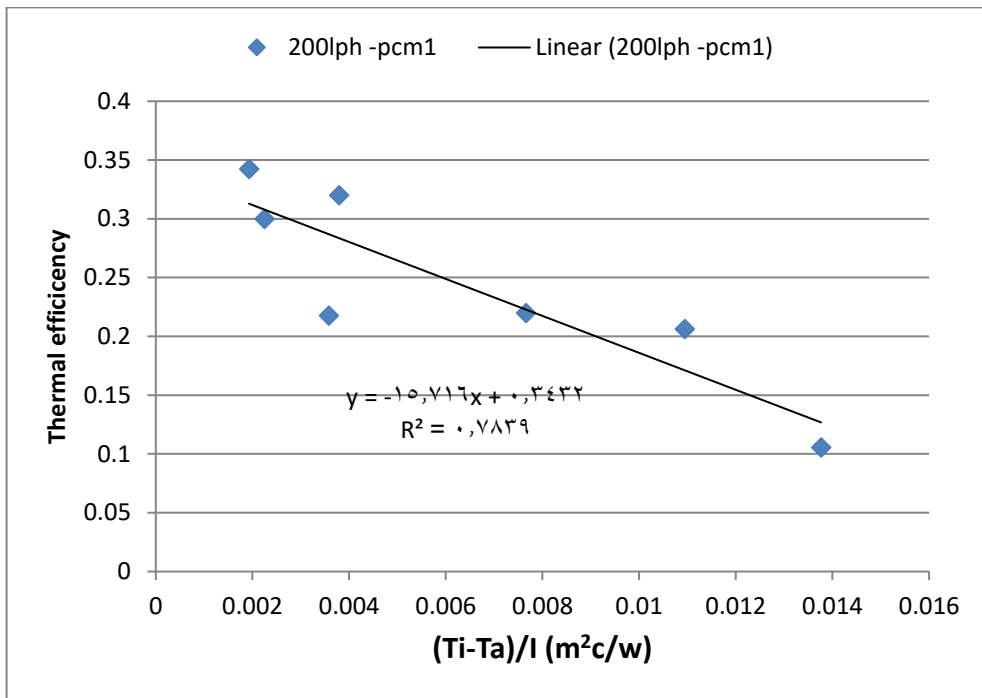


Figure 4.3 Operation curve of Solar Collector for flow rate of 200 lph.

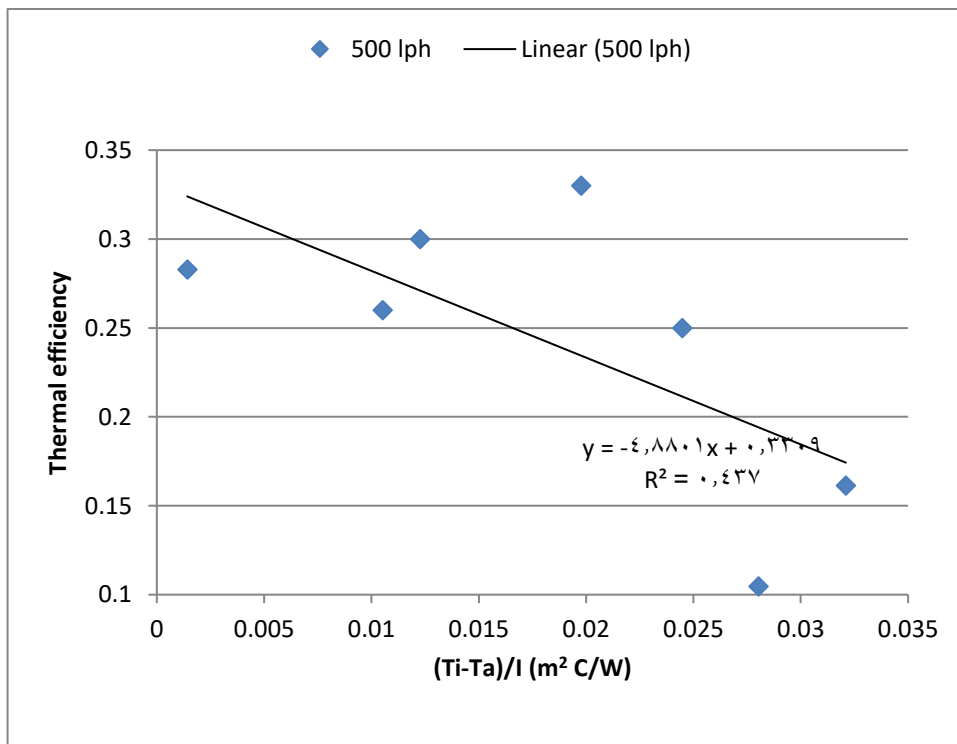


Figure 4.4 Operation curve of Solar Collector for flow rate of 500 lph .

4.3 PCM1 on Summer Season

Figures 4.5 and 4.6 shows the relation between water inlet temperature of inner tube and the PCM 1 temperatures versus hourly time for a water flow rates of 200 lph and 300 lph on 5th and 7th August 2016 respectively at the different angular direction. The water inlet temperature is noticed to be higher than the highest temperature of PCM1. It can be seen that the inlet water temperature and all the PCM1 temperatures are increased from 8:00 am to 17:00 pm due to increasing in the thermal energy observed from the solar radiation. The maximum temperatures of inlet water to inner tube and PCM1 are 73 °C and 64 °C for water flow rate of 200 lph which occurs at 17:00 pm. At 300 lph the maximum temperatures of inlet water to inner tube and PCM1 are 67.8 °C and 48.9 °C and they occur at 17:00 pm too. It can be seen that the melting process occurs at 12:00 noon for water flow rate of 200 lph and at 13:00 pm for water flow rate of 300 lph.

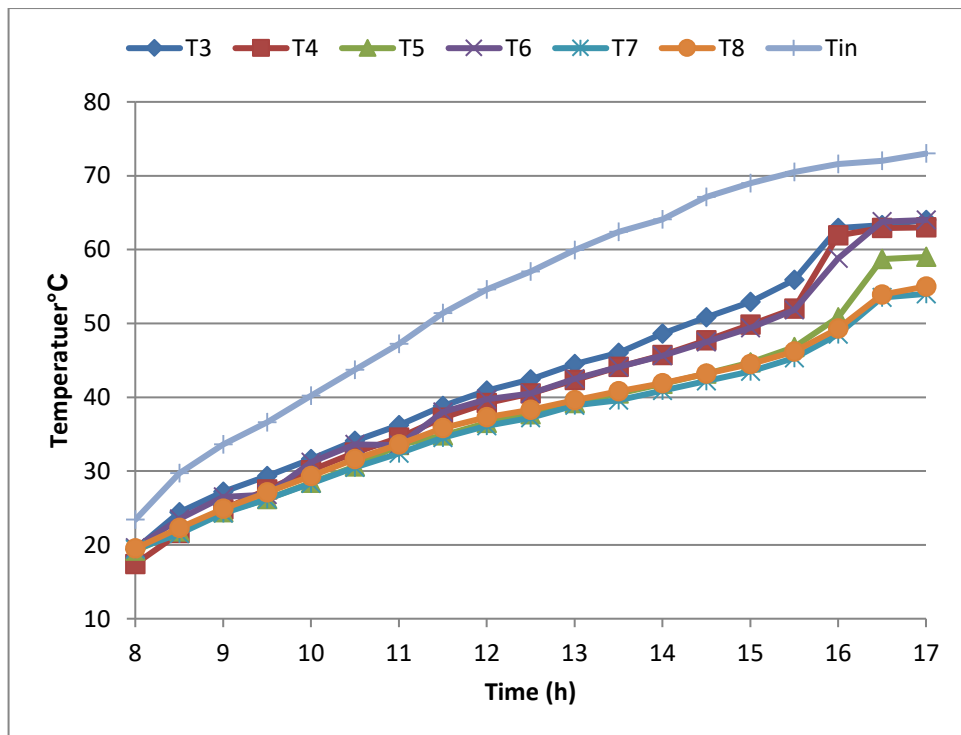


Figure 4.5 PCM1 temperatures for flow rate of 200 lph on 5th Aug 2016.

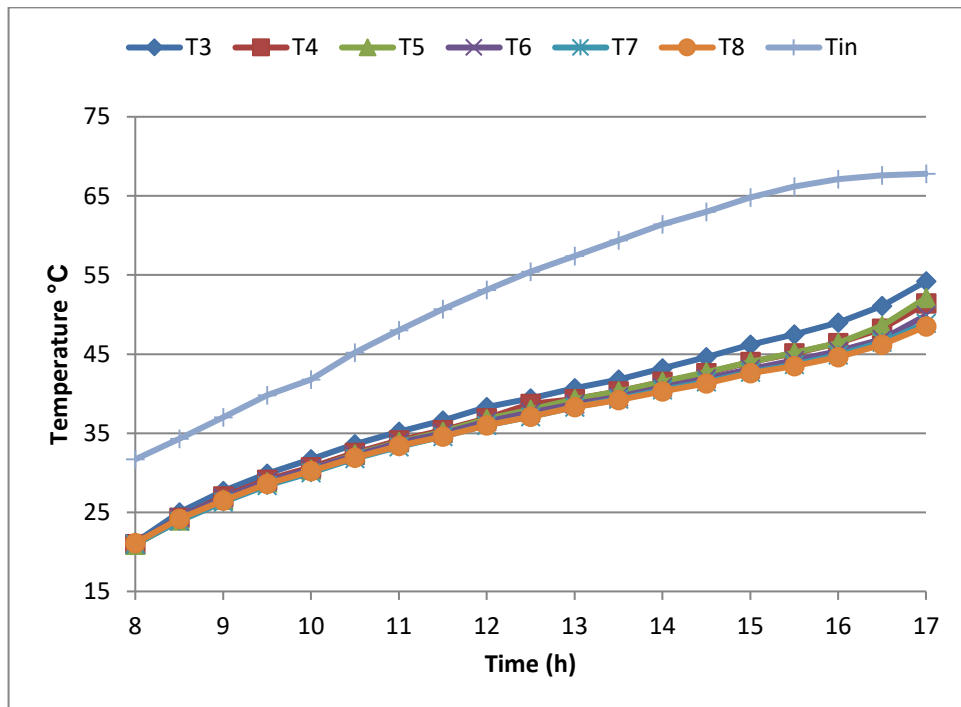


Figure 4.6 PCM1 temperatures for flow rate of 300 lph on 7th Aug 2016.

Fig. 4.7 shows the relation between water inlet temperature of inner tube and the PCM1 temperatures versus hourly time for a water flow rates of 500 lph on 11st August 2016 respectively at the different angular direction. The water inlet temperature is noticed to be higher than the highest temperature of PCM1. It can be seen that the inlet water temperature and all the PCM1 temperatures are increased from 8:00 am to 17:00 pm due to increasing in the thermal energy observed from the solar radiation. The maximum temperatures of inlet water to inner tube and PCM1 are 77.1 °C and 68.0 °C for water flow rate of 500 lph . It can be seen that the melting process occurs at 12:30 noon for water flow rate of 500 lph.

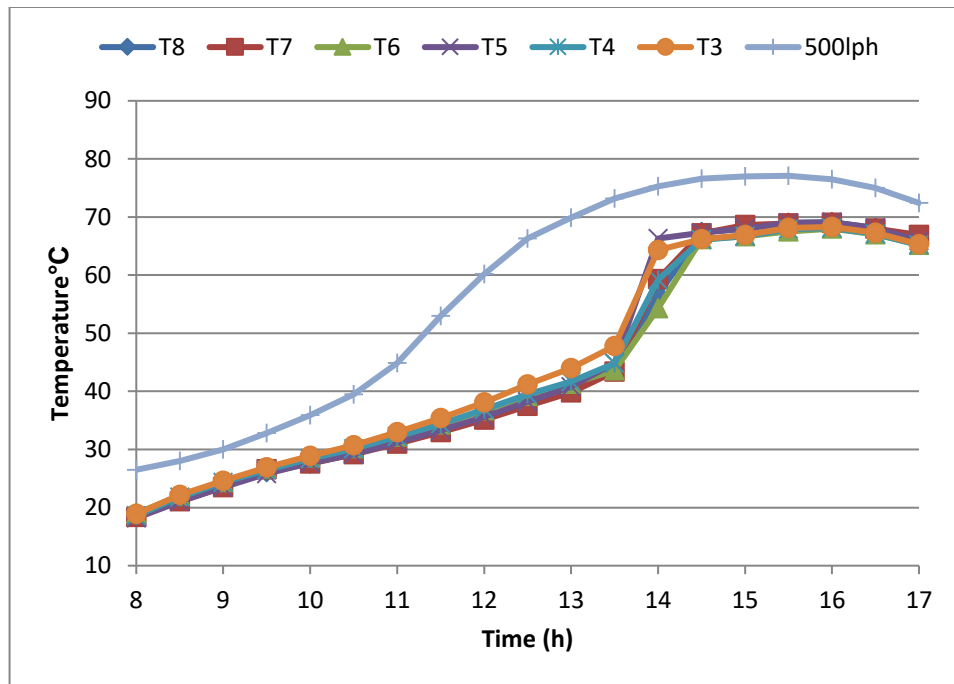


Figure 4.7 PCM1 temperatures for flow rate of 500 lph on 11 Aug 2016.

Figures 4.8 and 4.9, shows more details of the relation between water inlet temperature of inner tube and the PCM 1 temperatures versus hourly time for a water flow rate of 200 lph. One may observe that T3 and T6 are highest temperatures for PCM1 because of it are (T3 and T6) closest to inner tube surface that lead to increase the heat transfer at this locations faster than at the locations of T4, T5, T7, and T8. Also, it can be shown that T3 is higher than T6 because of unsymmetrical in its locations from the bulk temperature of water flow inside rectangular inner tube.

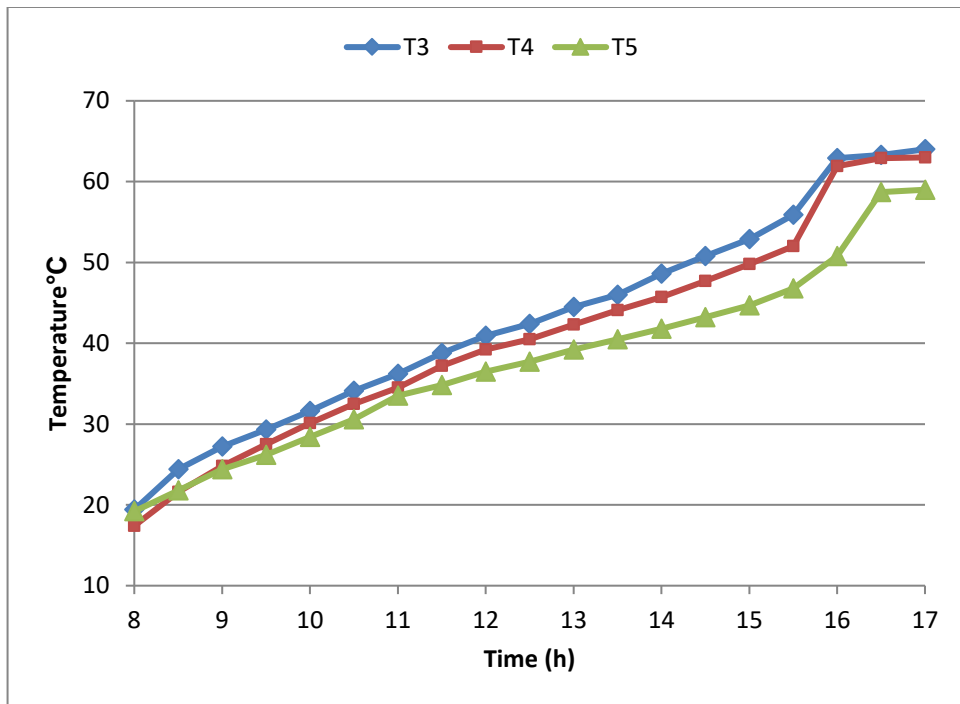


Figure 4.8 PCM1 temperatures (T3, T4, T5) for flow rate of 200 lph on 5th Aug. 2016.

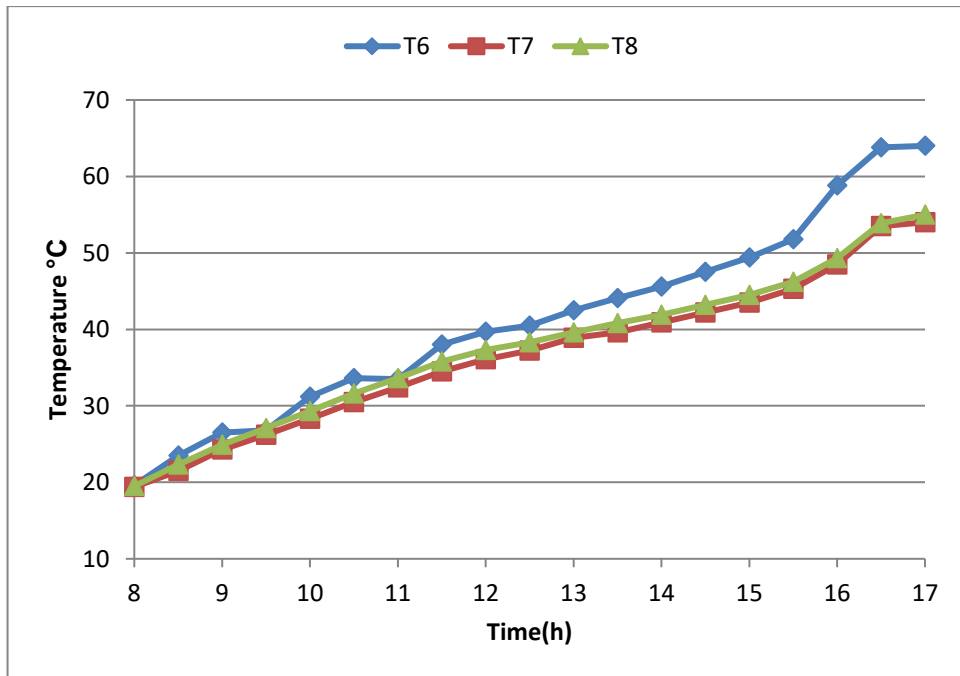


Figure 4.9 PCM1 temperatures (T6, T7, T8) for flow rate of 200 lph on 5th Aug. 2016.

Fig. 4.10 shows the relation between the middle temperatures (T_4) of PCM1 versus hourly time for a water flow rates of 200, 300, and 500 lph. It can be observed that the temperatures for the flow rate of 500 lph are highest temperatures than temperatures of the lower flow rates (200, 300) lph, because of the inlet temperatures for 500 lph water flow rate inside inner tube have highest temperatures than inlet temperatures of the lower flow rates (200, 300) lph.

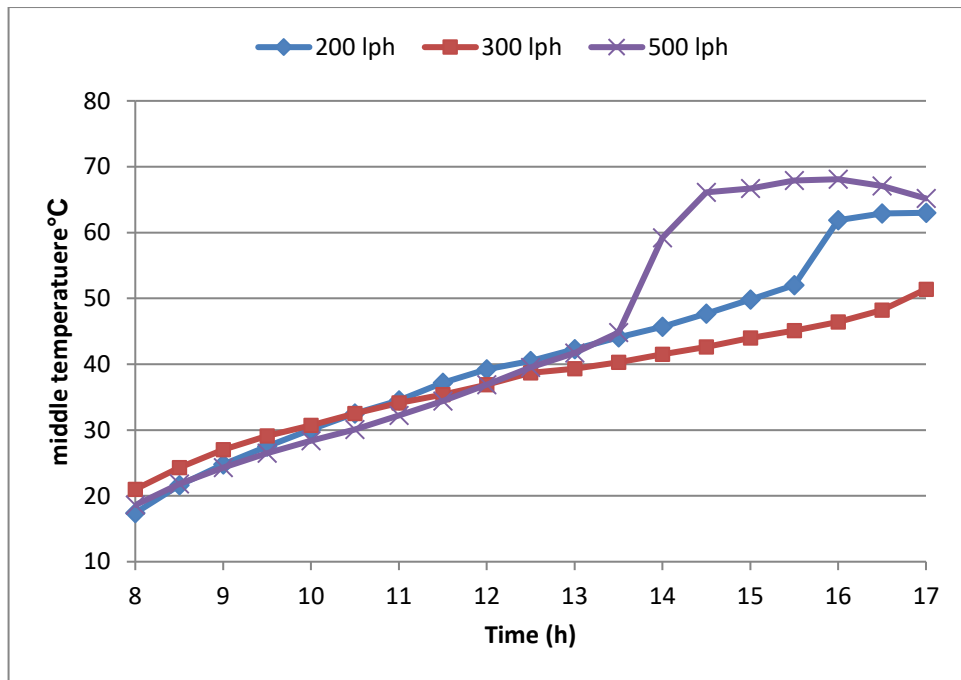


Figure 4.10 PCM1 middle temperatures (T_4) on 5th ,7th ,11th Aug 2016.

Fig. 4.11 shows the relation between the middle temperatures (T_7) of PCM 1 versus hourly time for a water flow rates of 200, 300, and 500 lph. It can be observed that the temperatures for the flow rate of 500 lph are highest temperatures than temperatures of the lower flow rates (200, 300) lph, because of the inlet temperatures for 500 lph water flow rate inside inner tube have highest temperatures than inlet temperatures(77.1C) of the lower flow rates (200, 300) lph.

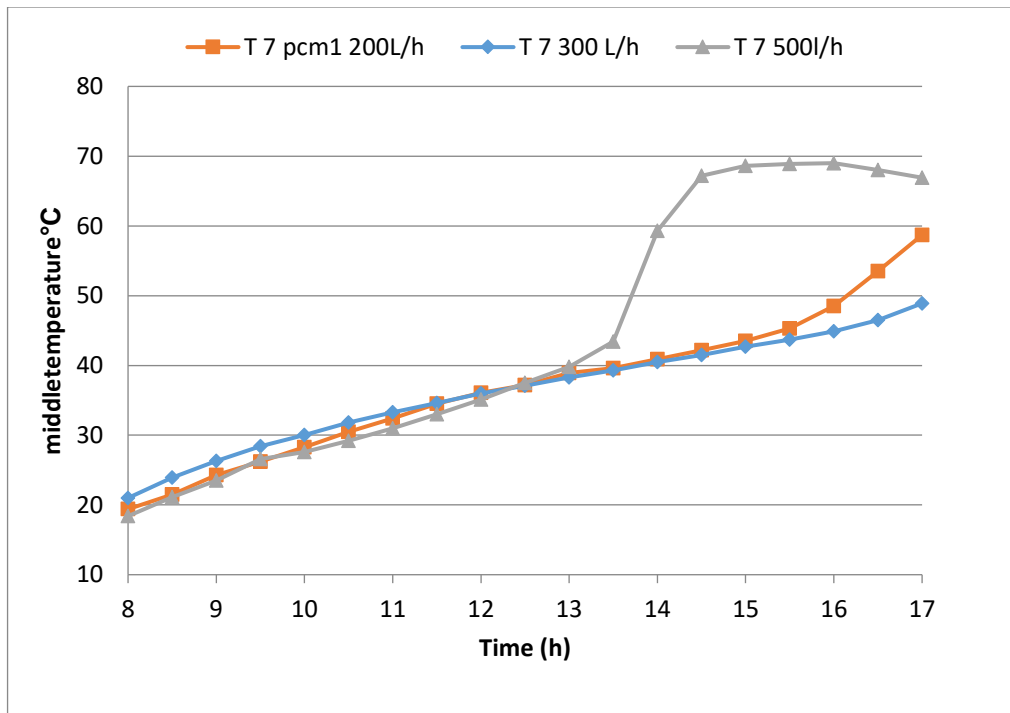


Figure 4.11 PCM1 middle temperatures (T7) on 5th, 7th, 11th Aug 2016.

Fig. 4.12 shows the relation between the Inlet water temperature inside inner tube (T1) for PCM1 versus hourly time for water flow rates of 200, 300, and 500 lph. It can be detected that the temperatures for the flow rate of 500 lph are the highest temperatures compared to the lower flow rates (200, 300) lph, due to the ambient temperatures for 500 lph water flow rate inside inner tube being the highest compared to the ambient temperatures of the lower flow rates (200, 300) lph as shown in Fig. 4.13.

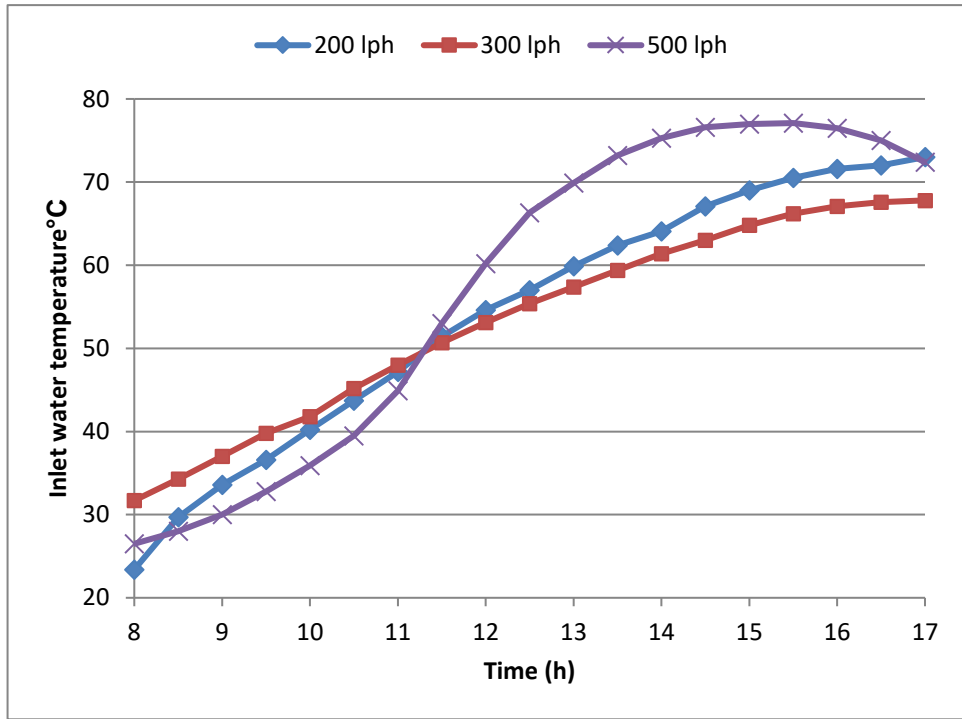


Figure 4.12 Inlet water temperature (T_{in}) for PCM1 on 5th ,7th ,11th Aug 2016.

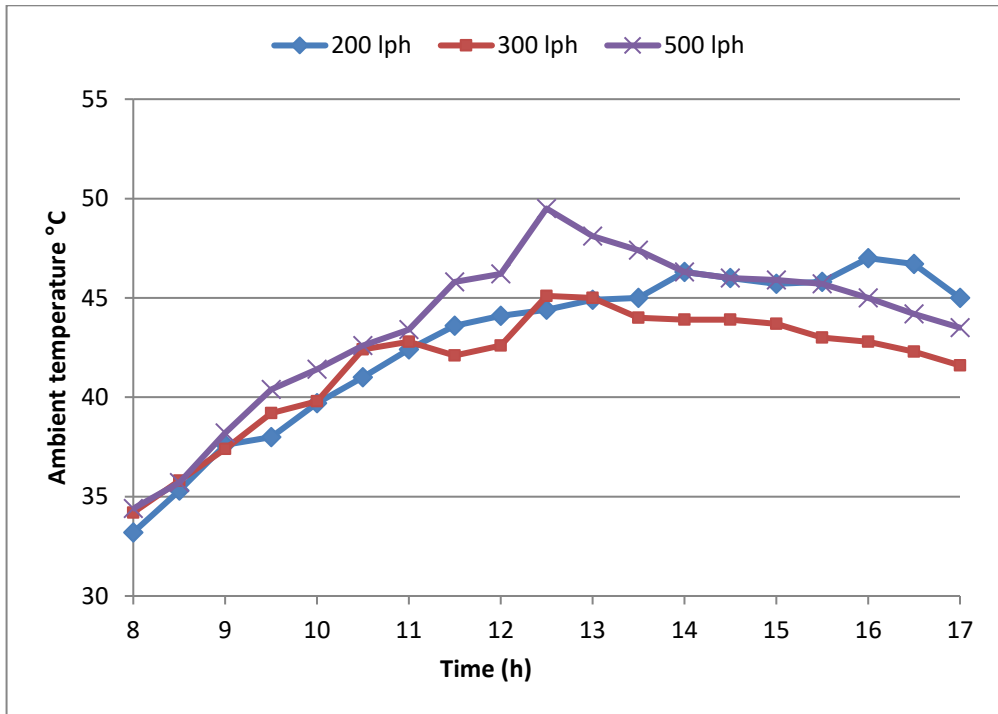


Figure 4.13 Ambient temperature (T_{amb}) for PCM1 on 5th ,7th ,11th Aug 2016.

Fig.4.14 shows the relation between the heat energy gained from the hot water flow inside inner tube for PCM1 versus hourly time for a water flow rates of 200, 300, and 500 lph. It can be observed that the heat gained for the flow rate of 200 lph are highest temperatures than that of the others flow rates (300, 500) lph, due to the temperatures differences for 200 lph water flow rate inside inner tube have highest values than that of the others flow rates (300, 500) lph as shown Fig. 4.15.

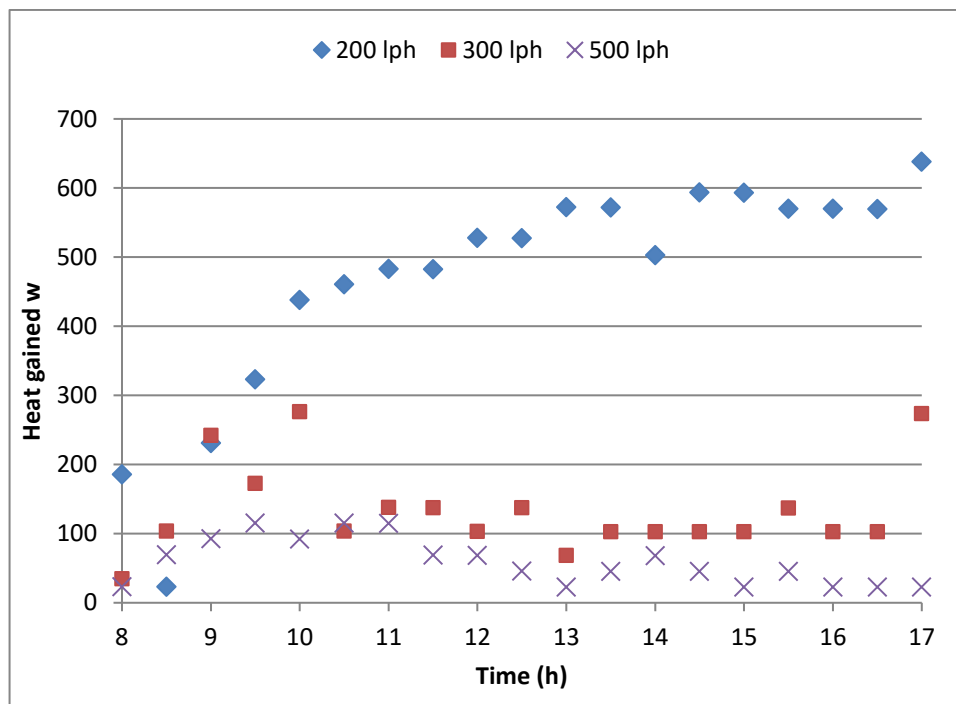


Figure 4.14 Heat gained for PCM1 on 5th ,7th ,11th Aug 2016

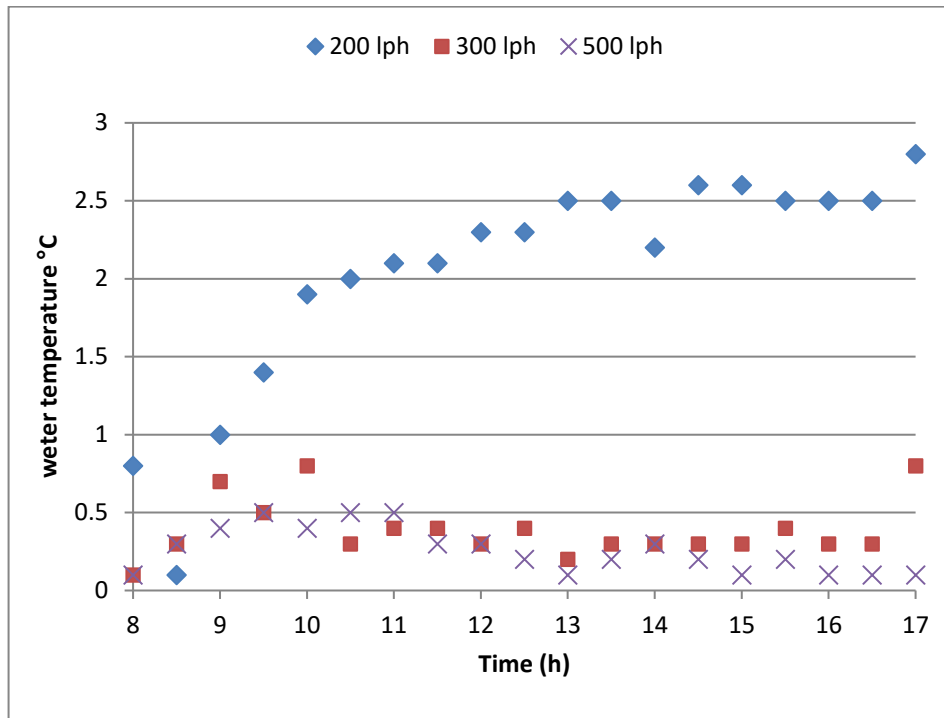


Figure 4.15 Water temperature difference of inner tube for PCM1 on 5th ,7th ,11th Aug 2016

Fig. 4.16 shows the relation between the raise of temperature for middle sensor (T4) for PCM1 versus hourly time for a water flow rates of 200, 300, and 500 lph. It can be observed that the maximum raising temperature is 14.3 °C found for the flow rate of 500 lph. These values are measured every half hour along daily test time.

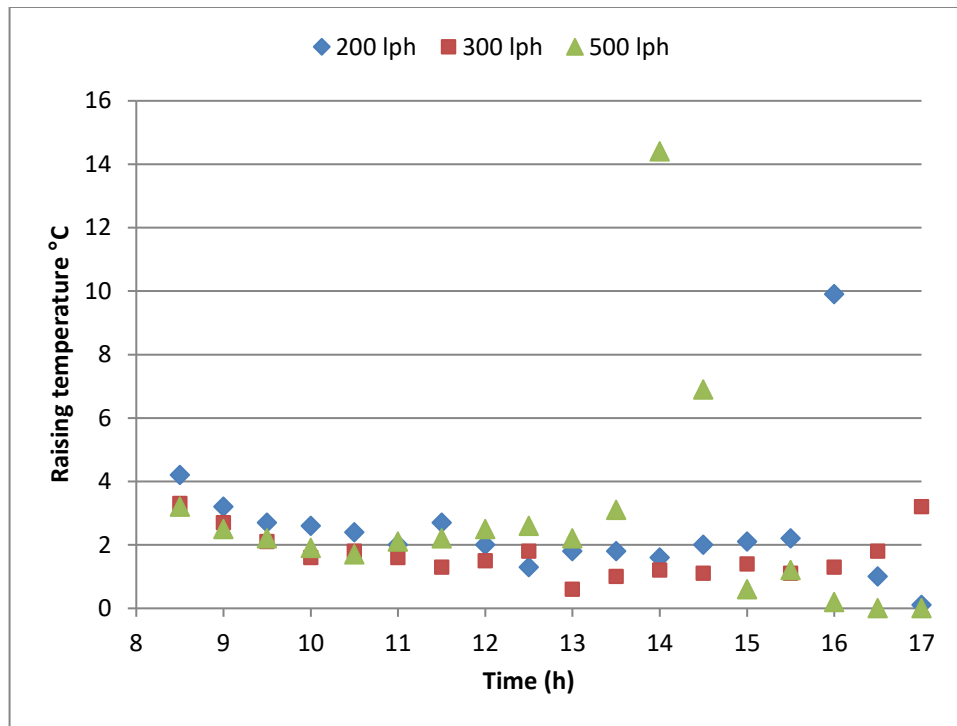


Figure 4.16 Raising of temperature for middle sensor (T4) for PCM1 on 5th ,7th ,11th Aug 2016.

Fig.4.17 shows the relation between the raise percent of temperature for middle sensor (T4) for PCM1 versus hourly time for a water flow rates of 200, 300, and 500 lph. It can be observed that the maximum raising percent of temperature is 34% found for the flow rate of 500 lph. The percent values are measured every half hour along daily test time.

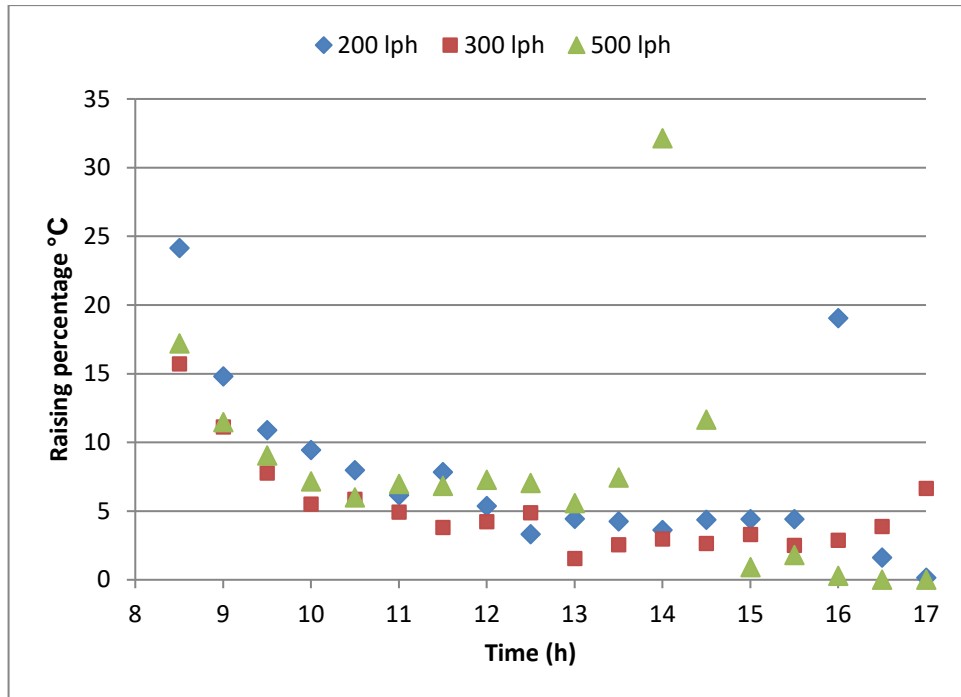


Figure 4.17 Raising percentage of temperature for middle sensor (T4) for PCM1 on 5th, 7th, 11th Aug 2016.

4.4 PCM1 on winter season.

Figures 4.18 and 4.19 shows the relation between water inlet temperature of inner tube and the PCM 1 temperatures versus hourly time for a water flow rates of 200 lph and 300 lph two each flow rate (26th,27th) and(28th,29th) Jan 2017 respectively in the different angular direction. The water inlet temperature is noticed to be higher than the highest temperature of PCM1. It can be shown that the inlet water temperature and all the PCM1 temperatures are increased with time due to increasing in the thermal energy observed from the solar radiation. The maximum temperatures of inlet water to inner tube and PCM1 are 55 °C and 41.7 °C for water flow rate of 200 lph respectively occurs after 16 hours 63.2°C and 44.2°C for water flow rate of 300 lph at the same time. It can be shown the melting process occurs after 16 hours for water flow rate of 200 lph and after 14 hours for water flow rate of 300 lph.

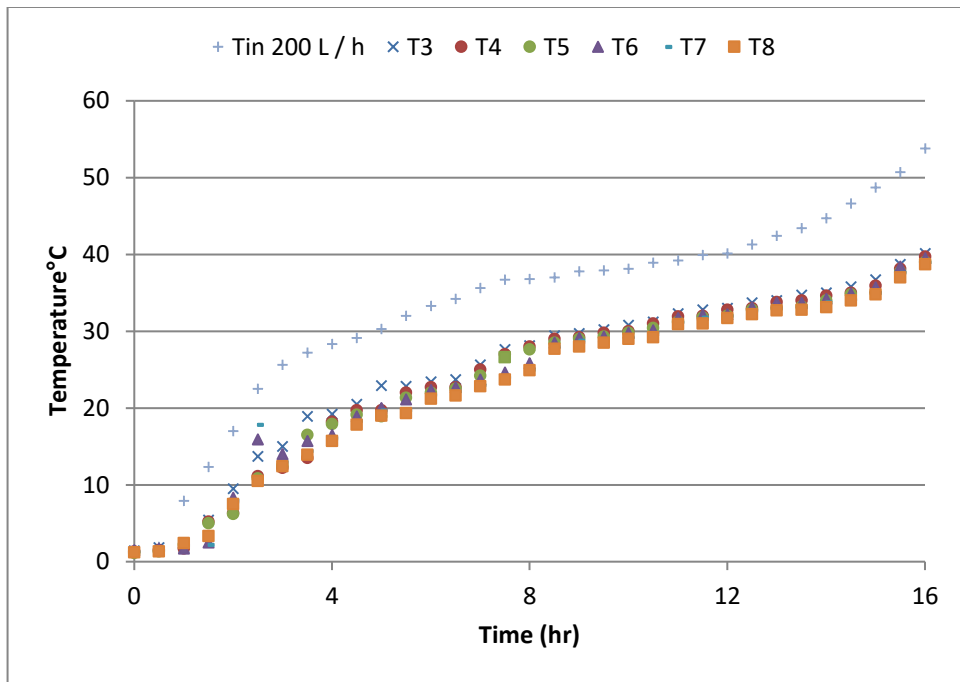


Figure 4.18 PCM1 temperatures for flow rate of 200 lph on 26th and 27th Jan 2017.

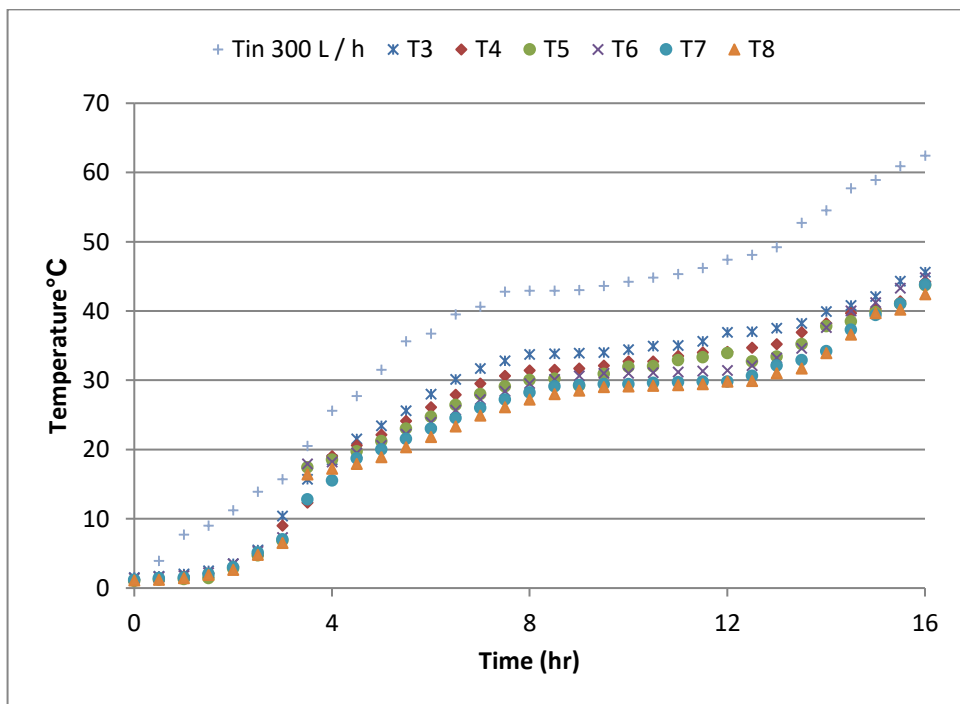


Figure 4.19 PCM1 temperatures for flow rate of 300 lph on 28th, 29th Jan 2017.

Fig. 4.20 shows the relation between water inlet temperature of inner tube and the PCM1 temperatures versus hourly time for a water flow rates of 500 lph on during two days 30th and 31th 2017 respectively at the different angular direction. The water inlet temperature is noticed to be higher than the highest temperature of PCM1. It can be seen that the inlet water temperature and all the PCM1 temperatures are increased from with time due to increasing in the thermal energy observed from the solar radiation. The maximum temperatures of inlet water to inner tube and PCM1 are 64.5°C °C and 4.8.5°C for water flow rate of 500 lph . It can be seen that the melting process occurs after 16 hours noon for water flow rate of 500 lph.

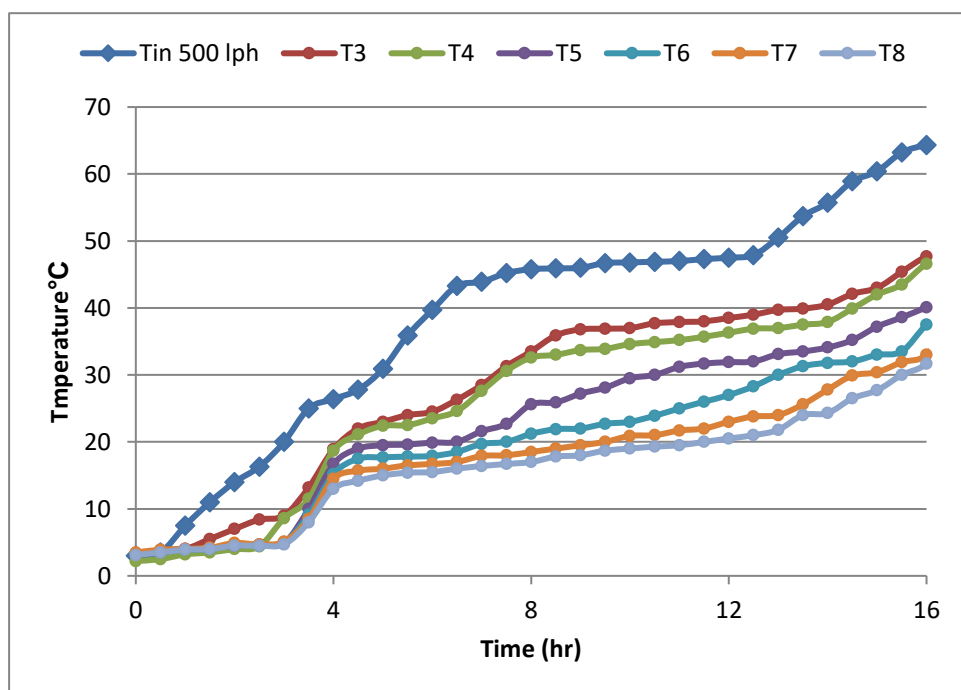


Figure 4.20 PCM1 temperatures for flow rate of 500 lph on 30th and 31th Jan2017

Figures 4.21 and 4.22 shows more details of the relation between water inlet temperature of inner tube and the PCM 1 temperatures versus hourly time for a water flow rate of 200 lph. One may observe that T3 and T6 are highest temperatures for PCM1 because of it are closest to inner tube surface that lead to increase the heat transfer at this locations faster than at the locations of T4,T5, T7, and T8. Also, it can be shown that T3 is higher than T6 because of unsymmetrical in its locations from the bulk temperature of water flow inside rectangular inner tube.

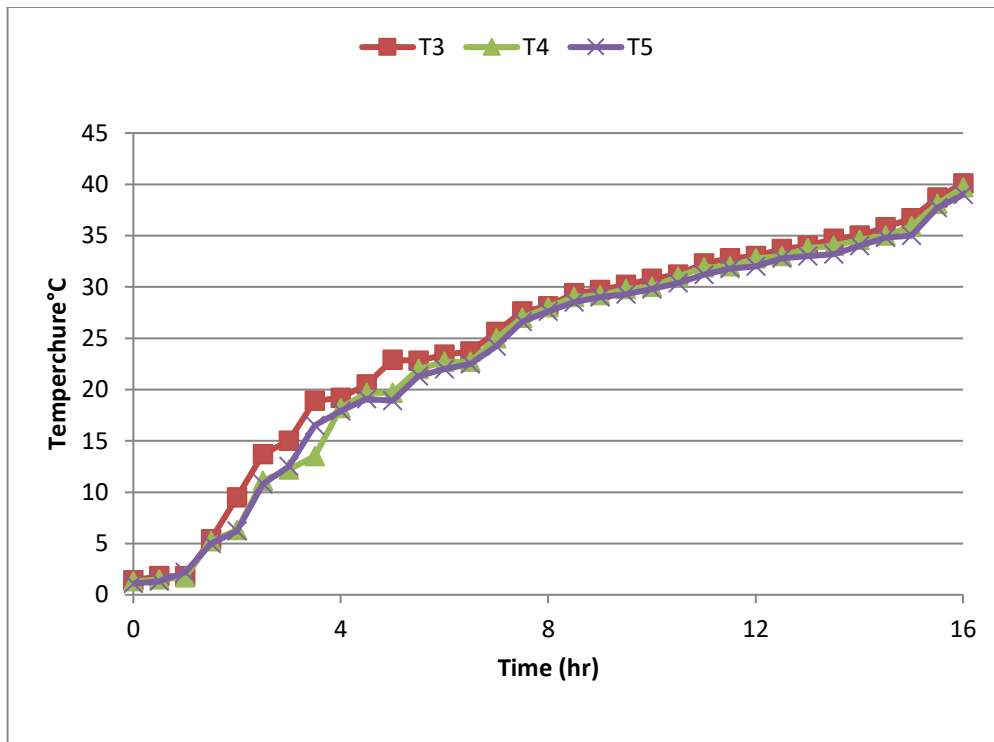


Figure 4.21 PCM1 temperatures (T3, T4, T5) for flow rate of 200 lph on 26th and 27th Jan 2017

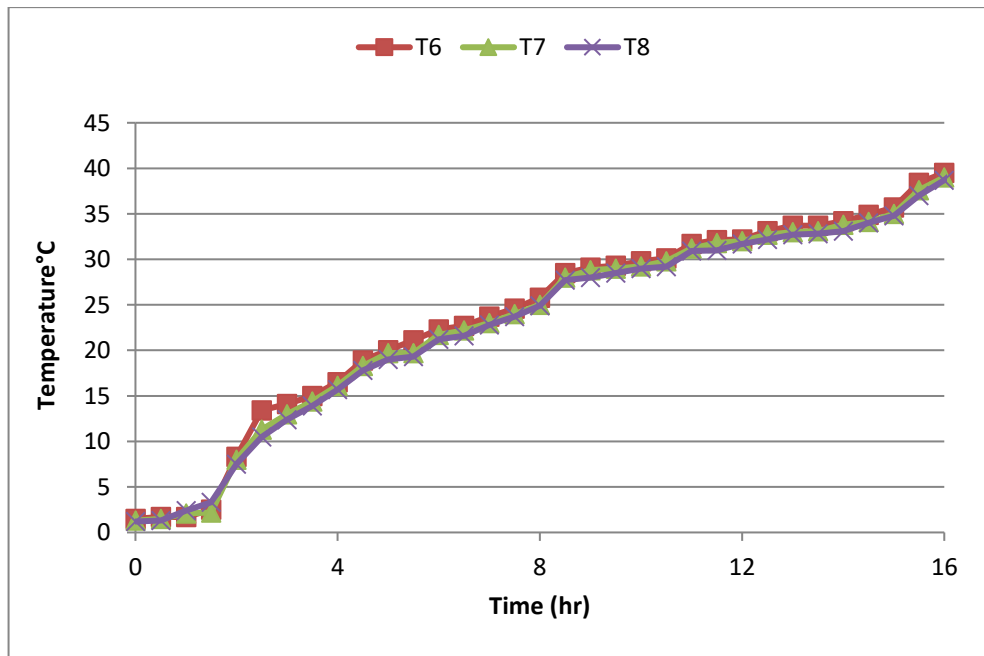


Figure 4.22 PCM1 temperatures (T6, T7, T8) for flow rate of 200 lph on 26th and 27th Jan 2017

Fig. 4.23 shows the relation between the middle temperatures (T4) of PCM 1 versus hourly time for a water flow rates of 200, 300, and 500 lph. It can be observed that the temperatures for the flow rate of 500 lph are highest temperatures than temperatures of the lower flow rates (200, 300) lph, because of the inlet temperatures for 500 lph water flow rate inside inner tube have highest temperatures than inlet temperatures of the lower flow rates (200, 300) lph.

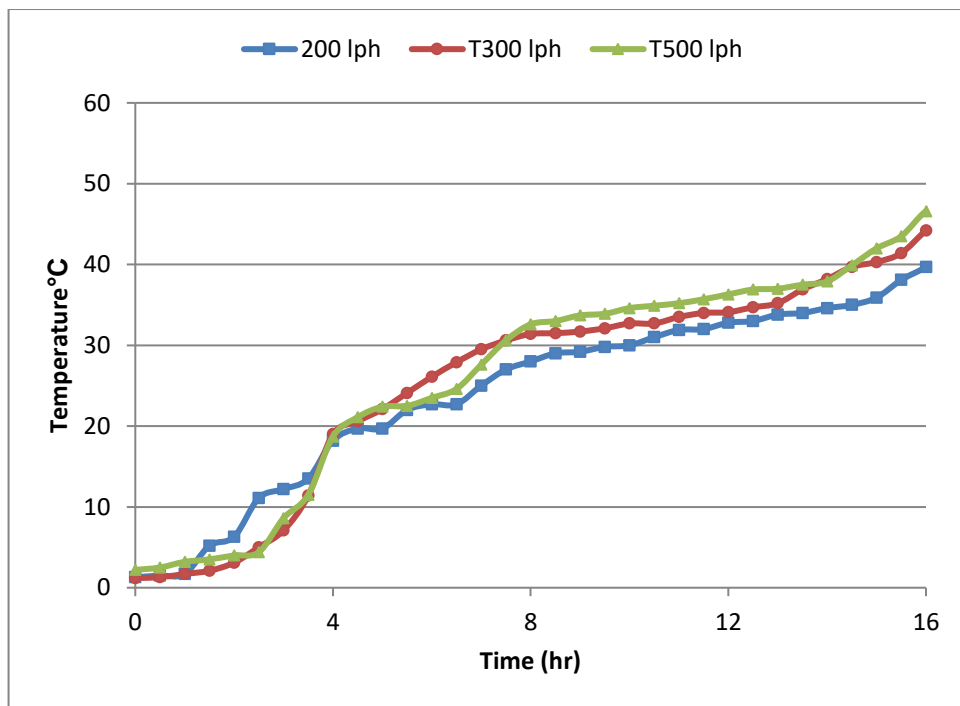


Figure 4.23 PCM1 middle temperatures (T4) of 200 lph on 26th, 27th, 28th, 29th, 30th and 31th Jan 2017

Fig. 4.24 shows the relation between the middle temperatures (T7) of PCM 1 versus hourly time for a water flow rates of 200, 300, and 500 lph. It can be observed that the temperatures for the flow rate of 300 lph are highest temperatures than temperatures of the lower flow rates (200, 500) lph, because of the inlet temperatures for 300 lph water flow rate inside inner tube have highest temperatures than inlet temperatures (64.5°C) of the lower flow rates (200, 500) lph.

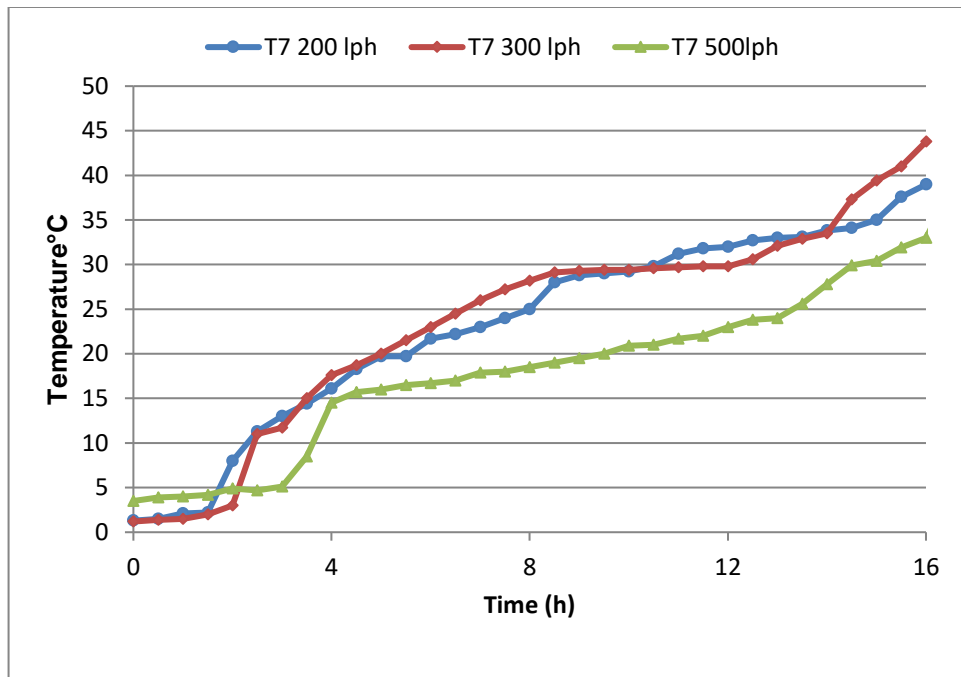


Figure 4.24 PCM1 middle temperatures (T7) of 200 lph on on 26th, 27th, 28th, 29th, 30th And 31th Jan 2017

Fig. 4.25 shows the relation between the Inlet water temperature inside inner tube (T1) for PCM1 versus hourly time for a water flow rates of 200, 300, and 500 lph. It can be detected that the temperatures for the flow rate of 500 lph are highest temperatures than temperatures of the lower flow rates (200, 300) lph, due to the ambient temperatures for 500 lph water flow rate inside inner tube have highest temperatures than ambient temperatures of the previous two cases (200 and 300 L/h) because the flow rate is higher and the paraffin needs less time to melt than (200, 300) lph as shows Figures 4.26 and 4.27.

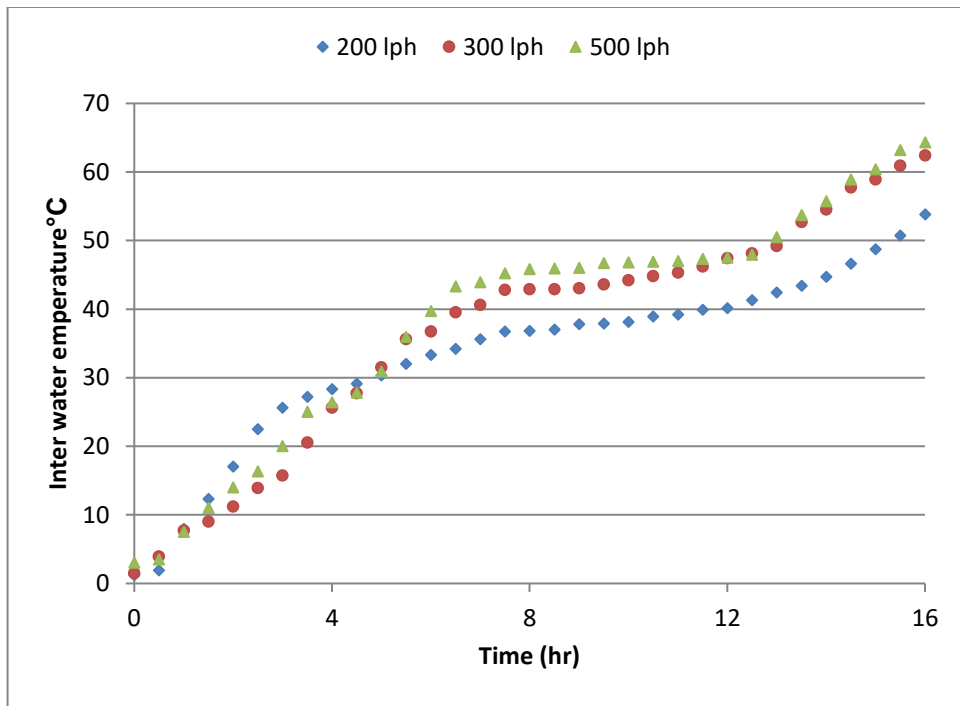


Figure 4.25 Inlet water temperature (T_{in}) for PCM1 on 26th,27th,28th,29th,30th and 31th Jan2017.

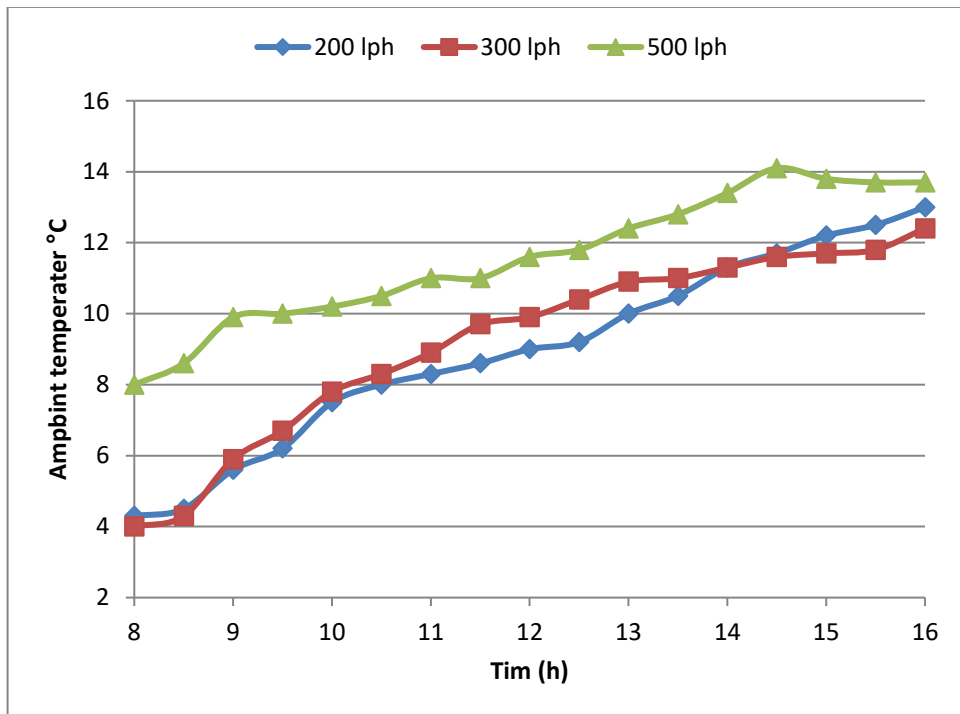


Figure 4.26 Ambient temperature (T_{amb}) for PCM1 on 26th,27th,28th,29th,30th and 31th Jan2017

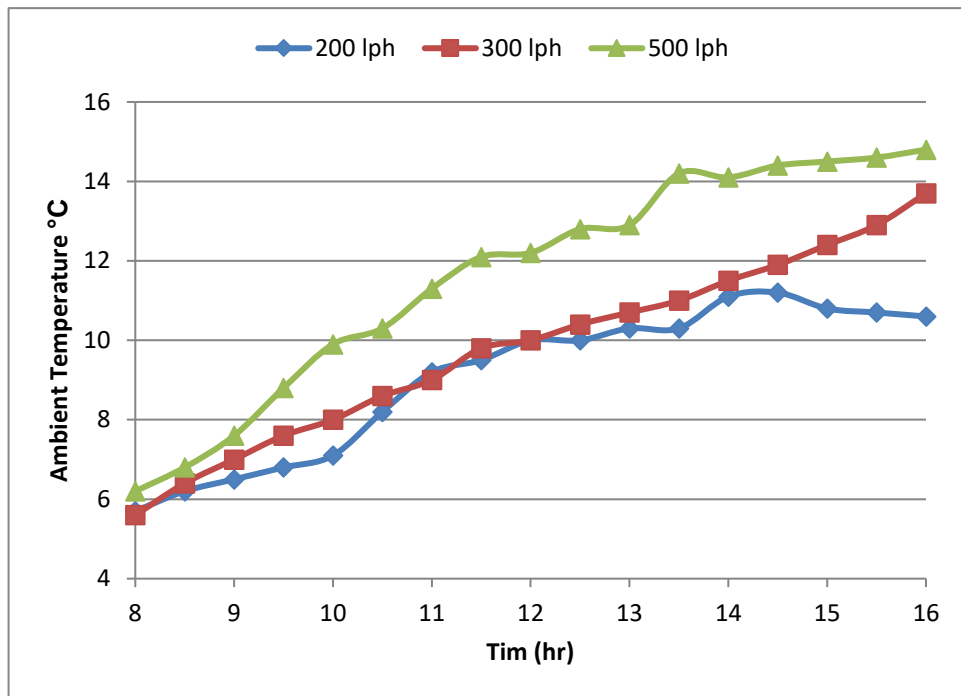


Figure 4.27 Ambient temperature (T_{amb}) for PCM1 on 26th, 27th, 28th, 29th, 30th and 31th Jan 2017.

Fig.4.28 shows the relation between the heat energy gained from the hot water flow inside inner tube for PCM1 versus hourly time for a water flow rates of 200, 300, and 500 lph. It can be observed that the heat gained for the flow rate of 500 lph are highest temperatures than that of the others flow rates (200, 300) lph, due to the temperatures differences for 500 lph water flow rate inside inner tube have highest values than that of the others flow rates (200, 300) lph as shown in Fig. 4.29.

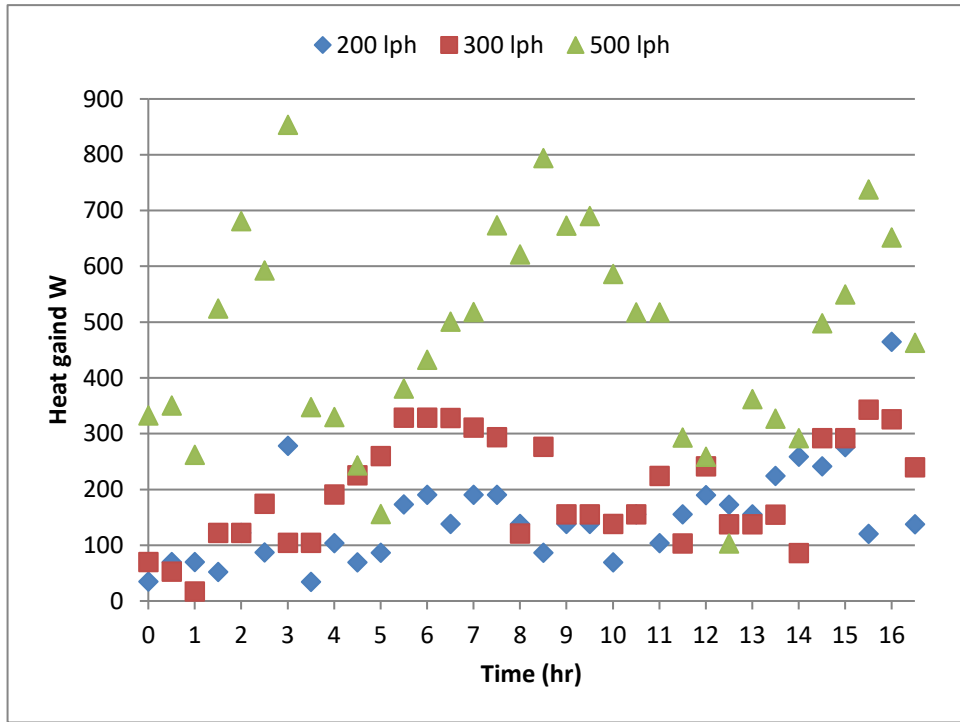


Figure 4.28 Heat gained for PCM1 on 26th,27th ,28th ,29th ,30th and31th Jan2017

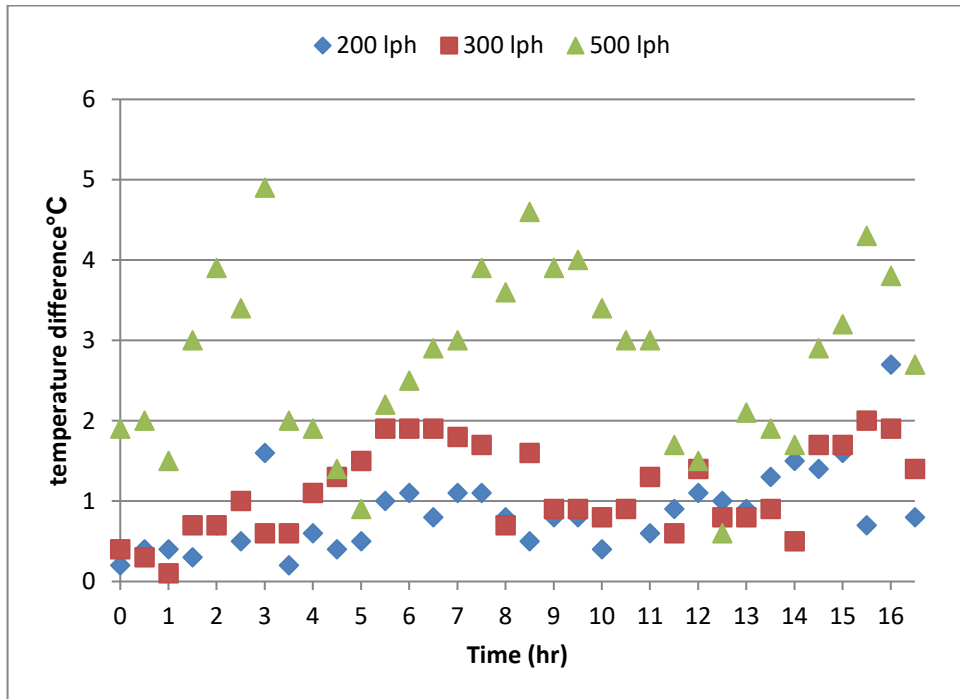


Figure 4.29 Water temperature difference of inner tube for PCM1 on 26th,27th ,28th ,29th ,30th and31th Jan2017

Fig. 4.30 shows the relation between the raise of temperature for middle sensor (T4) for PCM1 versus hourly time for a water flow rates of 200, 300, and 500 lph. It can be observed that the maximum raising temperature is 7.1 °C found for the flow rate of 500 lph. These values are measured every half hour along daily test time two-day the period 16 hours.

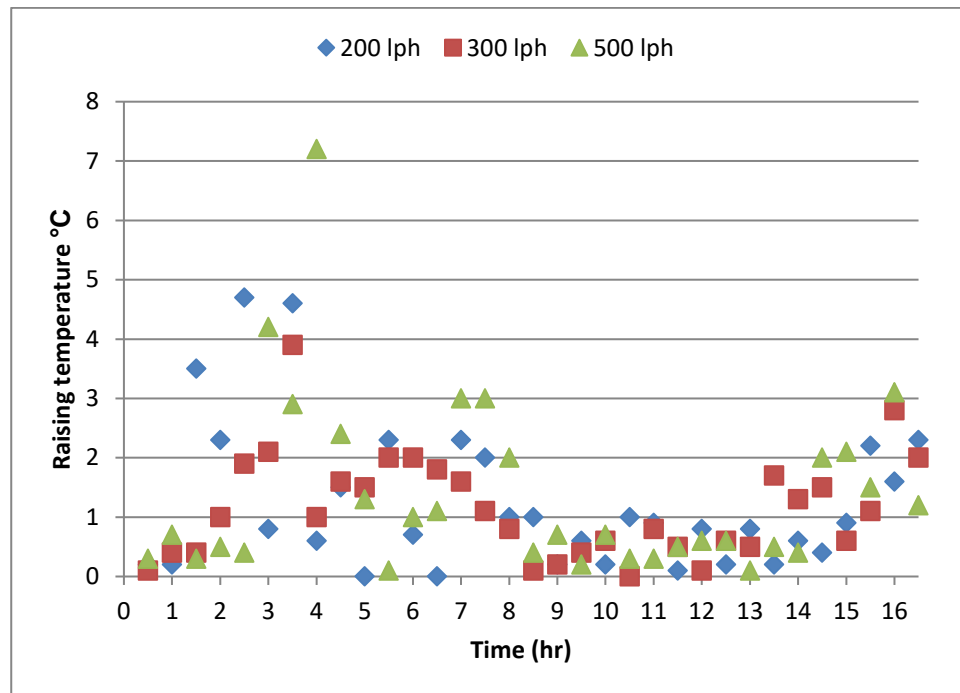
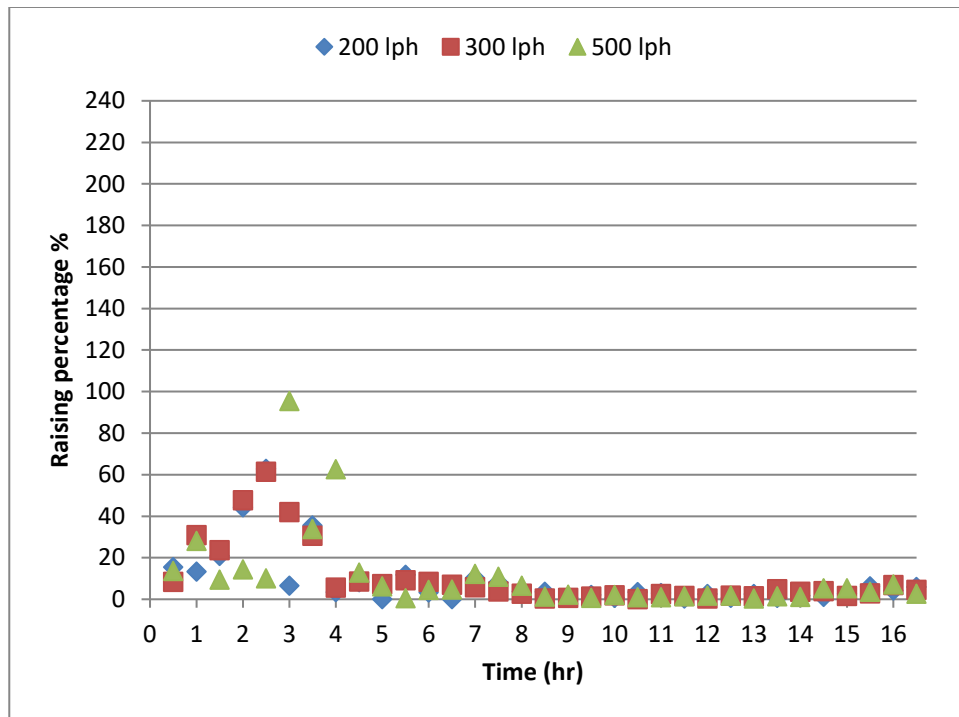


Figure 4.30 Raising of temperature for middle sensor (T4) for PCM1 on 26th, 27th, 28th, 29th, 30th and 31th Jan 2017.

Fig. 4.31 shows the relation between the raise percentage of temperature for middle sensor (T4) for PCM1 versus hourly time for a water flow rates of 200, 300, and 500 lph. It can be observed that the maximum raising percent of temperature is 95% found for the flow rate of 200 lph. The percent values are measured every half hour along daily test time two-day the period 16 hours.



Figure

4.31 Raising percent of temperature for middle sensor (T4) for PCM1 on 26th, 27th, 28th, 29th, 30th and 31th Jan 2017.

4.5 PCM2 on Summer Season

Figures. 4.32 and 4.33 shows the relation between water inlet temperature of inner tube and the PCM 2 temperatures versus hourly time for a water flow rates of 200 lph and 300 lph 16th and 15th Aug 2016 respectively in the different angular direction. The water inlet temperature is noticed to be higher than the highest temperature of PCM2. It can be shown that the inlet water temperature and all the PCM2 temperatures are increased from 8:00 am to 17:00 pm due to increasing in the thermal energy observed from the solar radiation. The maximum temperatures of inlet water to inner tube and PCM2 are 69.7 °C and 61.3 °C for water flow rate of 200 lph respectively occurs at 17:00 pm 73.8°C and 66.9°C for water flow rate of 300 lph at the same time. It can be shown the melting process occurs at 11:00 noon for water flow rate of 200 lph and at 11:30 pm for water flow rate of 300 lph.

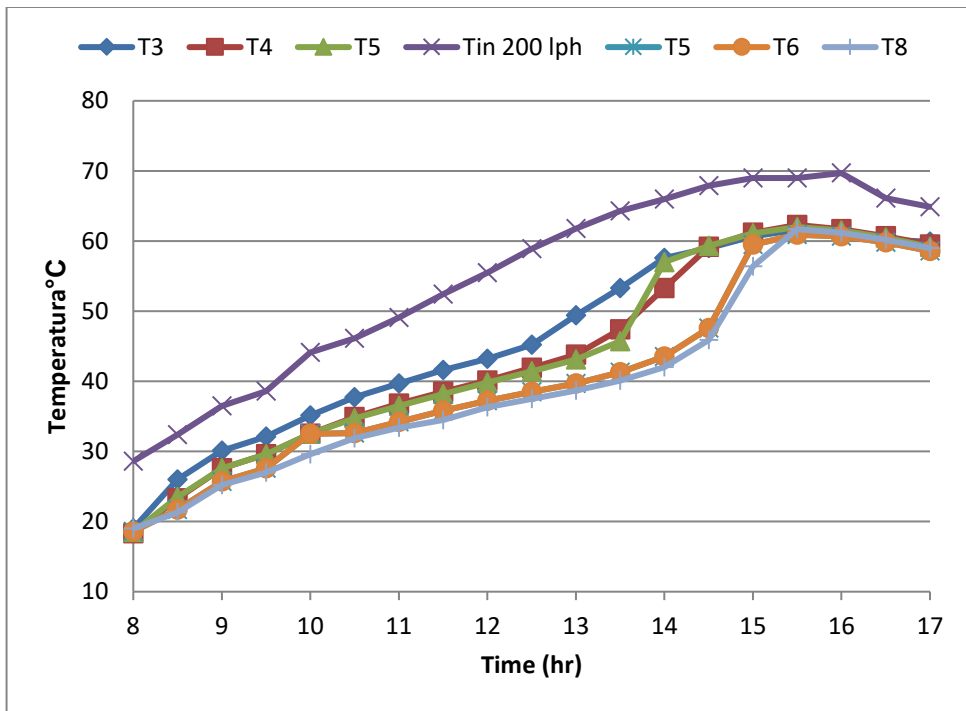


Figure 4.32 PCM2 temperatures for flow rate of 200 lph on 16th Aug 2016

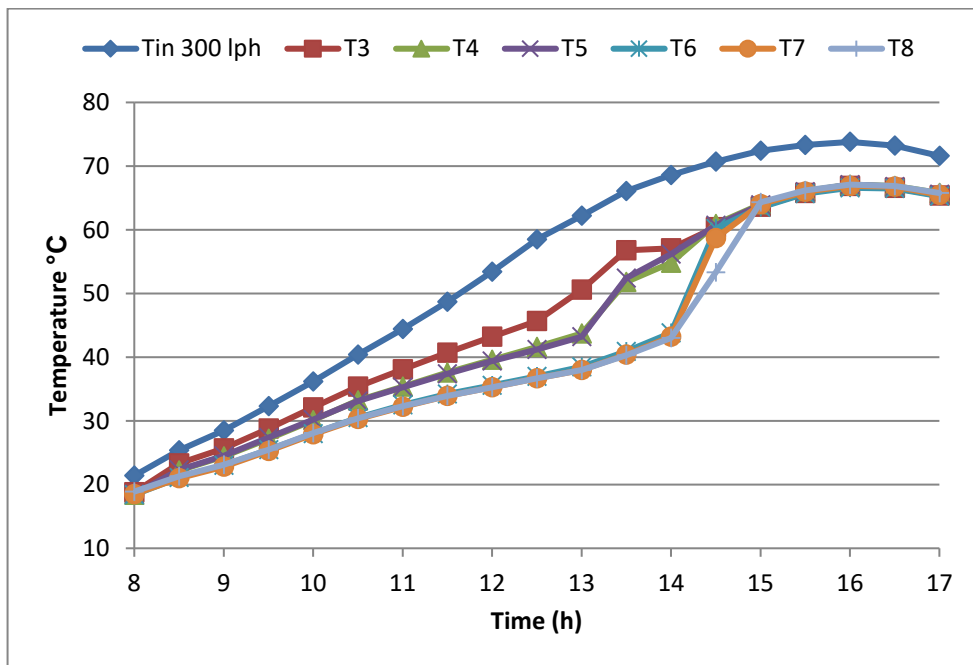


Figure 4.33 PCM2 temperatures for flow rate of 300 lph on 15th Aug 2016.

Fig.4.34 shows the relation between water inlet temperature of inner tube and the PCM2 temperatures versus hourly time for a water flow rates of 500 lph on one day's 14th AUG 2016 respectively at the different angular direction. The water inlet temperature is noticed to be higher than the highest temperature of PCM2. It can be seen that the inlet water temperature and all the PCM2 temperatures are increased with time due to increasing in the thermal energy observed from the solar radiation. The maximum temperatures of inlet water to inner tube and PCM2 are 62.7°C °C and 54.8°C for water flow rate of 500 lph. It can be seen that the melting process occurs after 12:30 hours after noon.

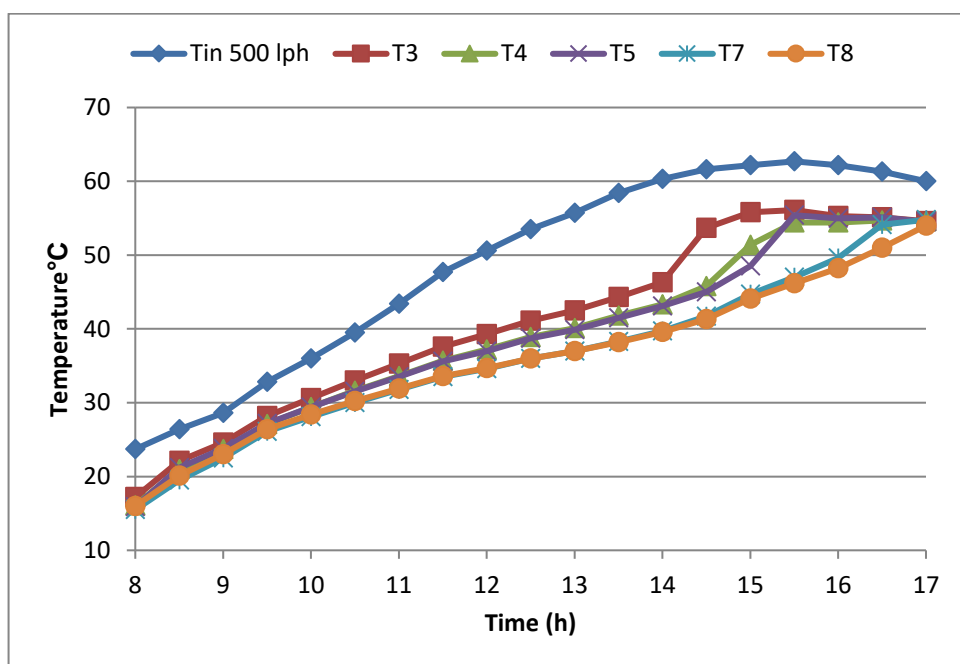


Figure 4.34 PCM2 temperatures for flow rate of 500 lph on 14th Aug 2016.

Figures. 4.35 and 4.36 shows more details of the relation between water inlet temperature of inner tube and the PCM2 temperatures versus hourly time for a water flow rate of 200 lph. One may observe that T3 and T6 are highest temperatures for PCM1 because of it are closest to inner tube surface that lead to increase the heat transfer at this locations faster than at the locations of T4,T5, T7, and T8. Also, it can be shown that T3 is higher than T6 because of unsymmetrical in its locations from the bulk temperature of water flow inside rectangular inner tube.

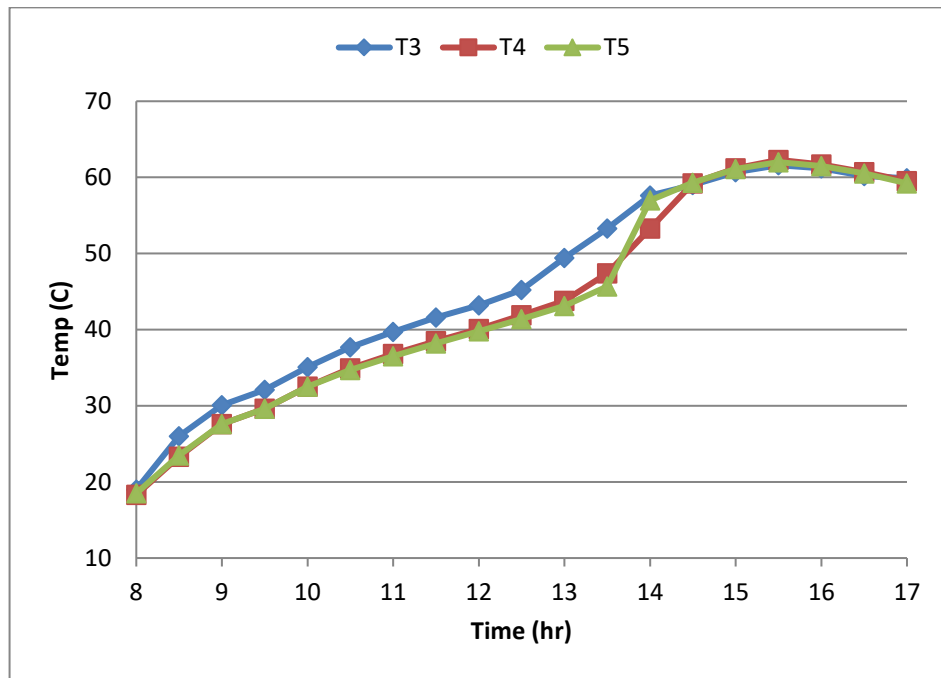


Figure 4.35 PCM2 temperatures (T3, T4, T5) for flow rate of 200 lph on 16th Aug - 2016

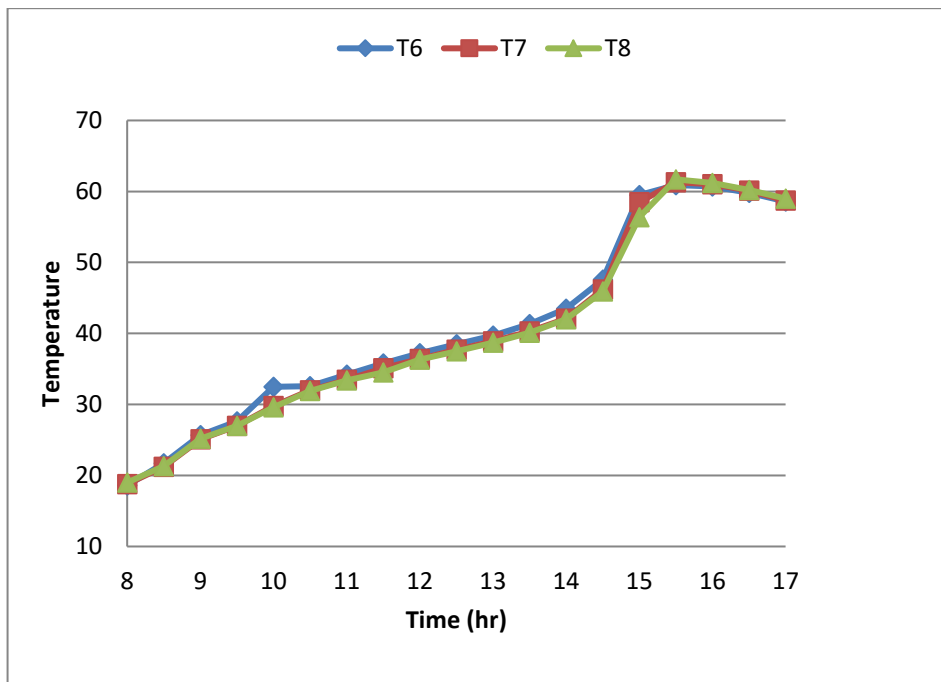


Figure 4.36 PCM2 temperatures (T6, T7, T8) for flow rate of 200 lph 16th Aug 2016

Fig.4.37 shows the relation between the middle temperatures (T4) of PCM2 versus hourly time for a water flow rates of 200, 300, and 500 lph. It can be observed that the temperatures for the flow rate of 300 lph are highest temperatures than temperatures of the lower flow rates (200, 500) lph, because of the inlet temperatures for 300 lph water flow rate inside inner tube. The maximum temperatures of inlet temperatures for 300lph is (73.8C) while temperatures of (200 and 500) (69.7°C, 62.7°C) respectively.

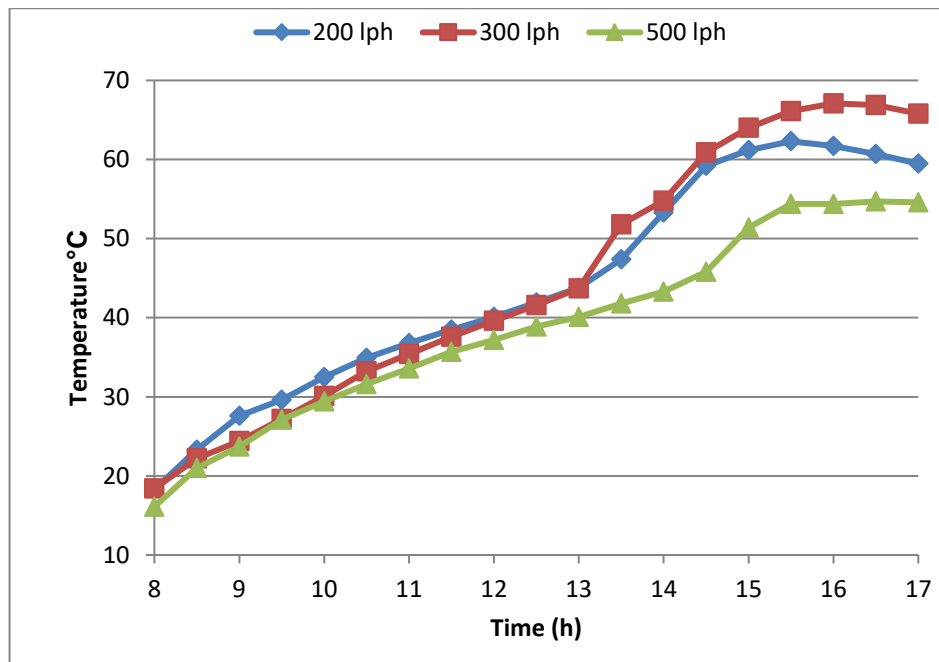


Figure 4.37 PCM2 middle temperatures (T4) of 200 lph on 16th Aug-2016.

Fig.4.38 shows the relation between the raise of temperature for middle sensor (T7) for PCM2 versus hourly time for a water flow rates of 200, 300, and 500 lph. It can be observed that the maximum raising temperature is 66.9 °C found for the flow rate of 300 lph. These values are measured every half hour along daily test time.

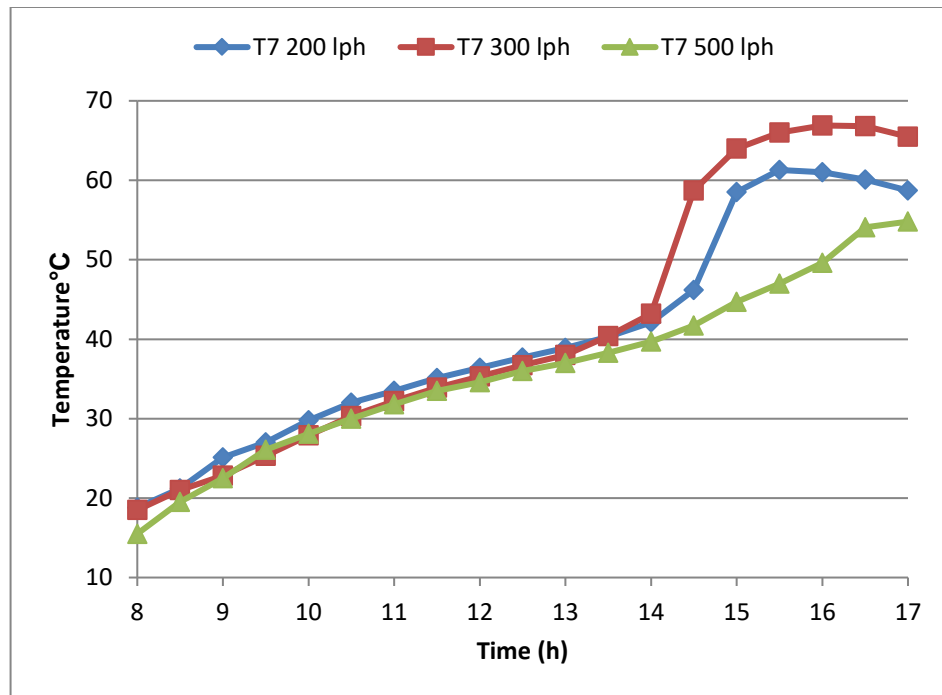


Figure 4.38 PCM2 middle temperatures (T7) of 200 lph on 16th Aug-2016.

Fig.4.39 shows the relation between the Inlet water temperature inside inner tube (T1) for PCM2 versus hourly time for a water flow rates of 200, 300, and 500 lph. It can be detected that the temperatures for the flow rate of 300 lph are highest temperatures than temperatures of the lower flow rates (200, 500) lph, due to the ambient temperatures for 300 lph water flow rate inside inner tube have highest temperatures than ambient temperatures of the lower flow rates (200, 500) lph expected this result due to weather changes and different sun light intensity during the different days of the experiment as shows Fig.4.40.

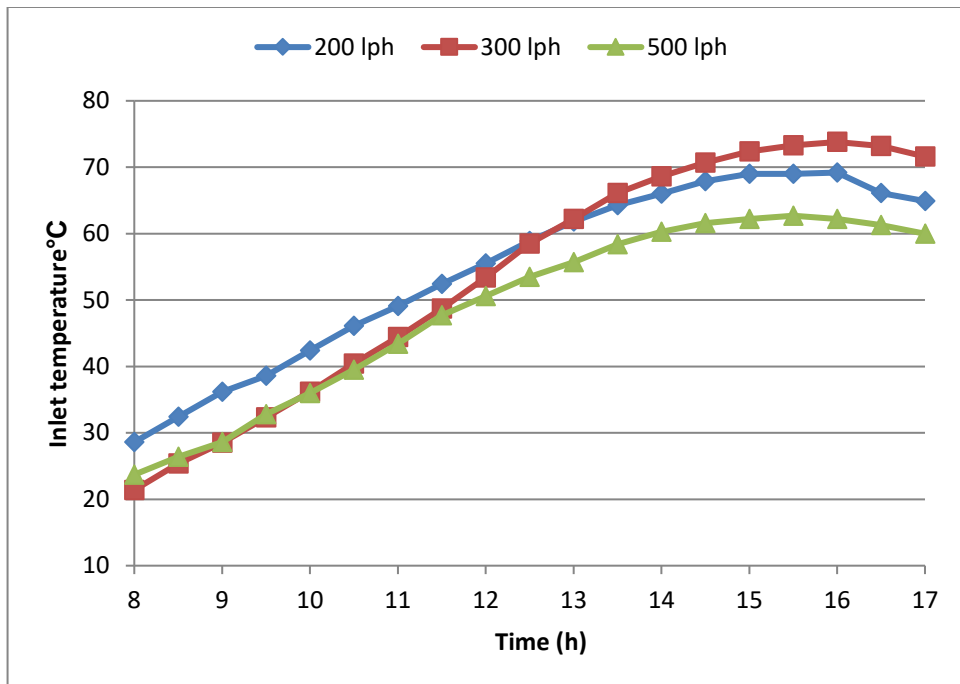


Figure 4.39 Inlet water temperature (T_{in}) for PCM2 on 14th,15th ,16th Aug -2016

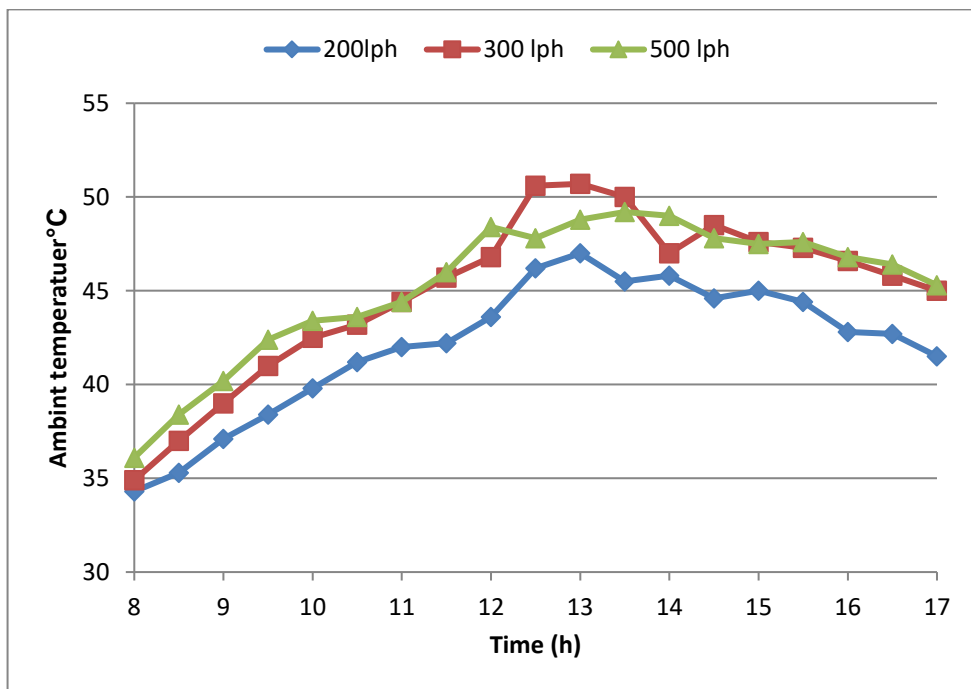


Figure 4.40 Ambient temperature (T_{amb}) for PCM2 on 14th,15th ,16th Aug 2016

Fig.4.41 shows the relation between the heat energy gained from the hot water flow inside inner tube for PCM2 versus hourly time for a water flow rates of 200, 300, and 500 lph. It can be observed that the heat gained for the flow rate of 300 lph are highest temperatures than that of the others flow rates (200, 500) lph, due to the temperatures differences for 300 lph water flow rate inside inner tube have highest values than that of the others flow rates (300, 500) lph as shown in Fig.4. 42.

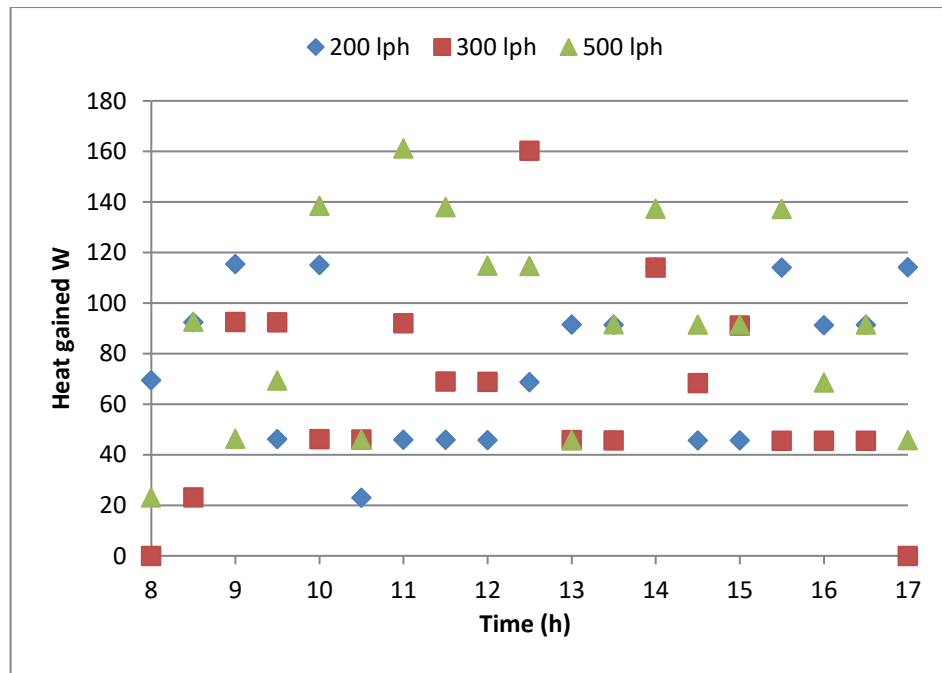


Figure 4.41 Heat gained for PCM2 on 14th, 15th, 16th Aug 2016

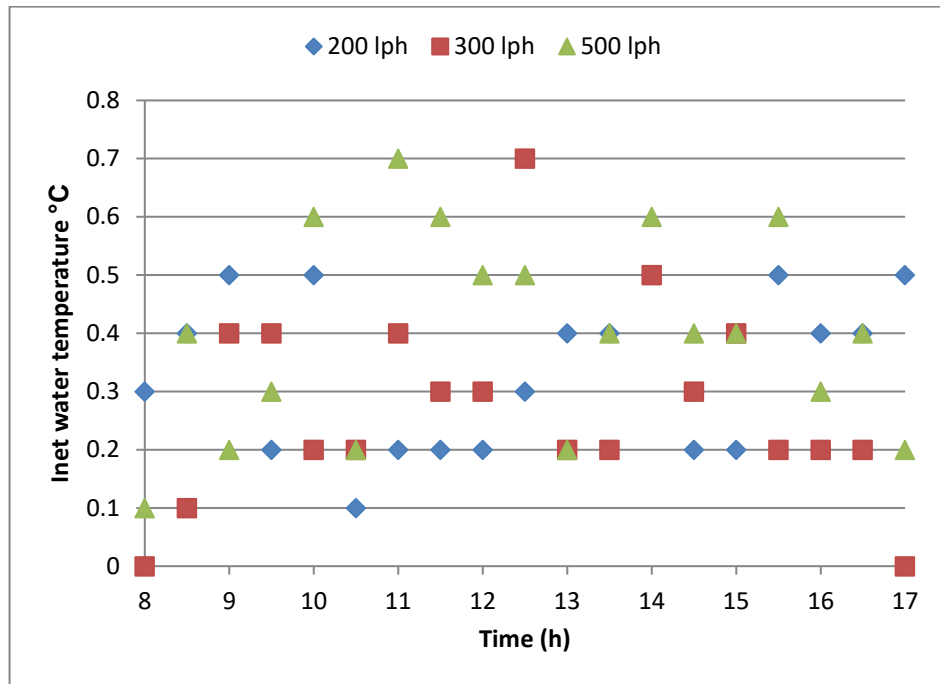


Figure 4.42 Inlet water temperature difference of inner tube for PCM2 on 14th,15th,16th Aug 2016

Fig.4.43 shows the relation between the raise of temperature for middle sensor (T4) for PCM2 versus hourly time for a water flow rates of 200, 300, and 500 lph. It can be observed that the maximum raising temperature is 8.1 °C found for the flow rate of 300 lph. These values are measured every half hour along daily test time.

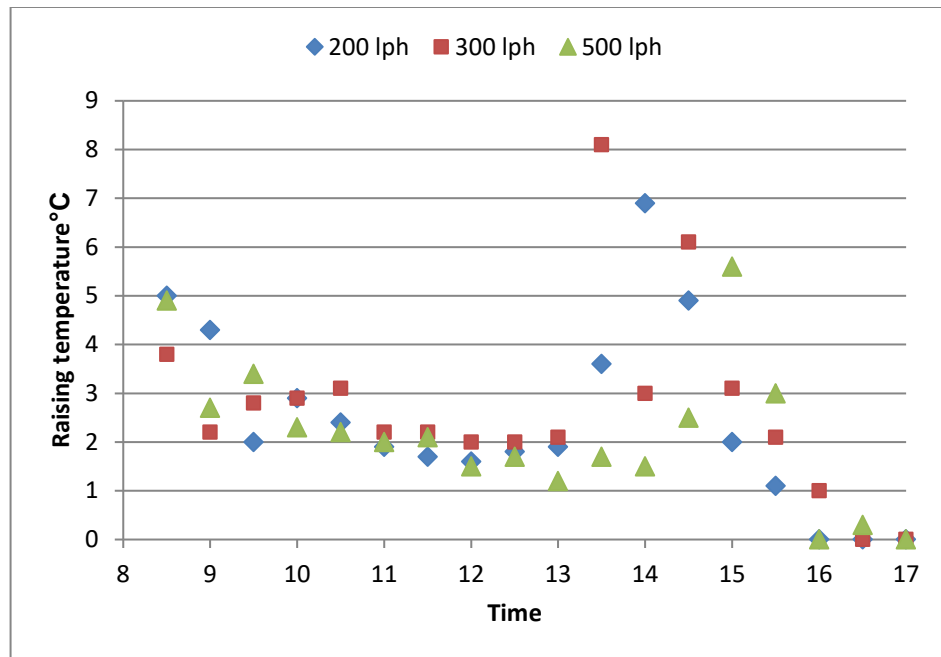


Figure 4.43: Raising of temperature for middle sensor (T4) for PCM1 on 14th, 15th, 16th Aug 2016

Fig.4.44 shows the relation between the raise percent of temperature for middle sensor (T4) for PCM2 versus hourly time for a water flow rates of 200, 300, and 500 lph. It can be observed that the maximum raising percent of temperature is 34% found for the flow rate of 500 lph. The percent values are measured every half hour along daily test time.

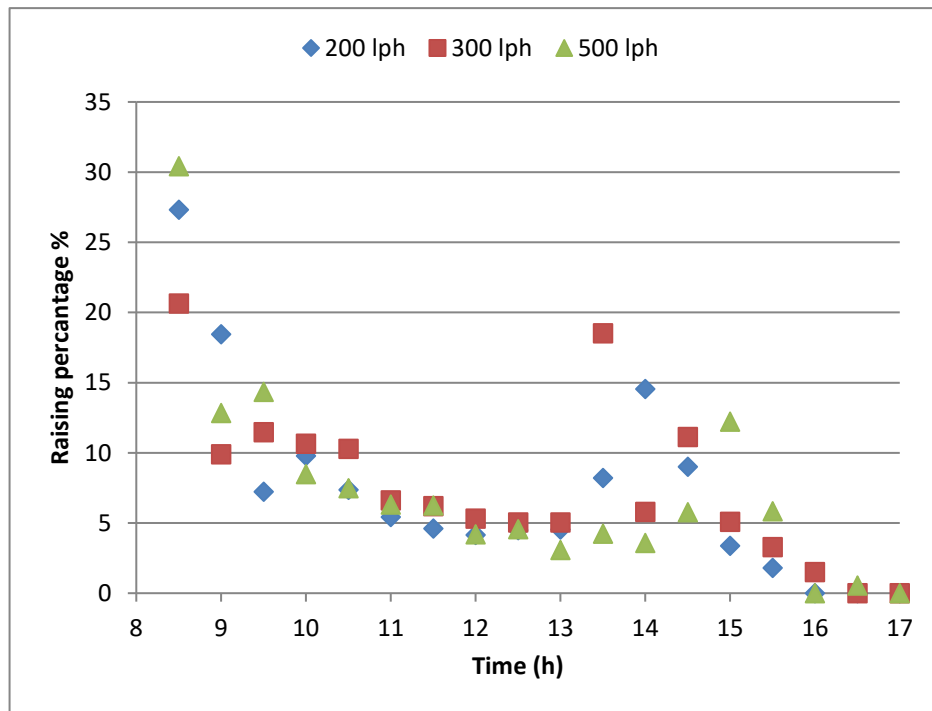


Figure 4.44 Raising percentage of temperature for middle sensor (T4) for PCM2 on 14th, 15th, 16th Aug 2016

4.6 PCM2 Winter Season

Figures. 4.45 and 4.46 shows the relation between water inlet temperature of inner tube and the PCM 2 temperatures versus hourly time for a water flow rates of 200 lph and 300 lph two each flow rate (19th, 20th) and (21th, 22th) Dec 2016 respectively in the different angular direction. The water inlet temperature is noticed to be higher than the highest temperature of PCM2. It can be shown that the inlet water temperature and all the PCM2 temperatures are increased with time due to increasing in the thermal energy observed from the solar radiation. The maximum temperatures of inlet water to inner tube and PCM2 are 61.8 °C and 51 °C for water flow rate of 200 lph respectively occurs after 16 hours 61.9°C and 53°C for water flow rate of 300 lph at the same time. It can be shown the melting process occurs after 14 hours noon for water flow rate of 200 lph and after 13 hours for water flow rate of 300 lph.

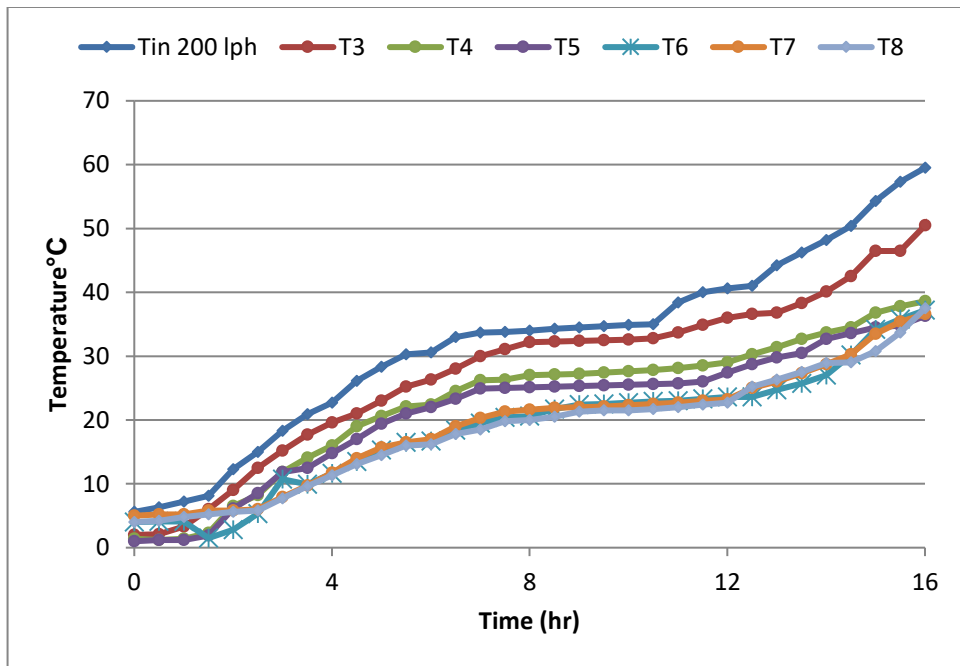


Figure 4.45 PCM2 temperatures for flow rate of 200 lph on 19th, 20th Dec 2016.

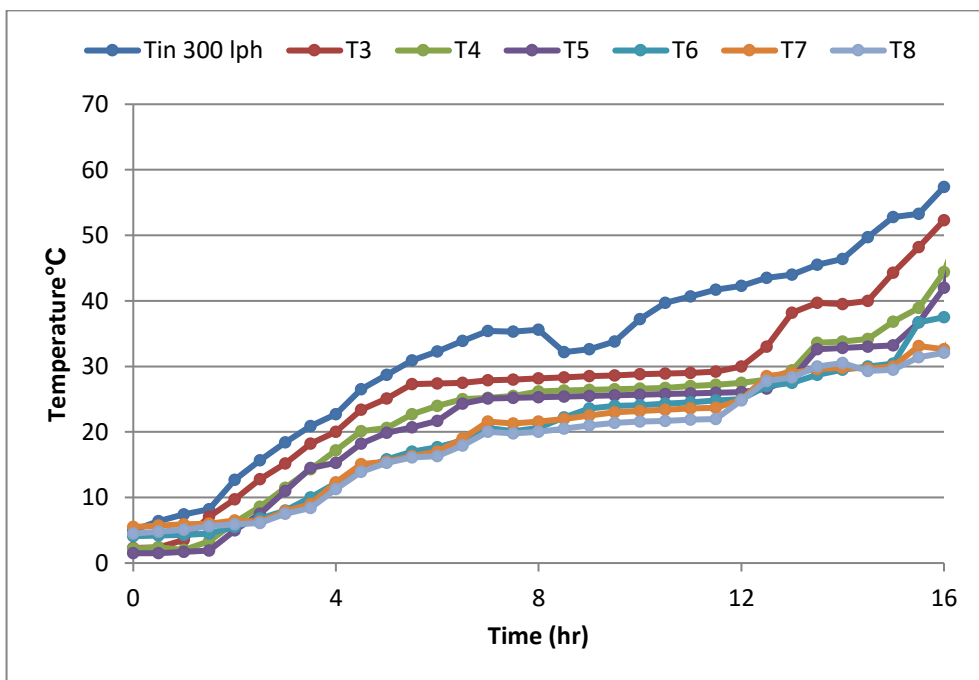


Figure 4.46 PCM2 temperatures for flow rate of 300 lph on 21th, 22th Dec 2016

Fig.4.47 shows the relation between water inlet temperature of inner tube and the PCM1 temperatures versus hourly time for a water flow rates of 500 lph identified the experiment lasted for 16 hours 27th and 28th Dec 2016 respectively at the different angular direction. The water inlet temperature is noticed to be higher than the highest temperature of PCM2. It can be seen that the inlet water temperature and all the PCM2 temperatures are increased from with time due to increasing in the thermal energy observed from the solar radiation. The maximum temperatures of inlet water to inner tube and PCM2 are 61.9°C °C and 45°C for water flow rate of 500 lph . It can be seen that the melting process occurs after 13 hours noon for water flow rate of 500 lph. occurs in shorter time.

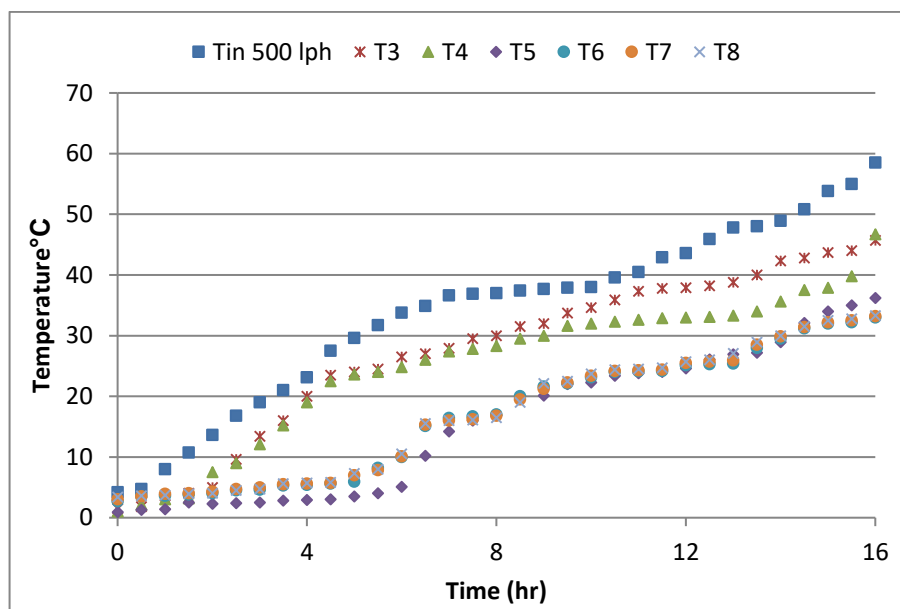


Figure 4.47 PCM2 temperatures for flow rate of 500 lph on 27th,28th Dec 2016

Figures 4.48 and 4.49 shows more details of the relation between water inlet temperature of inner tube and the PCM 2 temperatures versus hourly time for a water flow rate of 200 lph. One may observe that T3 and T6 are highest temperatures for PCM2 because of it are closest to inner tube surface that lead to increase the heat transfer at this locations faster than at the locations of T4,T5, T7, and T8. Also, it can be shown that T3 is higher than T6 because of unsymmetrical in its locations from the bulk temperature of water flow inside rectangular inner tube. Prefers to use drainage 500lph because gives the best temperatures due to high speed and the friction between water molecules. Produces high temperatures supports melt the paraffin.

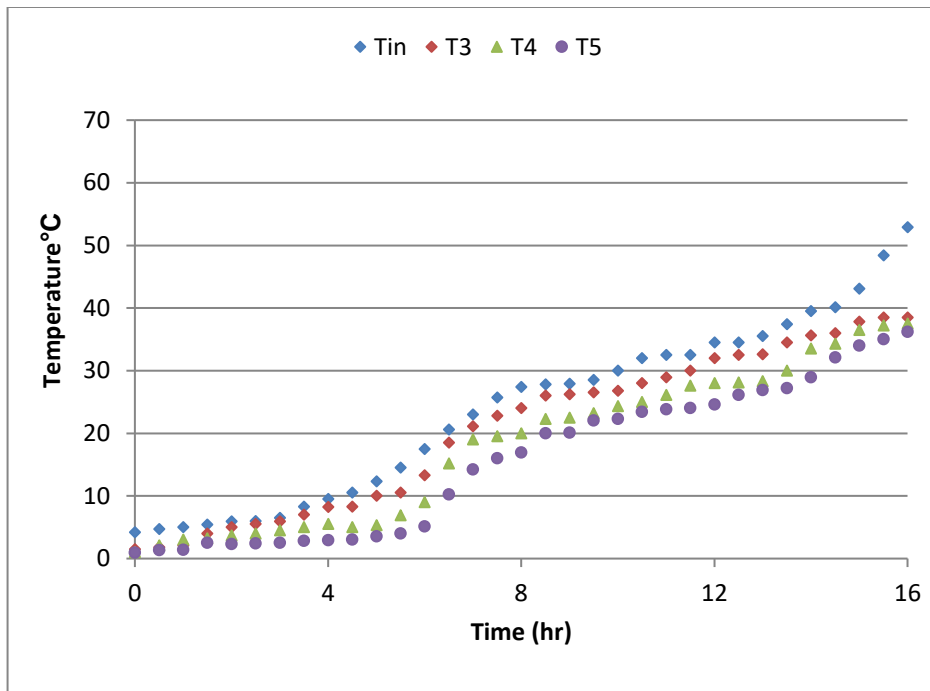


Figure 4.48 PCM2 temperatures (T3, T4, T5) for flow rate of 200 lph on 19th and 20th Dec 2016

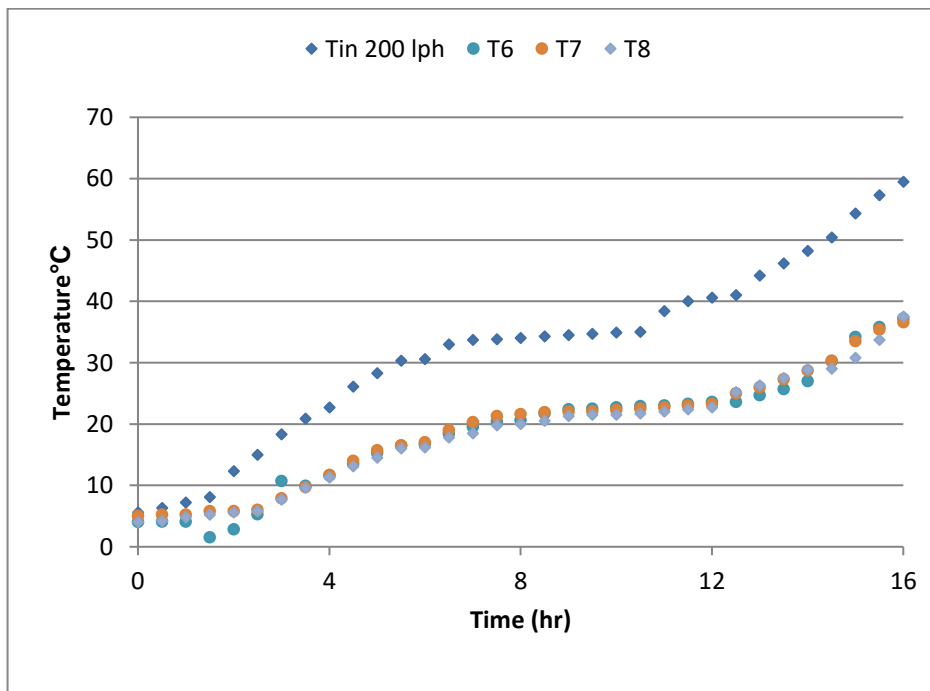


Figure 4.49 PCM2 temperatures (T6, T7, T8) for flow rate of 200 lph 19th and 20th Dec 2016

Fig.4.50 shows the relation between the middle temperatures (T_4) of PCM2 versus hourly time for a water flow rates of 200, 300, and 500 lph. It can be observed that the temperatures for the flow rate of 500 lph are highest temperatures than temperatures of the lower flow rates (200, 300) lph, because of the inlet temperatures for 500 lph water flow rate inside inner tube have highest temperatures than inlet temperatures of the lower flow rates (200, 300) lph with increasing the flow rate, the melting rate increases and the PCM2 melts in shorter time.

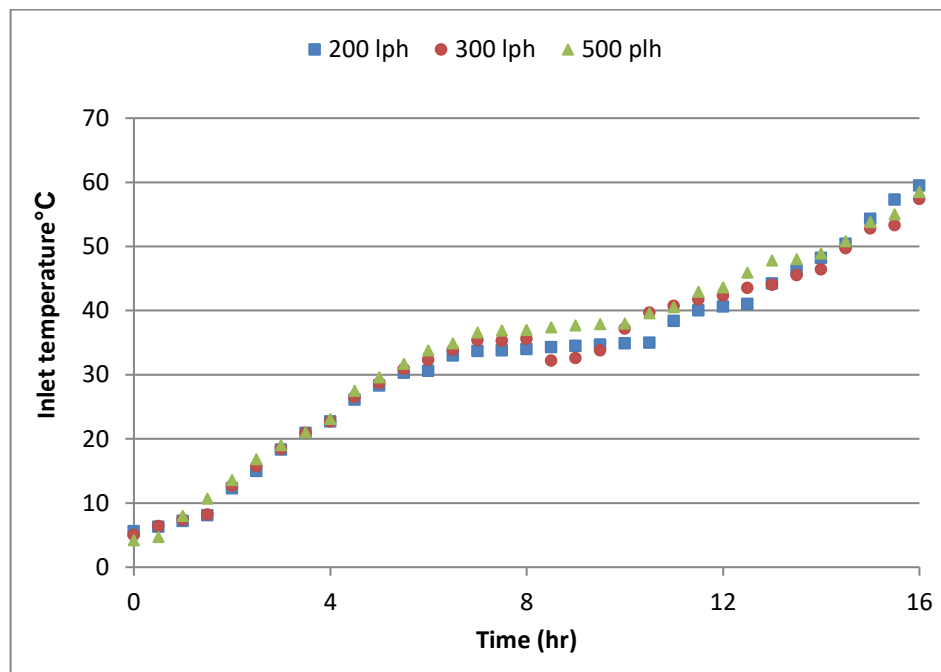


Figure 4.50 PCM2 middle temperatures (T_4) of 200 lph on 19th, 20th, 21th, 22th, 27th and 28th Dec 2016

Fig. 4.51 shows the relation between the Inlet water temperature inside inner tube (T_1) for PCM2 versus hourly time for a water flow rates of 200, 300, and 500 lph. It can be detected that the temperatures for the flow rate of 500 lph are highest temperatures than temperatures of the lower flow rates (200, 300) lph, due to the ambient temperatures for 500 lph water flow rate inside inner tube have highest temperatures than ambient temperatures increased even more than the previous two cases (200 and 300 L/h) because the flow rate is higher and the paraffin needs less time to melt (200, 300) lph as shows Figures 4.52 and 4.53.

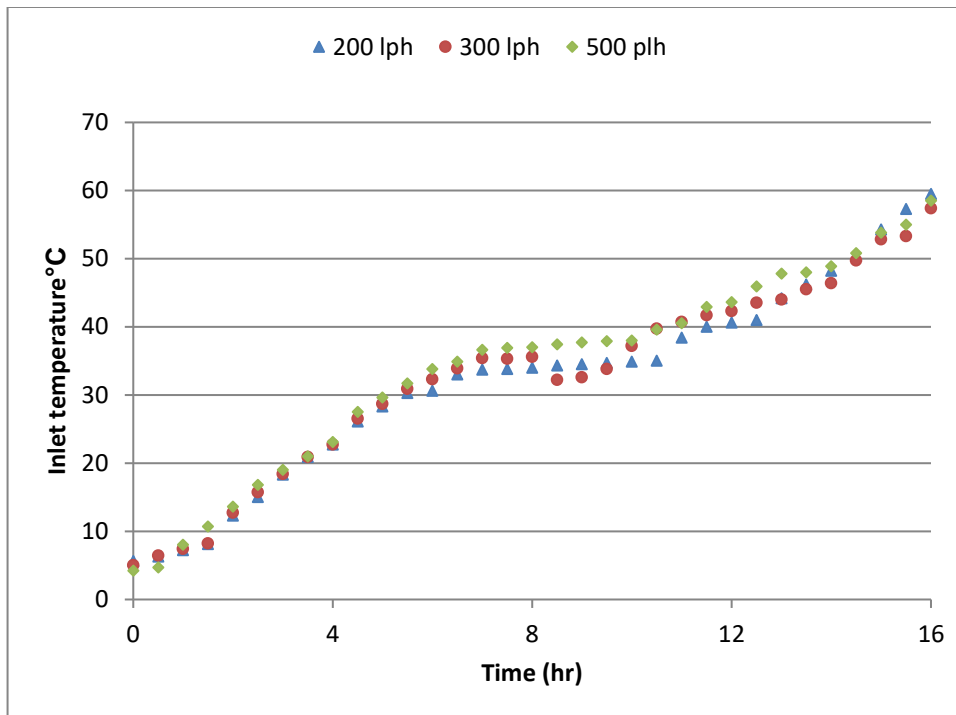


Figure 4.51 Inlet water temperature (T_{in}) for PCM2 on 19th, 20th, 21th, 22th, 27th and 28th Dec 2016

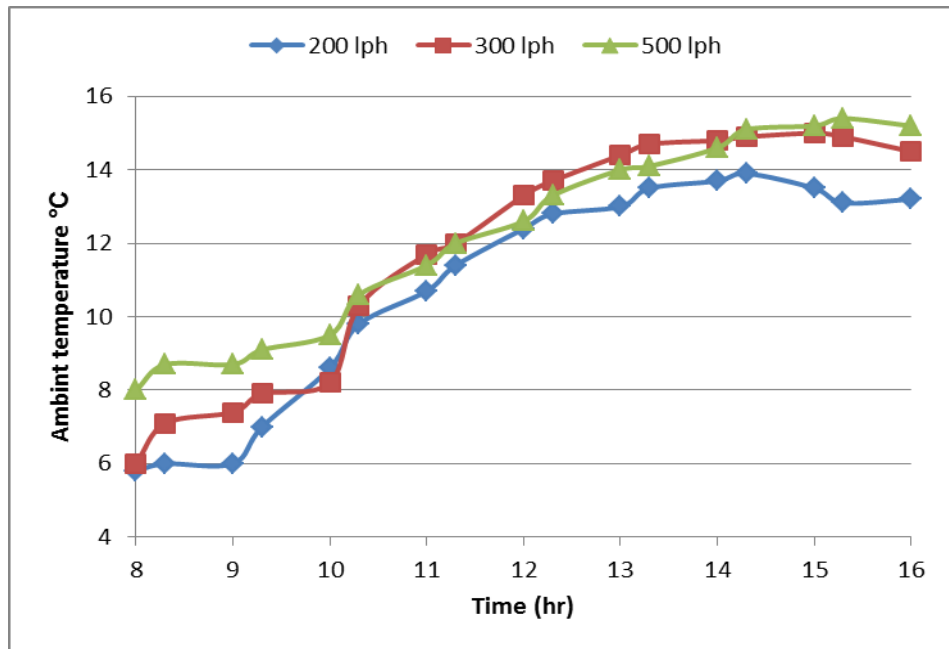


Figure 4.52 Ambient temperature (T_{amb}) for PCM2 on 19th, 20th, 21th, 22th, 27th and 28th Dec 2016.

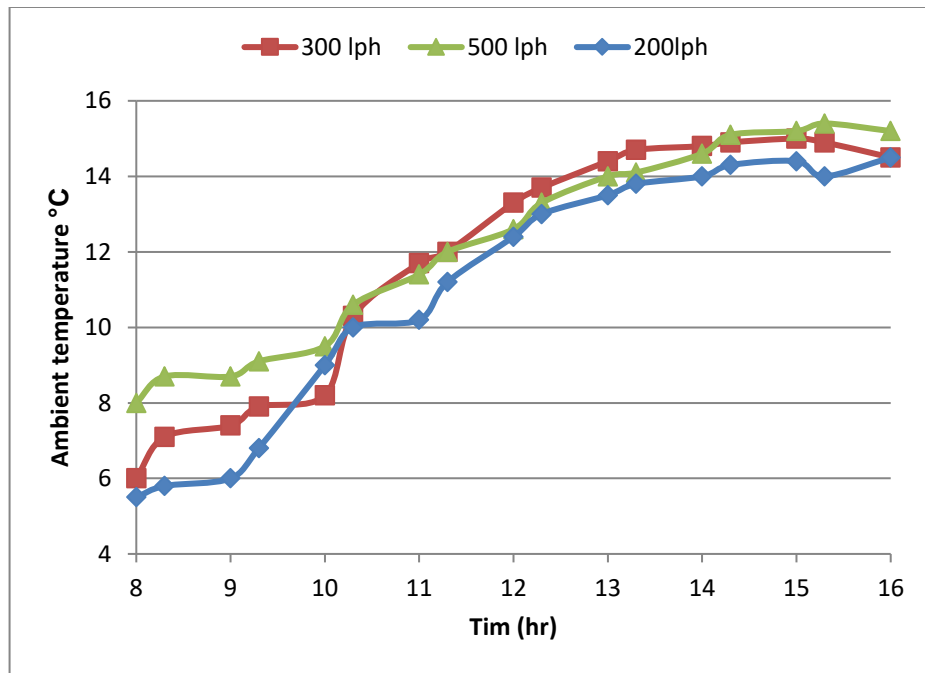
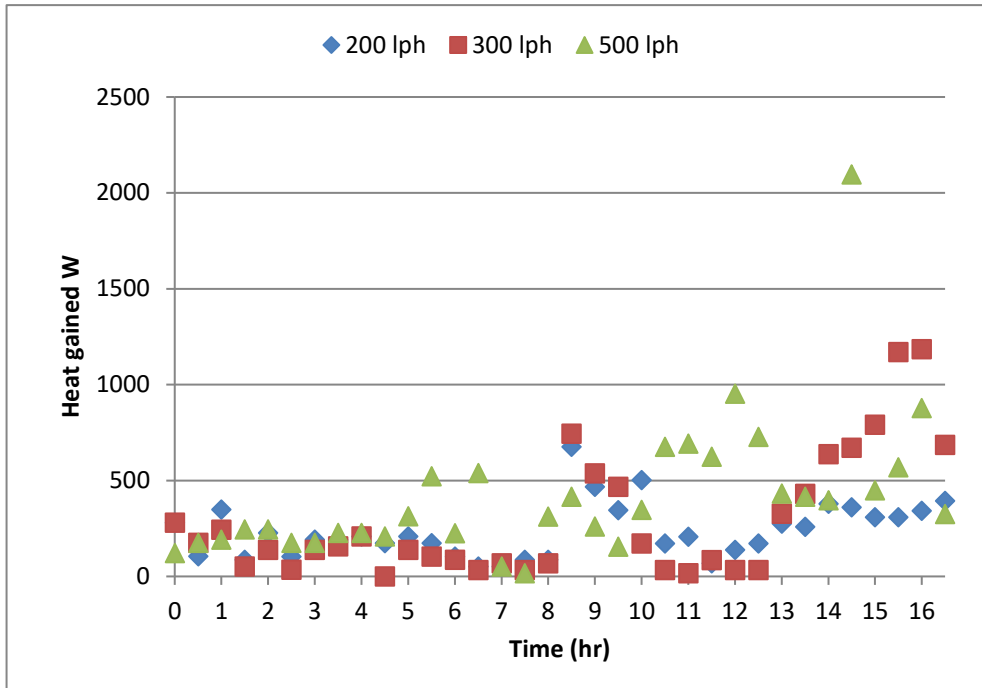


Figure 4.53 Ambient temperature (T_{amb}) for PCM2 on 19th, 20th, 21th, 22th, 27th and 28th Dec 2016.

Fig.4.54 shows the relation between the heat energy gained from the hot water flow inside inner tube for PCM2 versus hourly time for a water flow rates of 200, 300, and 500 lph. It can be observed that the heat gained for the flow rate of 500 lph are highest temperatures than that of the others flow rates (200, 300) lph, due to the temperatures differences for 500 lph water flow rate inside inner tube have highest values than that of the others flow rates (200, 300) lph as shown in Fig.4.55.



4.54 Heat gained for PCM2 on on19th,20th ,21th ,22th ,27th and 28th Dec2016

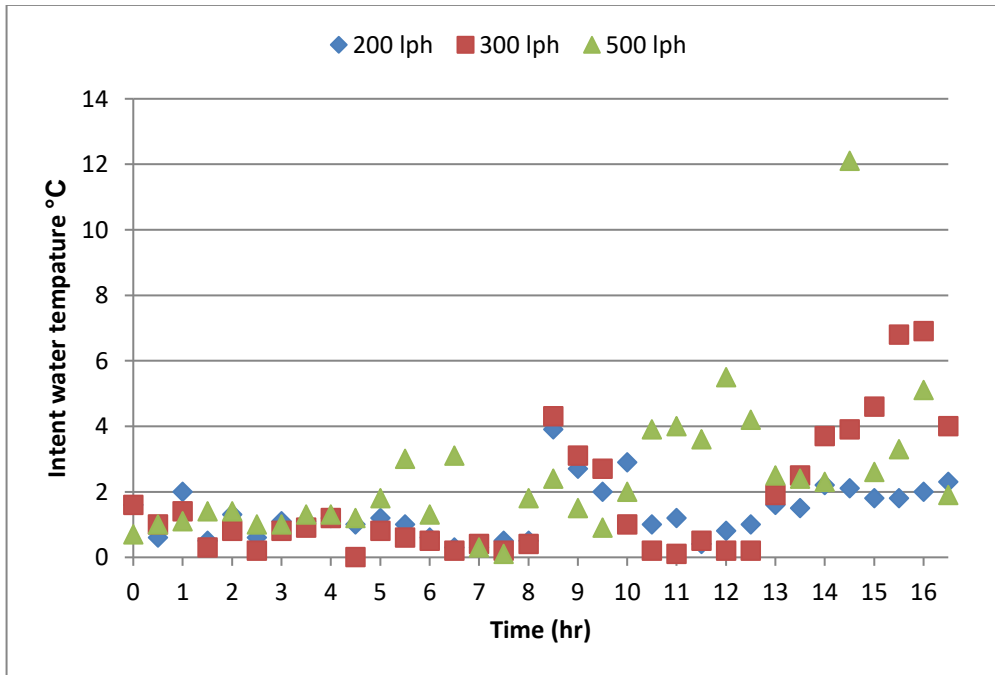


Figure 4.55 Intent water temperature difference of inner tube for PCM2 on 19th,20th ,21th ,22th ,27th and 28th Dec 2016.

Fig. 4.56 shows the relation between the raise of temperature for middle sensor (T4) for PCM2 versus hourly time for a water flow rates of 200, 300, and 500 lph. It can be observed that the maximum raising temperature is 6.2 °C found for the flow rate of 500 lph. These values are measured every half hour along daily test time.

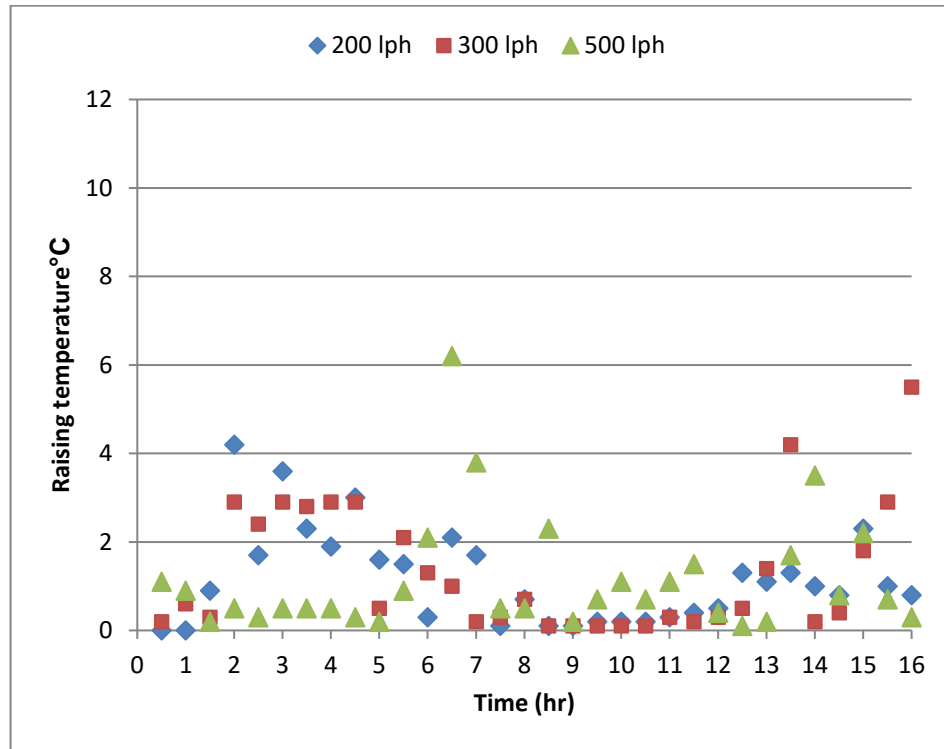


Figure 4.56 Raising of temperature for middle sensor (T4) for PCM2 on 19th, 20th das 20016.

Fig.4.57 shows the relation between the raise percent of temperature for middle sensor (T4) for PCM2 versus hourly time for a water flow rates of 200, 300, and 500 lph. It can be observed that the maximum raising percent of temperature is 31% found for the flow rate of 200 lph. The percent values are measured every half hour along daily test time two-day period 16 hours.

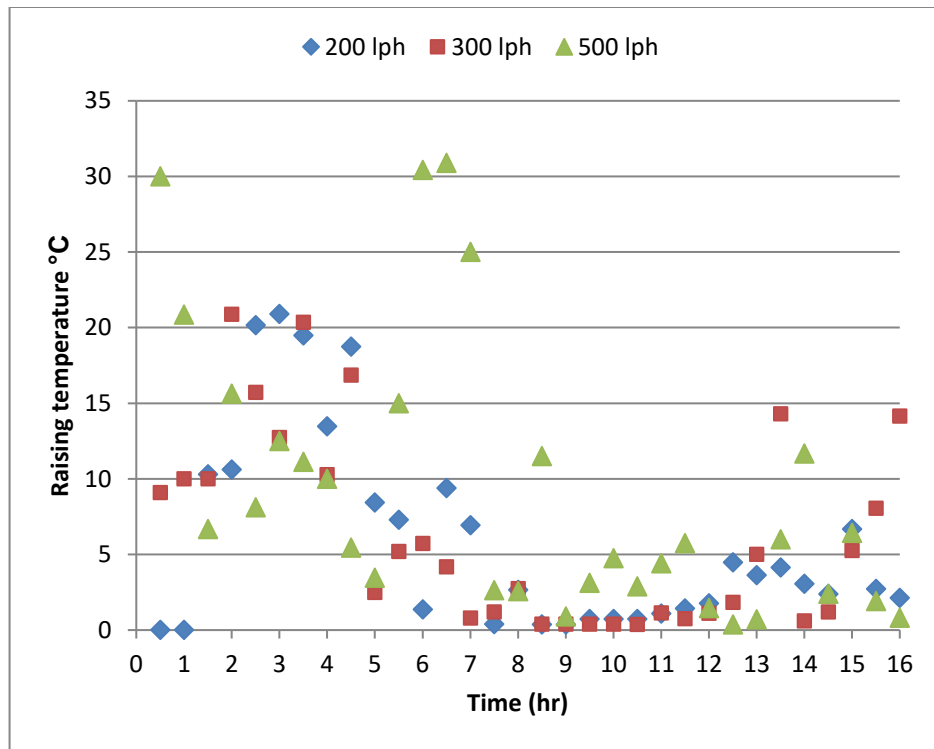


Figure 4.57 Raising percentage of temperature for middle sensor (T4) for PCM2 on 19th, 20th das 20016

Fig.5.58 shows the relationship between the latent heat of (PCM2) versus discharge rates of water flow from 200, 300, and 500 lph on summer season and winter season . It can results indicate that the heat stored in the flow rate 300 lph is the highest heat stored of other flow (200,500), du to 200 lph have a maxim temperature difference between initial temperature and final temperature, which have initial temperature (2.2°C) and the final temperature (51.4°C).

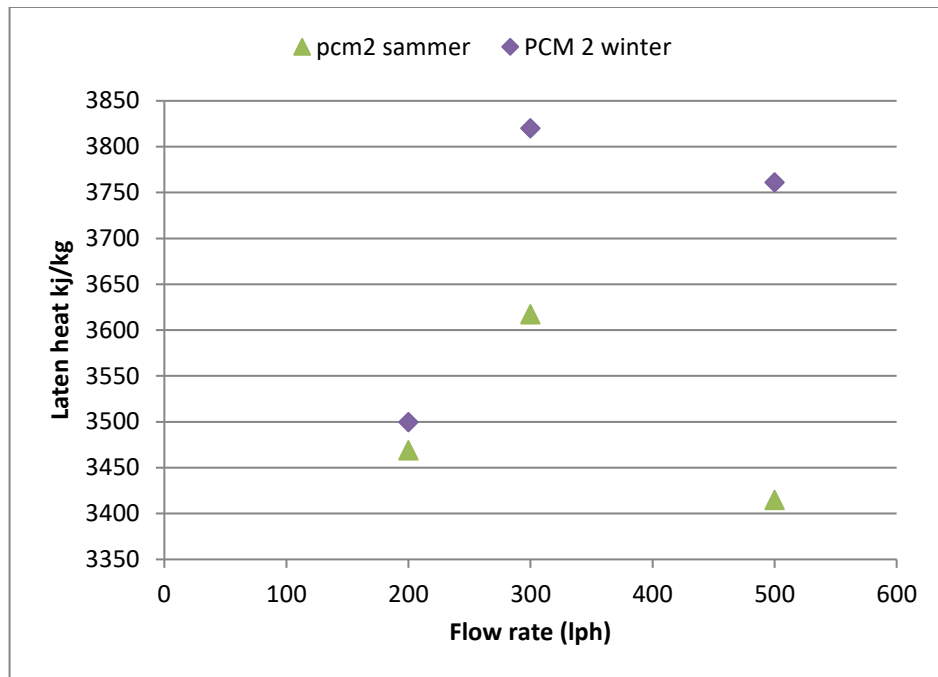
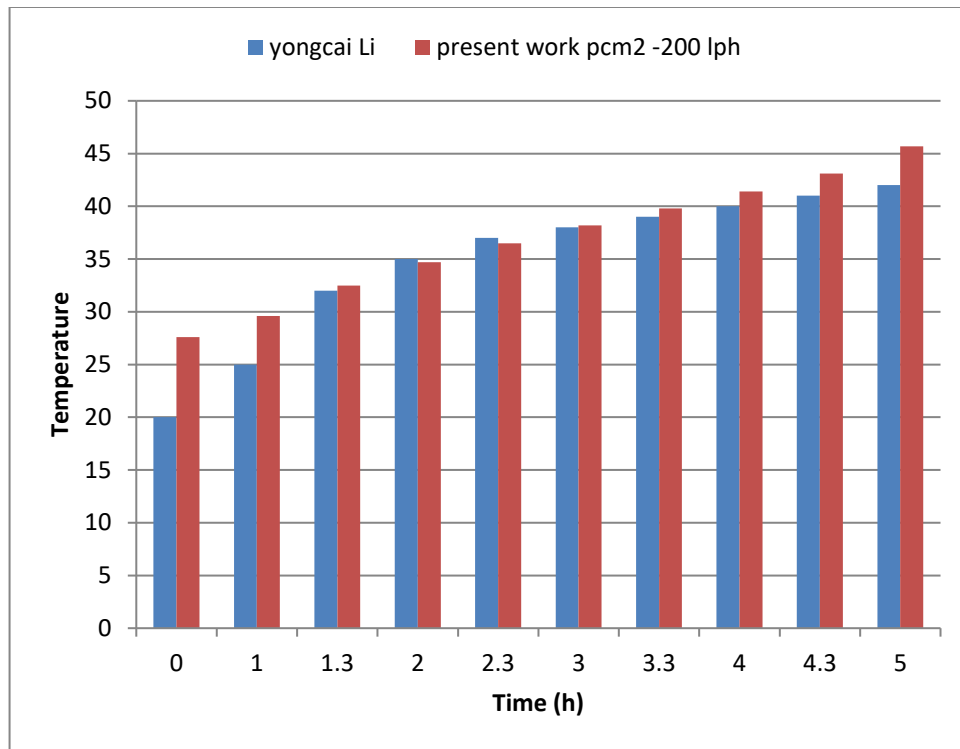


Figure 4.58 Latent Heat of PCM2.

Fig. 4.59 shows a comparisons between the present experiments results and (yongcai Li) experiment results, which included relationship between PCMS middle temperature and time. PCMS of the present work and (yongcai Li) work have the same physical properties. It can be observed that the temperature of present work are higher than the temperature of (yongcai Li) by 15% due to the present work is done under natural solar radiation while (yongcai Li) work is done under a group of light radiation in the laboratory.



4.59 Compares on between the present work and (yongcai Li) work [39].

4.7 Summary

- PCM2 gives higher rates of melting than PCM1 due to its higher purity and heat transfer.
- T4 is the temperature that should be considered for the melting process because of the location of its thermocouple. This thermocouple is not very close to the heat exchanger (as T3) and it is not close to the storage container wall (as T5).
- The melting rate is mainly affected by the flow rate and the best melting was obtained at the highest flow rate (500 l/h). However, the weather condition changes, atmospheric temperature and sun light intensity also affect the thermocouple temperatures and melting rates

Chapter Five

Conclusion and Recommendations

5.1 Conclusion

In this study, two types of paraffin PCM1 and PCM2 were tested in both the summer season and winter season. The experiment was conducted at different flow rates (200, 300 and 500 l/h) for each paraffin type. The followings conclusion remark from the experiment results:

- In the summer season, the highest temperature measured by middle thermocouple (T4) at flow rate 500 l/h was (68.1°C) and the Because of high flow speeds, the kinetic energy of the water molecules increase and consequently, the melting process speed increases needed time of (3-4) hours only. While it needed more time (14-16) hours in winter season. Increasing solar radiation and ambient temperature reduces the melting time for both PCM types.
- The best results for paraffin melting were obtained for PCM1 and PCM2 on Aug 2016 summer season at flow rate 500l/h. Because at high flow speeds, the kinetic energy of the water molecules increase and consequently, the melting process speed increases.
- The inlet temperature has a great effect on paraffin melting.
- Heat transfer characteristics from the heat exchanger to melt the paraffin undergoes three stages:
 - 1- The heat transfers by conduction.
 - 2- The heat transfers by conduction and conviction together.
 - 3- The heat transfers by conduction and convection alternatively.
- It conclude that the white paraffin (PCM2) starts melting at 40.2°C where the black paraffin (PCM1) starts melting at 44°C.
- PCM2 shows a better performance than PCM1 because of the high purity of PCM2
- The flow rate of 300lph gave the fastest paraffin melting compared with the (200,500) due to weather changes, low sun light and low temperature in the summer season for PCM2.

- The present experimental results compared with the available previous studied and give a good agreement.

5.2 Recommendations

- Using a circular internal tube with a fin.
- Using heat exchanger made of copper for more heat conduction.
- Using a parabolic type solar collectors.
- Changing the setup to use the paraffin for coolant.
- Can using the ability of the procedure of this study to be employed in air conditioner with gas instead of paraffin.

References

- [1] D. Fernandez a ,at, Thermal energy storage: “How previous findings determine current research priorities .energy 39(2012)-246 -275.
- [2] M.Ravikumar and DR.Pss, Phase change material as a thermal energy for cooling of, 2005-2008 Joint. All rights reserved.
- [3] Edina Milisic, Modelling of energy storage using phase-change materials (PCM materials: July 2013).
- [4] Lavinia Gabriela, Thermal Energy Storage with Phase Change Material. Issue 20, January-June 2012, p. 75-98.
- [5] Fabio anono , Thiess the use of phase changing material for cooling of Buildings. Combined with night sky radidiant cooling. 2014-2015.
- [6] A. ABHA ,et,Low temperature latent heat thermal energy storage : heat storage materials, Vol 10, No. 4. pp 313-332. 1983..
- [7] Daniel,et,An Overview of Phase Change Materials and their Implication on Power Demand, 2009-IEEE-Motreal- PCM
- [8] H. Mehling and L. F. Cabeza, Heat and cold storage with PCM: an up to date introduction into basics and applications. Berlin: Springer Science & Business Media, 2008, pp. 11–55.
- [9] Louis and Robyn Murray,et, Phase Change Material Selection in the Design of a Latent Heat Energy Storage System Coupled with a Domestic Hot Water Solar Thermal , 2011.
- [10] Luisa F. Cabeza a ,*, Cecilia Castello´n a , Miquel Nogue´s a , Marc Medrano a , Ron Leppers b , Oihana Zubillaga Use of microencapsulated PCM in concrete walls for energy savings. Energy and Buildings 39 (2007) 113–119.
- [11] Lavinia Gabriela SOCACIU, Thermal Energy Storage with Phase Change Material, Issue 20, January-June 2012 p. 75-98.
- [12] Abduljalil A. Al-Abidi n , Sohif Bin Mat, K. Sopian, M.Y. Sulaiman, C.H. Lim, Abdulrahman Th, Review of thermal energy storage for air conditioning systems Energy Reviews 16 (2012) 5802–5819.
- [13] Shuo Peng,1 Alan Fuchs,1 R. A. Wirtz2Polymeric Phase Change Composites for Thermal Energy Storage , 19 January 2004 DOI 10.1002/app.20578.
- [14] Murat Kenisarin, Khamid Mahkamov, Solar energy storage using phase change materials, 11 (2007) 1913–1965.

- [15] Qi Qi, Yiqiang Jiang, Shiming Deng. A Simulation Study on Solar Energy Seasonal Storage by Phase Change Material. ICSET 2008.
- [16] Waqar A. Qureshi, Student Member, IEEE, Nirmal-Kumar C. Nair, Member, IEEE, Mohammed M. Farid, Non-member, IEEE, Demand Side Management Through Efficient Thermal Energy Storage Using Phase Change Material, 2008 Australasian Universities Power Engineering Conference (AUPEC'08).
- [17] Atul Sharma, C. R. Chen, Solar Water Heating System with Phase Change Materials, International Review of Chemical Engineering (I.RE.CH.E.), Vol. 1, N. 4 July 2009.
- [18] Vasishta D. Bhatt*, Kuldip Gohil, Arunabh Mishra, Thermal Energy Storage Capacity of some Phase changing Materials and Ionic Liquids, ISSN : 0974-429 Vol.2, No.3, pp 1771-1779, July-Sept 2010 .
- [19] Yan Quanying Li Lisha Shen Deyan , The experimental research on the thermal Characterizations of shape-stabilized Paraffin to be used in a Wall , 978-1-4244-4813-5/10©2010 Crown.
- [20] P. Zhang, L. Xia, R.Z. Wang , The thermal response of heat storage system with paraffin and paraffin/expanded graphite composite for hot water supply, 8-13 My 2011 linkoping ,Sweden.
- [21] Eduard Oróa , Antoni Gila , Laia Miróa , Gerard Peiróa , Servando Álvarezb , Luisa F. Cabeza , Thermal energy storage implementation using phase change materials for solar cooling and refrigeration applications , Energy Procedia 30 (2012) 947 – 956 .
- [22] Ronald Warzoha, Omar Sanusi, Brian McManus, Amy S. Fleischer, Evaluation of Methods to Fully Saturate Carbon Foam with Paraffin Wax Phase Change Material for Energy Storage, 978-1-4244-9532-0/12©2012 IEEE.
- [23] S. Harikrishnan¹ , S. Kalaiselvam¹, experimental investigation of solidification and melting characteristics of nanofluid as pcm for solar water heating systems , Technologies for Sustainable Development, 07-09 February 2013, Howrah, India.
- [24] Jianqing Chena,b, Donghui yanga, c, Jinghua Jiang a,d, Aibin Maa,d, Dan Songa, Research progress of phase change materials (PCMs) embedded with metal foam (a review) Jianqing Chen et al. / Procedia Materials Science 4 (2014) 389 – 394 .
- [25] M. J. Hosseini¹ , M. Rahimi¹ , and R. Bahrampoury, Thermal analysis of PCM containing heat exchanger enhanced with normal annular fines, Mech. Sci., 6, 221–234, 2015

- [26] Arun Kumar and S.K.Shukla, A Review on Thermal Energy Storage Unit for Solar Thermal Power Plant Application. Energy Procedia 74 (2015) 462 – 469
- [27] Sekar Sinaringati, Nandy Putra, Muhammad Amin and Fitri Afriyanti, The Utilization of paraffin and beeswax as heat energy storage in infant incubator, vol.11.NO.2, January 2016.
- [28] Abhat, A., 1983, "Low temperature latent heat thermal energy storage: heat storage materials", Solar Energy, 30, 4, 313-331.
- [29] Gerald permutt, Thesis, Absolute viscosity of the n – Paraffin liquids, Newark 1960.
- [30] Lane, G., 1983, "Latent heat materials", Volume 1, CRC Press, Boca Raton, Florida.
- [31] Buddhi, D. and Sawhney, R.L., 1994, "Proc: Thermal energy storage and energy conversion", School of Energy and Environmental Studies, Devi Ahilya University, Indore, India
- [32] Ettouney, H.M., Alatiqi, I., Al-Sahali, M., Al-Ali, S.A., 2004, "Heat transfer enhancement by metal screens and metal spheres in phase change energy storage systems", Renewable Energy, 29, 841 - 860.
- [33] Colvin, D.P. and Bryant, Y.G., 1998, " Protective clothing containing encapsulated phase change materials", Proceedings of the 1998 ASME International Mechanical Engineering Congress and Exposition, Anaheim, CA, USA, 23–32.
- [34] Ashrae applications handbook, chapter 32 by american society of heating, solar energy use. Atlanta, ga: 1999.
- [35] J. ma, w. sun, j. ji, y. zhang, a. zhang, and w fan. "experimental and theoretical study of the efficiency of a dual function solar collector". applied thermal engineering (2011); 31: 1751–1756.
- [36] Bhaskaran Rajesh "Introduction to CFD Basics". 2013.
- [37] Lane ga . solar heat storage latent heat materials, vol.1. boca raton fl: crc press, inc.; 1983.
- [38] Baylin F. Low temperature thermal energy storage: a state of the art survey. Report no. SERI/RR/-54-164. Golden, Colorado, USA: Solar Energy Research Institute; 1979.
- [39] yongcai Li, thesis, Thermal Performance Analysis of A PCM Combined Solar Chimney System for Natural Ventilation and Heating/Cooling ,September, 2013